RADIATION CHARACTERISTIC ANALYSIS OF TAPERED SLOT ANTENNAS

A THESIS SUBMITTED TO
THE GRADUATE SCHOOL OF NATURAL AND APPLIED SCIENCES
OF
MIDDLE EAST TECHNICAL UNIVERSITY

BY

AYKUT CİHANGİR

IN PARTIAL FULFILLMENT OF THE REQUIREMENTS
FOR
THE DEGREE OF MASTER OF SCIENCE
IN
ELECTRICAL AND ELECTRONICS ENGINEERING

AUGUST 2010

Approval of the thesis:

RADIATION CHARACTERISTIC ANALYSIS OF TAPERED SLOT ANTENNAS

submitted by **AYKUT CİHANGİR** in partial fulfillment of the requirements for the degree of **Master of Science in Electrical and Electronics Engineering Department, Middle East Technical University** by,

Prof. Dr. Canan Özgen ____________
Dean, Graduate School of **Natural and Applied Sciences**

Prof. Dr. İsmet Erkmen ____________
Head of Department, **Electrical and Electronics Dept., METU**

Assist. Prof. Dr. Lale Alatan ____________
Supervisor, **Electrical and Electronics Dept., METU**

Assoc. Prof. Dr. Özlem Aydın Çivi ____________
Co-supervisor, **Electrical and Electronics Dept., METU**

Examining Committee Members:

Prof. Dr. Gülbin Dural ____________
Electrical and Electronics Engineering Dept., METU

Assist. Prof. Dr. Lale Alatan ____________
Electrical and Electronics Engineering Dept., METU

Assoc. Prof. Dr. Sencer Koç ____________
Electrical and Electronics Engineering Dept., METU

Assoc. Prof. Dr. Şimşek Demir ____________
Electrical and Electronics Engineering Dept., METU

M.Sc. Can Barış Top ____________
ASELSAN

Date: **23/08/2010**

I hereby declare that all information in this document has been obtained and presented in accordance with academic rules and ethical conduct. I also declare that, as required by these rules and conduct, I have fully cited and referenced all material and results that are not original to this work.

Name Surname: Aykut Cihangir

Signature:

ABSTRACT

RADIATION CHARACTERISTIC ANALYSIS OF TAPERED SLOT ANTENNAS

Aykut Cihangir
M.Sc., Department of Electrical and Electronics Engineering
Supervisor: Assist. Prof. Dr. Lale Alatan
Co-Supervisor: Assoc. Prof. Dr. Özlem Aydın Çivi

August 2010, 87 pages

The aim of this study is to investigate the effects of changes in the physical parameters of tapered slot antennas (TSA) on their radiation characteristics and also to explore the possibility of reconfiguration in the radiation pattern of TSA by switching between two different types of tapering.

There are mainly three physical parameters that affect the radiation pattern of TSAs. These are antenna length, aperture width and the ground extension. After designing a wideband microstrip line to slot line transition, the effect of antenna parameter variations on the beamwidth and sidelobe level of the antenna are investigated through the use of a commercially available electromagnetic simulation software HFSS by ANSOFT. The radiation characteristics of constant width slot antennas (CWSA) and linearly tapered slot antennas (LTSA) are compared. It is observed that CWSAs exhibit narrower beamwidth and higher sidelobe level whereas linearly tapered slot antennas (LTSA) have wider beamwidth with lower sidelobe level compared to each other. A novel switching architecture between CWSA and LTSA is proposed to obtain a reconfigurable antenna.
Keywords: Tapered slot antennas, reconfigurable antennas, microstrip line to slotline transition.

ÖZ

SÖNÜMLENEN YARIK ANTENLERİN IŞIMA KARAKTERİSTİĞİ ANALİZİ

Aykut Cihangir
Yüksek Lisans, Elektrik ve Elektronik Mühendisliği Bölümü
Tez Yöneticisi: Yrd. Doç. Dr. Lale Alatan
Eş Tez Yöneticisi: Doç. Dr. Özlem Aydın Çivi

Ağustos 2010, 87 sayfa

Bu çalışma ile sönümlenen yarık antenlerin fiziksel özelliklerinin ışıma örüntüsüne etkilerini araştırmak ve iki farklı sönümlenme tipi arasında yapılacak geçişlerle ışıma örüntüsünde yeniden şekillendirilebilirlik elde edilebilme olasılığını araştırmak hedeflenmiştir.

Genel olarak bir sönümlenen yarık antenin ışıma örüntüsünü etkileyen üç fiziksel özellik vardır. Bunlar anten boyu, açıklık genişliği ve toprak uzantısı parametreleridir. Geniş bantlı bir mikroşerit hattan yarık hatta geçiş tasarımı sonrasında, ANSOFT firmasının ticari bir elektromanyetik benzetim yazılımı olan HFSS ile anten parametrelerinin yarım açı huzme genişliği ve yan lob seviyesi üzerine etkileri araştırılmıştır. Sabit Genişlikli ve Doğrusal Sönümlenen Yarık Antenlerin ışıma karakteristikleri karşılaştırılmıştır. Analiz sonucunda Doğrusal Sönümlenen Yarık Antenlerin daha dar huzme genişliği ve daha yüksek yan lob seviyesine, Doğrusal Sönümlenen Yarık Antenlerin ise daha geniş huzme genişliği ve daha düşük yan lob seviyesine sahip olduğu gözlemlenmiştir. Yeniden şekillendirilebilir bir anten elde etmek için Sabit Genişlikli ve Doğrusal Sönümlenen Yarık Antenler arasında bir geçiş mimarisi önerilmiştir.

Anahtar Kelimeler: Sönümlenen yarık antenler, yeniden şekillendirilebilirlik, mikroşerit hattan yarık hatta geçiş.

ACKNOWLEDGEMENTS

I would like to express my gratitude to my supervisor Assist. Prof. Dr. Lale Alatan, for her guidance, support, understanding and tolerance throughout this study.

I wish to thank my co-supervisor Assoc. Prof. Dr. Özlem Aydın Çivi, for her contribution and guidance in my study.

I would also want to thank Assoc. Prof. Dr. Sencer Koç, Ömer Bayraktar and Erdinç Yurdakul for their support in the antenna manufacturing and pattern measurement phase of the study.

Finally, I am indebted to my family and friends, who never let me lose my motivation and who never withheld their help from me, in all circumstances.

TABLE OF CONTENTS

LIST OF TABLES

LIST OF FIGURES

CHAPTER 1

INTRODUCTION

Electrical and Electronics Engineering Department of Middle East Technical University (METU) is a member of EU supported COST ASSIST project. The scope of this project is the design of reconfigurable antennas at millimeter-wave frequency band. Millimeter-wave band is considered in this project since the Personal Communication Systems (PCS) operate with high data rates that correspond to a large bandwidth requirement which can be easily satisfied in this frequency band. In millimeter-wave designs that are used in applications like PCS, automotive collision avoidance radars and local cellular radio networks, an integrated antenna that rests on a substrate and has ease to be integrated with other RF circuits on a common board or module is usually preferred. It is important for the antenna and rest of the system to be located on a single substrate to get a compact layout. Due to the easy integration and large bandwidth requirements, Tapered Slot Antenna (TSA) is chosen to be the antenna configuration that will be studied within the scope of this work. Different types of reconfigurable antennas are studied at METU. In those antennas generally reconfiguration is done either on the operating frequency of the antenna or on the polarization of the antenna. Since the bandwidth of TSA is already wide and excitation of different polarizations in TSA requires the design of complex structures, a different type of reconfiguration is searched for TSA. During the literature survey about TSA, it is found that the tapering profile of TSA significantly affects the radiation characteristics of the antenna. Consequently in this thesis, it is aimed to investigate the radiation characteristics of TSA and to explore the possibility of reconfiguring the radiation pattern of TSA by switching between different tapering profiles.

Tapered slot antennas (TSA) are travelling wave antennas. In general, all antennas whose voltage or current distribution can be modeled by one or more travelling waves are called travelling wave (nonresonant) antennas. Unlike standing wave (resonant) antennas, the phase distribution along a traveling wave antenna can not be assumed to be constant as stated in [1]. The reflected wave in resonant antennas is totally or partially minimized in the traveling wave antennas by proper termination. An example to this phenomenon is the long wire antenna which is actually a resonant dipole antenna terminated by a matched load.

There are two types of traveling wave antennas: slow wave antennas and fast wave antennas. Slow wave antennas are antennas whose phase velocities are equal to or smaller than the speed of light. For surface wave antennas, a type of slow wave antennas, the radiation takes place at the discontinuities, nonuniformities and curvatures where the bound wave on the antenna surface is interrupted. The travelling wave antennas of this class are endfire or near endfire radiators. Fast wave antennas on the other hand have phase velocities larger than the speed of light. Consequently, leaky wave antennas are considered as fast wave antennas. This type of antenna couples power discretely or continuously through its length. The result is a tilted main beam from the endfire direction.

A tapered slot antenna uses a slot line etched on a dielectric material, which is widening through its length to produce an endfire radiation [2]. An electromagnetic wave propagates through the surface of the antenna substrate with a velocity less than the speed of light which makes TSAs gain slow wave antenna properties. The EM wave moves along the increasingly separated metallization tapers until the separation is such that the wave detaches from the antenna structure and radiates into the free space from the substrate end. The E-plane of the antenna is the plane containing the electric field vectors of the radiated electromagnetic (EM) waves. For TSAs, this is parallel to the substrate since the electric field is established between two conductors that are separated by the tapered slot. The H plane, the plane containing the magnetic component of the radiated EM wave runs perpendicular to the substrate.

TSAs have moderately high directivity (on the order of 10-17 dB) and narrow beamwidth because of the traveling wave properties and almost symmetric E-plane and H-plane radiation patterns over a wide frequency band as long as antenna parameters like shape, total length, dielectric thickness and dielectric constant are chosen properly. Other important advantages of TSAs are that they exhibit broadband operation, low sidelobes, planar footprints and ease of fabrication. A TSA can have large bandwidth if it exhibits a good match both at the input side (transition from the feed line to slot line) and the radiation side (transition from the antenna to free space) of the antenna [3]. The gain of a TSA is proportional to the length of the antenna in terms of wavelength. Tapered slot antennas are also suitable to be used at high operating frequencies (greater than 10 GHz), where a long electrical length corresponds to a considerably short geometrical length. The main disadvantage of the TSA is that only linear polarization can be obtained with conventional geometries.

As shown in Figure 1, several TSA types exist according to the shape of tapering. Most common types are Linearly Tapered Slot Antenna (LTSA), Vivaldi or Exponentially Tapered Slot Antenna and Constant Width Slot Antenna (CWSA).

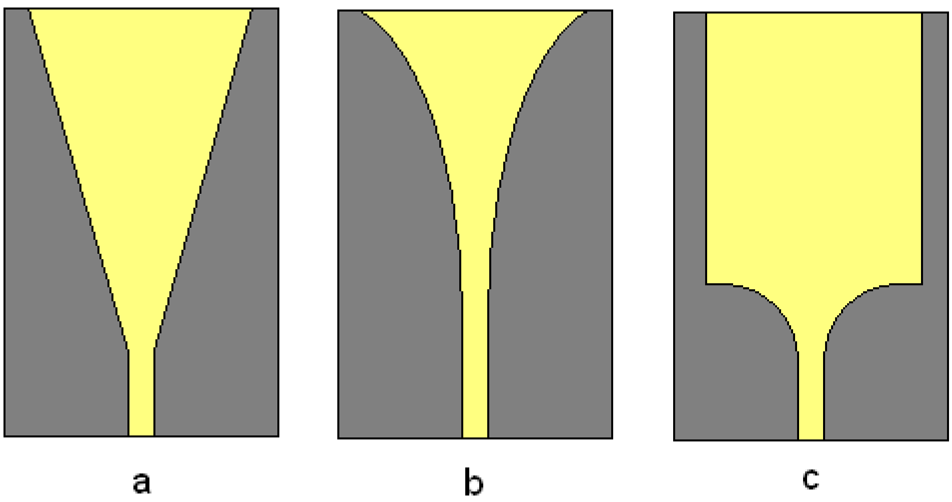

Figure 1 Tapered Slot Antenna Types

(a) Linearly Tapered Slot Antenna (b) Exponentially Tapered Slot Antenna (Vivaldi) (c) Constant Width Slot Antenna

These three main types of TSAs are compared in [4] in terms of beamwidths and side lobe levels. For a TSA with the same antenna length, aperture width and substrate parameters, CWSA has the narrowest beamwidth, followed by LTSA and then Vivaldi. The sidelobe levels are highest for CWSA, followed by LTSA and then Vivaldi. So a transition between the LTSA and CWSA structures could provide reconfigurability about antenna beamwidth and sidelobe levels. Within the scope of this thesis, the two configurations are studied separately and the changes in the radiation patterns of LTSA and CWSA are examined.

TSAs are first introduced in 1979 in the 9th European Microwave Conference by two independent presentations [5], [6]. In [5], an ETSA (Vivaldi) to be used in a 8-40 GHz video receiver module is proposed. The antenna had a usable bandwidth of 2-20 GHz with a gain of approximately 10dBi and -20dB sidelobe level. Exponential taper was chosen in this work in order to achieve a wideband performance with an aperiodic continuously scaled structure. It is stated that the energy in the travelling wave on the tapered slot becomes weaker as the separation between the arms of the slot line increases and at last the energy couples to the radiated field.

In [6], an X-band LTSA excited by a microstrip line on alumina substrate is proposed. The antenna was designed to be used in short range radar and phased array systems. The LTSA had a gain of 6dBi and a sidelobe level of -10dB. The antenna had a %5 bandwidth centered at 9 GHz. The slot width at the open end of the slot line was changed while keeping the antenna length constant and the change in the gain and sidelobe levels were observed.

In 1985, CWSA is proposed in [7]. In this study, the effective thickness value required for compliance with Zucker's curves for travelling wave antennas are stated. Effects of the parameters of the dielectric substrate and the dimensions of the antenna on the radiation characteristics of the antenna were investigated experimentally for LTSA, Vivaldi and CWSA geometries.

Until 1986, only experimental studies had been conducted for the analysis of TSAs. The numerical analysis of TSAs through the use of Method of Moments (MoM) is first proposed by Janaswamy in his Ph.D. dissertation [8]. In 1989, Johansson also demonstrated the MoM analysis of LTSAs to determine the surface currents on the antenna [9]. In [10], analyses of TSAs are also performed by MoM and the dielectric constant profile of the substrate is optimized to achieve a required radiation pattern.

After the work of Yngvesson et al [4] that emphasizes the easy integration feature of TSAs, they started to be widely used in millimeter-wave and array applications. TSAs operating at millimeter-wave frequency band are designed and studied in [11]-[13]. In [11], two types of TSAs (LTSA and ETSA) operating at 23-80 GHz band are designed. According to simulation results the input return loss values of both of the antennas are below -10dB within the frequency band. However, when the radiation characteristics of the antennas are investigated, it is observed that the antenna starts to be more directive as the frequency increases. Therefore the gain of the antenna varies between 7-12 dBi for the LTSA and between 8-10 dBi for the ETSA. It is concluded that the radiation pattern bandwidth of the ETSA is wider compared to LTSA. In [12], a LTSA operating at 45-75 GHz band is designed on a low temperature cofired ceramic (LTCC) substrate. It is observed that the high dielectric constant of the LTCC substrate degrades the radiation characteristics of the antenna by lowering the gain and distorting the radiation pattern. Therefore an air cavity at the back of the antenna is introduced to lower the effective dielectric constant of the substrate. In this way, the distortions in the radiation pattern of the antenna are eliminated but still a variation of 4.9dBi to 5.9dBi is observed in the gain of the antenna within the frequency band. In [13], the effective dielectric constant of the substrate is reduced by selectively machining holes in the dielectric substrate. The radiation characteristics of the designed antenna are investigated at 24, 30 and 36 GHz both with and without holes. It is observed that the introduction of the holes lowers the sidelobe levels, significantly decreases 10dB beamwidths and increases the gain of the antenna. However, the dependency of the gain of the antenna on frequency is same as the examples discussed so far.

Arrays of TSAs can be used to obtain higher directivity and some demonstrative TSA antenna array examples can be found in [14]-[16].

Since the tapered slot antennas are extensions of a slot line, one should generally design a transition between a slot line and some other type of transmission line that feeds the antenna. These transitions can be classified into two groups as stated in [3]:

Electromagnetically coupled transitions:

The coupling is through EM fields rather than direct electrical contact as shown in Figure 2. The feed line is printed on one side of the substrate and the slot line is etched on the other side. This type of transitions may use microstrip line, coplanar waveguide (CPW) or stripline as the feed line.

Directly coupled transitions:

Coupling is through a direct current path like a wire or a solder connection. Transitions that use a coaxial line, bond wires or ribbons are directly coupled transitions. Coplanar waveguide type feed line can be directly coupled to the antenna as well. In that case, feed line is printed on the same side of the substrate with the antenna and one of the slots of CPW line is extended to be the slot line of the antenna whereas the other slot in the feed is properly terminated as illustrated in Figure 3.

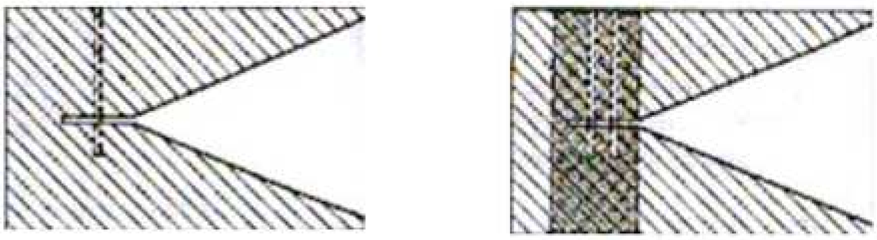

Figure 2 Examples of electromagnetically coupled transitions

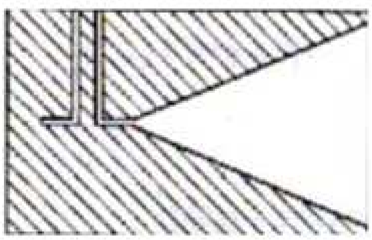

Figure 3 Directly coupled transition for CPW feed line

Many studies have been conducted on the design of transitions from various transmission line types to slot lines. Most popular of the input transmission line types are coplanar waveguide and microstrip line. In [17], different transition topologies between coplanar waveguide to slot line are studied. Wideband microstrip line to slot line transitions can be found in [18], with reference to the simplified circuit models of the transitions. The designs studied are orthogonal microstrip line to slotline transitions where two transmission lines intersect at a right angle on different faces of a dielectric substrate. Different topologies and transition models have been investigated with measurement results.

The second chapter of the thesis starts with the discussions about the proper choice of the dielectric substrate in the design of TSAs followed by the design of microstrip line to slot line transition used in this work. Next, the parametric study results for the LTSA and CWSA are presented in this chapter.

The third chapter includes the radiation characteristic and bandwidth comparisons between LTSAs and CWSAs having same physical dimensions. The reconfiguration method proposed for the switching between LTSA and CWSA configurations is also presented in this chapter.

In the fourth chapter, the radiation patterns obtained through measurement of LTSA and CWSA configurations will be evaluated. First, the measurement data will be compared to simulation data, then differences between the radiation patterns of LTSA and CWSA will be discussed and finally the variations in the radiation patterns with respect to frequency will be investigated.

The “Conclusion” chapter will sum up the general results deduced from this study.

CHAPTER 2

PARAMETRIC STUDY ON THE RADIATION CHARACTERISTICS OF TSA

In this section, how antenna substrate choice is made will be explained first. The design of microstrip line to slot line transition that will be used to feed the TSAs will be given next. The LTSA and CWSA design and the parametric study results for the LTSA and CWSA will be interpreted. This section will end with a bandwidth comparison of CWSA with linear and exponential taper profiles.

2.1.Substrate Choice

Tapered slot antennas are well-behaved travelling-wave antennas as long as a condition about the parameters of the substrate is satisfied. In order to state this condition, first the effective thickness of the dielectric substrate (t_{eff}) need to be defined as follows [19].

$$\frac{t_{eff}}{\lambda_0} = \left(\sqrt{\varepsilon_r} - 1\right)\frac{t}{\lambda_0} \tag{1}$$

where λ_0 is the free space wavelength at the center frequency, t is the thickness and ε_r is the dielectric constant of the substrate. The necessary condition for a TSA to possess travelling wave antenna characteristics is [19]:

$$0.005 \le \frac{t_{eff}}{\lambda_0} \le 0.03 \tag{2}$$

As stated in [13] and [16], for a t_{eff}/λ_0 value below 0.005, the antenna will have decreased directivity whereas for values larger than 0.03, unwanted substrate modes will develop that will deviate the antenna from travelling wave antenna characteristics and introduce grating lobes to the radiation pattern.

The dielectric materials that are available at METU are listed in Table 1 together with their parameters and effective thickness values at 35 GHz. Among the substrates considered, two dielectric materials, shown shaded in Table 1, with three different thickness values satisfy the condition given in Equation (2). 0.51mm thick RO5880 Duroid substrate is chosen to be used in this thesis study.

Table 1 Parameters of available dielectric materials

Material	ε_r	tan δ	t(mm)	t_{eff}/λ_0
TMM 10	9.2	0.0017	0.81	0.192
RO4003	3.38	0.0027	0.51	0.049
			0.81	0.079
			1.52	0.148
RO5880	2.2	0.0009	0.127	0.007
			0.51	0.028
			0.78	0.044
			1.57	0.088
R06006	6.15	-	1.27	0.219
RO6010	10.2	-	0.635	0.162
FR3	4	-	1.52	0.177
FR4	4.4	0.022	1.52	0.195
Cuflon	2.1	0.00045	0.127	0.006
			0.78	0.041

2.2.Design of microstrip line to slot line transition

The bandwidth goal for the LTSA and CWSAs to be designed is decided to be between 30-40 GHz centered at 35 GHz so a wideband transition between microstrip line and slot line is needed. Due to the simplicity in design and manufacturing, microstrip line is chosen as the feed line. The microstrip line to slot line transition proposed in [18] is considered. The geometry of the transition is shown in Figure 4. The transition is employing a microstrip line and a slot line crossing each other at a right angle. The microstrip extends about one quarter of a guided wavelength beyond the slot, and the slot extends about a quarter of a guided wavelength beyond the microstrip.

In order to obtain a transition that has low return loss over a wide frequency band, the impedances of the microstrip line and the slot line should be matched to each other to minimize the reflections. The slot line width shall be chosen not to have too large impedance values in order to be able to achieve impedance matching between microstrip line and slot line. The characteristic impedance of a slot line increases with increasing slot width, so the width of the slot should be chosen as small as possible to obtain an impedance value close to 50Ω. Because of the manufacturing limitations, a minimum slot width of 0.254 mm (10 mils) is chosen. To calculate the characteristic impedance and guided wavelength of the slot line, empirical formulas proposed in [20] and presented in Appendix A are used.

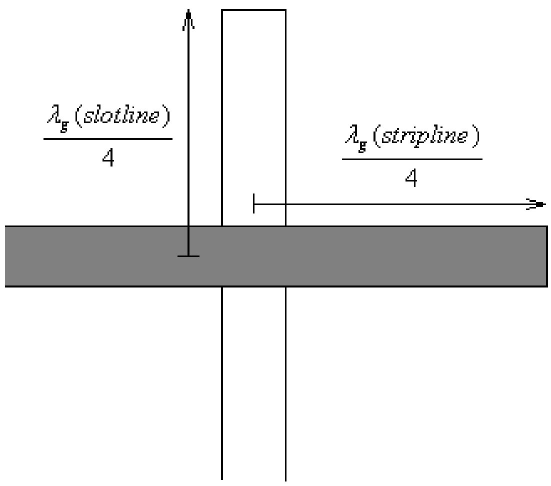

Figure 4 Orthogonal microstrip line to slot line transition

The characteristic impedance and the guided wavelength (at 35 GHz) of 0.254 mm wide slot line are calculated as 152.76Ω and 7.24 mm, respectively. A wideband impedance transformer needs to be designed in order to match the 50Ω microstrip line to 152Ω slot line. So, a Chebyshev impedance transformer circuit, studied in [21] and [22], is designed with three sections (N=3). As shown in Figure 5, the impedance transformer circuit consists of three microstrip segments of quarter guided wavelength long between the input microstrip line and the load. The input impedance (Z_0) of the Chebyshev Transformer will be the characteristic impedance of the microstrip line and the load impedance will be the characteristic impedance of the slot line.

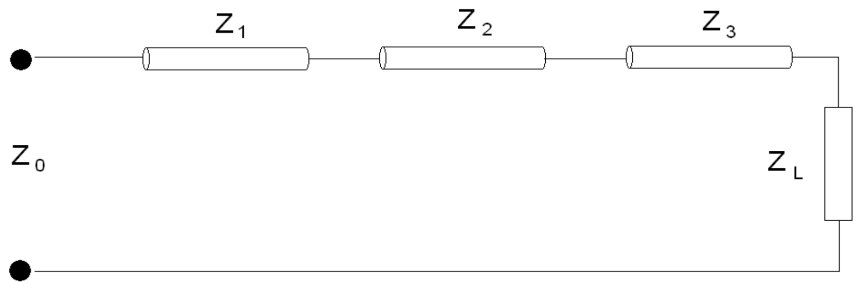

Figure 5 Chebyshev impedance transformer circuit

The characteristic impedance values of the three quarter wavelength long segments are calculated by using the equations given in Appendix B and listed as:

- $Z_1 = 61.01\ \Omega$
- $Z_2 = 87.39\ \Omega$
- $Z_3 = 125.19\ \Omega$

The line widths and effective dielectric constant (ε_{eff}) values corresponding to these impedances are determined by using the equations given in Appendix A. Guided wavelengths of microstrip segments are determined by Equation (3).

$$\lambda_g = \frac{\lambda_0}{\sqrt{\varepsilon_{eff}}} \qquad (3)$$

The width and length values of each microstrip line segment are listed in Table 2.

Table 2 Calculated width and length values of microstrip line segments

	Strip Width	Quarter Guided Wavelength
Z_0=50 Ω	1.58 mm	1.56 mm
Z_1=61.01 Ω	1.16 mm	1.58 mm
Z_2=87.39 Ω	0.6 mm	1.61 mm
Z_4=125.19 Ω	0.26 mm	1.63 mm

In order to improve the accuracy of width and length values calculated from empirical formulas, simulations on HFSS are performed. Microstrip lines are modeled as two port networks with two wave ports at both ends. The characteristic impedance of the line is calculated from s_{11} results and the guided wavelength of the line is found from the phase of s_{12} parameter. A couple of simulations are performed to fine tune the width and length of the microstrip line such that the desired impedance and guided wavelength values are achieved. With the help of the simulation results, for 50Ω, 61.01 Ω, 87.39 Ω and 125.19 Ω transmission lines, the width and the quarter guided wavelength values are determined as given in Table 3.

Table 3 Microstrip Line Parameters

	Values Calculated		**Values obtained from HFSS**	
	strip width	$\lambda_g/4$	strip width	$\lambda_g/4$
Z_0=50 Ω	1.58 mm	1.56 mm	1.58 mm	1.54 mm
Z_1=61.01 Ω	1.16 mm	1.58 mm	1.08 mm	1.56 mm
Z_2=87.39 Ω	0.6 mm	1.61 mm	0.54 mm	1.60 mm
Z_4=125.19 Ω	0.26 mm	1.63 mm	0.2 mm	1.63 mm

To investigate the performance of the designed microstrip line to slot line transition, two structures are connected back to back as show in Figure 6. The simulation results for the return loss and insertion loss of this structure from 20 to 50GHz are presented in Figure 8 and the dimensions of the final structure are given in Figure 7. It can be seen from the simulation results of the designed transition that, it exhibits return loss lower than -10dB and a good level of insertion loss (lower than 3 dB) over the frequency band of 27-40 GHz.

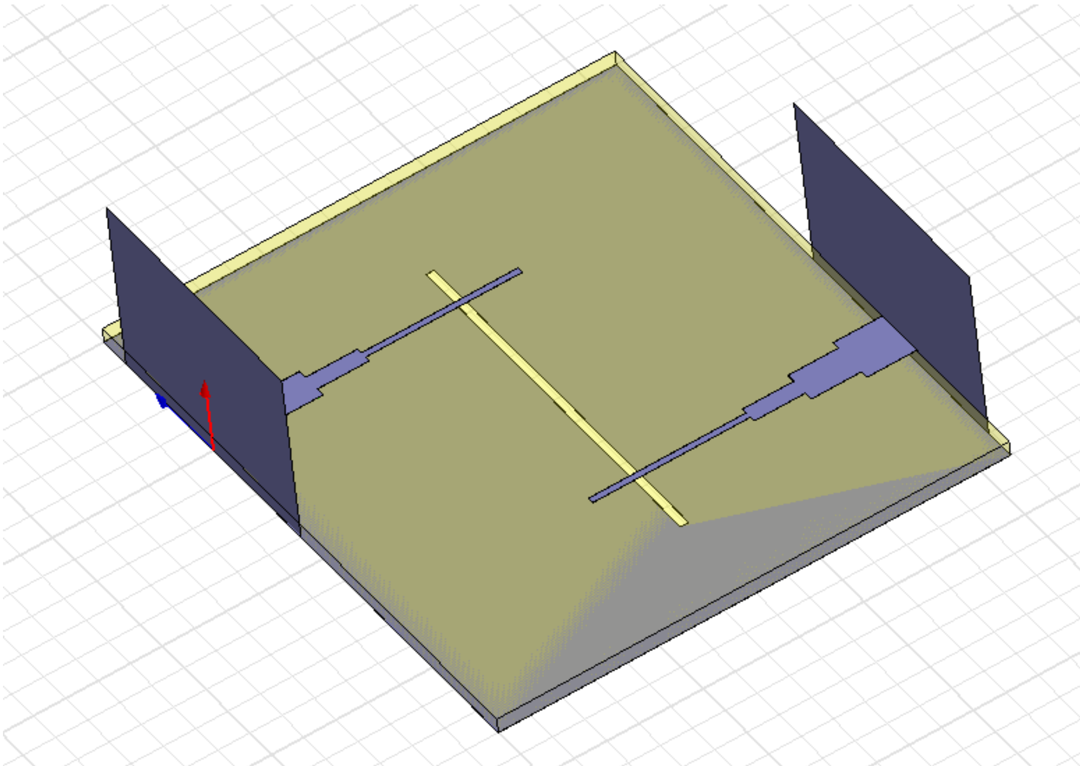

Figure 6 Back to back connected microstrip line to slot line transitions

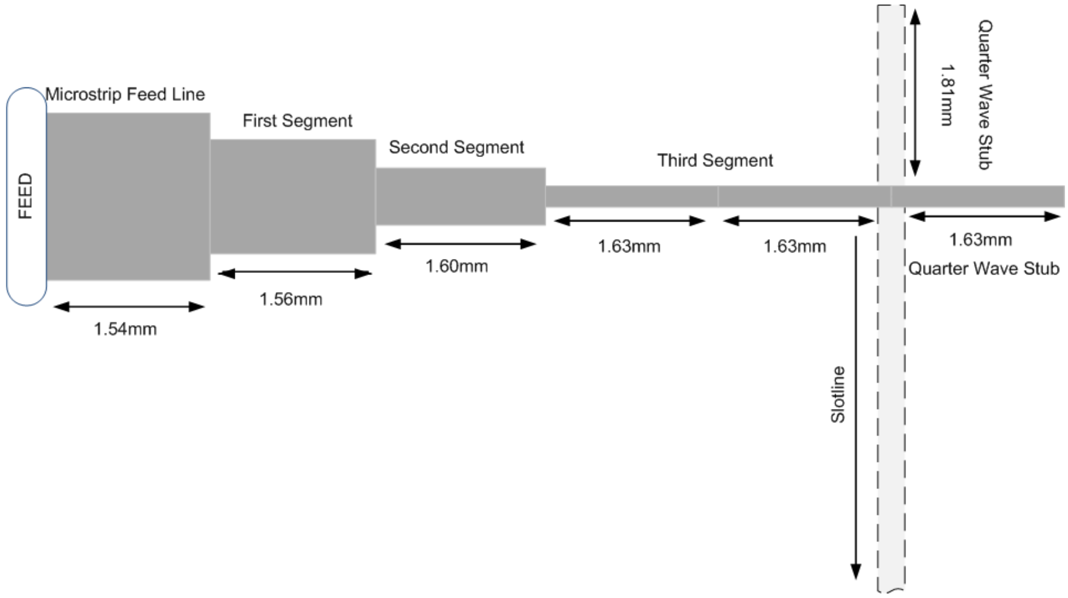

Figure 7 Final dimensions of the microstrip line to slot line transition

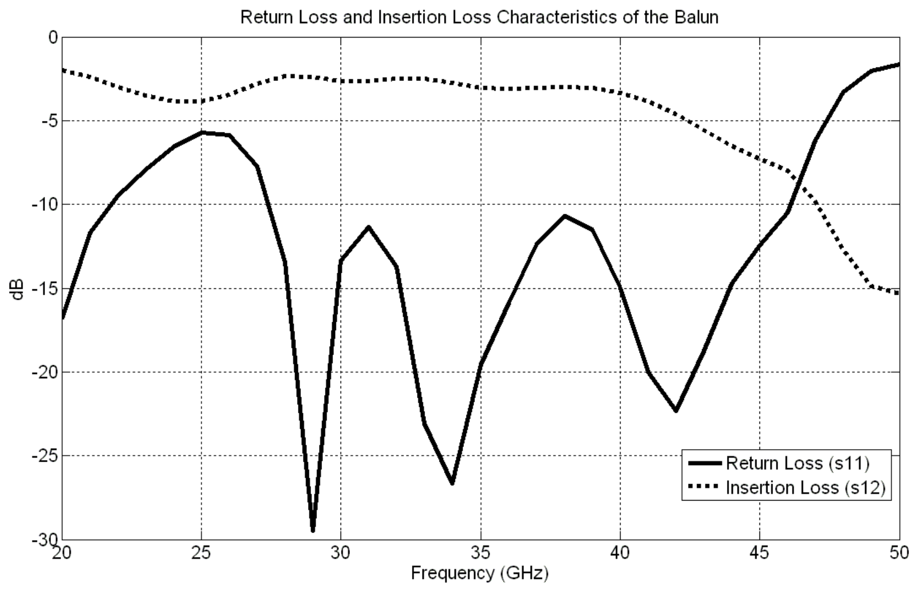

Figure 8 Simulation results of the microstrip line to slot line transition

2.3.Parametric Study of LTSA

A linearly tapered slot antenna (LTSA) consists of a slot line that gets wider linearly through the antenna length. As shown in Figure 9, there are basically three main parameters that determine the radiation characteristics of a LTSA. These are:

- Antenna length (L)
- Aperture width (W)
- Ground extension (H)

In order to determine the behavior of the radiation pattern with the changes in these three parameters, a parametric study has been carried out, where one of these parameters are changed and the other two are kept constant.

It is stated in [10] that for an LTSA to have endfire beam with no split in the beam, the antenna length should be longer than three wavelengths at the center frequency. Hence, for the antenna length four different values ($3\lambda_0$, $4\lambda_0$, $5\lambda_0$, $6\lambda_0$) are considered during the parametric study. According to [7], for an LTSA to radiate efficiently, the aperture width of the antenna should be larger than half wavelength at the center frequency. Two aperture width values are chosen as $\lambda_0/2$ and λ_0 for this purpose. Finally, three different values (λ_0, $3\lambda_0/2$, $2\lambda_0$) for the ground extension parameter are studied. In summary, LTSA configurations having totally 24 (4x2x3) different parameters are modeled and simulated at 35 GHz to observe the variations in the radiation characteristics of the antenna. Directivity, E-plane and H-plane half-power beamwidths and E-plane and H-plane first sidelobe levels are compared and the effects of antenna length, aperture width and ground extension on these antenna performance measures are observed. These parametric study results are also compared with the parametric study data of an air substrate LTSA presented in [10].

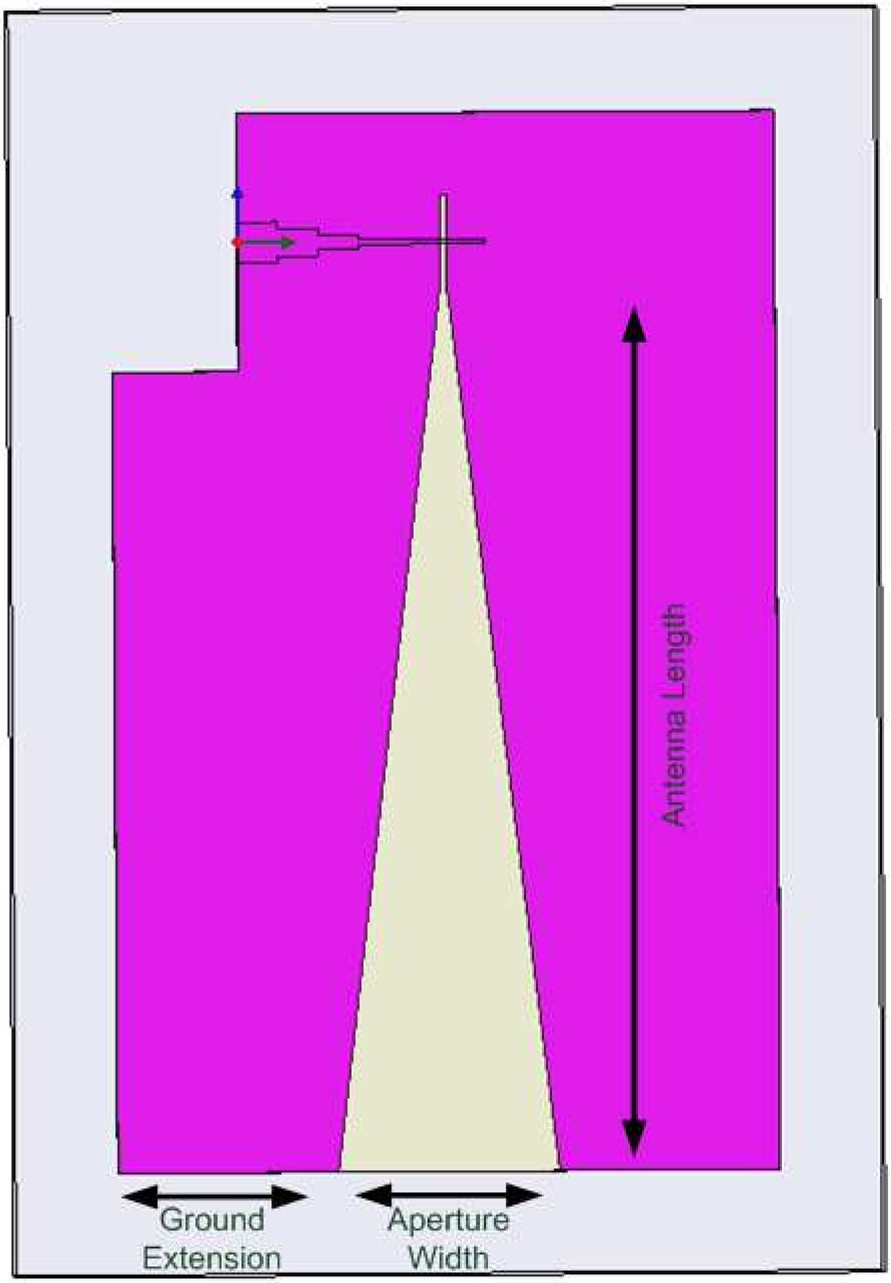

Figure 9 The geometry of LTSA

The simulation results are summarized in Table 4 in which the varying parameters of the antenna are given in terms of λ_0=8.57mm at 35GHz. The rows that are shown shaded in Table 4 correspond to configurations that deviate from the endfire antenna characteristics because of having tilted or split beams. When the aperture width is small and the antenna is long, the amount of tapering along the antenna becomes insufficient and the travelling wave can not properly detach from the antenna to cause an endfire radiation. The flare angle, which is the angle between two arms of the LTSA is below 6^0 for these three configurations. The results in Table 4 are presented such that the effects of variations in the antenna length could be easily observed. When the antenna length is increased, the antenna is expected to be more directive. It is observed that the H-plane half power beamwidth decreases with increasing antenna length. This result stems from the fact that as the antenna length is increased with aperture width is kept constant, the flare angle decreases and the e-field distribution along the aperture approaches a uniform field distribution. The E-plane beamwidth also generally decreases with increasing antenna length, with some exceptions as in W=0.5 λ_0 and H=1 λ_0 case. Therefore these observations are consistent with initial expectations. When the effects on the sidelobe levels are studied, it is observed that H-plane sidelobe level slightly increase with increasing antenna length. The flare angle again is the reason of this increase in sidelobe level. As the flare angle decreases, the E-field along the aperture gets more uniform resulting in a higher sidelobe level. On the other hand, when the E-plane sidelobe levels are investigated it is observed that the sidelobe level in this plane depends also on the width of the aperture. For the case of W=0.5 $\lambda_{0,}$ the E-plane sidelobe levels increase as the antenna length increases while for W=1 λ_0, the E-plane sidelobe level decreases with increasing length. Since the E-plane is parallel along the width of the aperture, a dependence on the width is expected for this plane. For narrow apertures, the flare angle will be the dominant parameter that affects the amount of tapering along the aperture. However for wider apertures, the increase in the amount of tapering due to the increase in the antenna length becomes more effective then the decrease in the amount of tapering due to decreasing flare angle.

Table 4 Parametric study results for the LTSA

W	H	L	Directivity (dB)	E-plane HPBW (degrees)	H-plane HPBW (degrees)	E-plane SLL (dB)	H-plane SLL (dB)
0.5	1	3	10,24	26	34	-4,19	-8,92
		4	10,03	37	27	-7,53	-8,54
		5	8,96	48	22	-5,38	-5,74
		6	8,13	44	21	-3,85	-1,35
	1.5	3	9,5	40	32	-7,41	-7,62
		4	10,2	30	27	-7,02	-7,82
		5	9,72	34	24	-6,92	-7,57
		6	8,06	45	21	-5,82	-5,52
	2	3	8,91	45	32	-6,85	-7,04
		4	10	33	28	-8	-6,02
		5	10,28	23	26	-4,74	-5,15
		6	9,13	25	23	-4,25	-3,59
1	1	3	11,72	26	34	-15,05	-9,16
		4	12,51	24	30	-12,15	-9,64
		5	12,83	23	26	-12,73	-9,82
		6	12,14	23	26	-12,56	-8,97
	1.5	3	10,94	38	33	-12,96	-8,13
		4	12,05	28	29	-13,04	-7,84
		5	12,65	24	26	-16,94	-7,63
		6	12,55	22	23	-15,77	-7,66
	2	3	10,94	40	34	-13,49	-8,95
		4	11,49	34	27	-14,49	-8,5
		5	12,31	29	26	-15,27	-7,02
		6	12,69	21	25	-16,55	-6,29

To demonstrate the changes in the radiation pattern of the antenna with respect to variations in the antenna length, E-plane and H-plane patterns for three different L values are plotted respectively in Figure 10 and Figure 11 for $W=\lambda_0$, $H=1.5\lambda_0$.

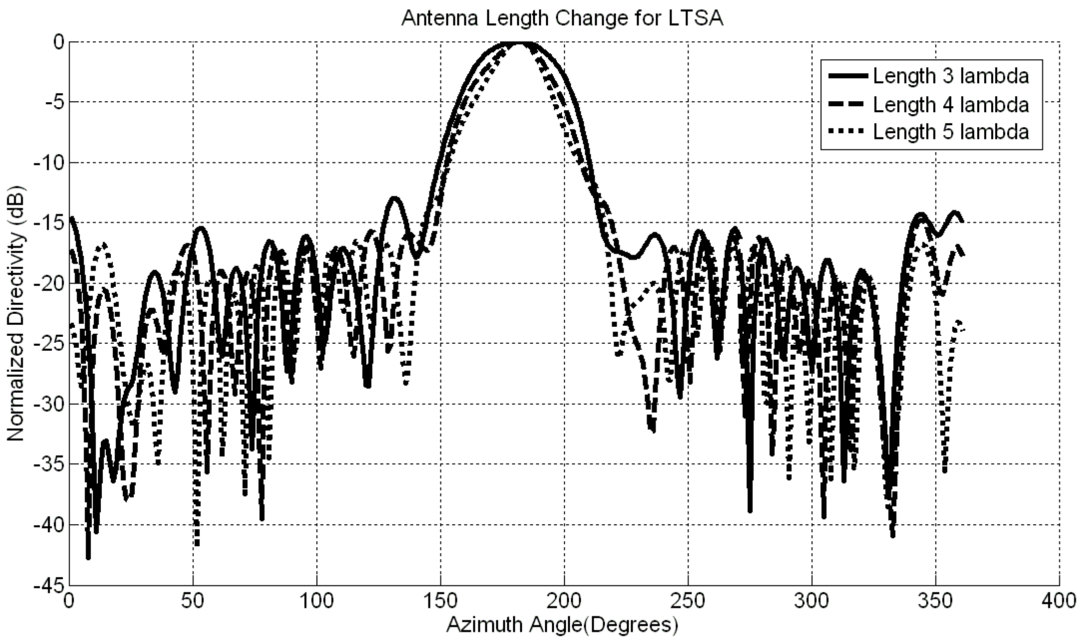

Figure 10 Effect of antenna length variations on E-Plane pattern for LTSA

Figure 11 Effect of antenna length variations on H-Plane pattern for LTSA

In order to easily observe the effects of the aperture width parameter on E-plane and H-plane radiation patterns, Table 4 is rearranged as Table 5.

Table 5 Effects of the aperture width parameter variations for LTSA

L	H	W	Directivity (dB)	E-plane HPBW (degrees)	H-plane HPBW (degrees)	E-plane SLL (dB)	H-plane SLL (dB)
3	1	0.5	10,24	26	34	-4,19	-8,92
		1	11,72	26	34	-15,05	-9,16
	1.5	0.5	9,5	40	32	-7,41	-7,62
		1	10,94	38	33	-12,96	-8,13
	2	0.5	8,91	45	32	-6,85	-7,04
		1	10,94	40	34	-13,49	-8,95
4	1	0.5	10,03	37	27	-7,53	-8,54
		1	12,51	24	30	-12,15	-9,64
	1.5	0.5	10,2	30	27	-7,02	-7,82
		1	12,05	28	29	-13,04	-7,84
	2	0.5	10	33	28	-8	-6,02
		1	11,49	34	27	-14,49	-8,5
5	1	0.5	8,96	48	22	-5,38	-5,74
		1	12,83	23	26	-12,73	-9,82
	1.5	0.5	9,72	34	24	-6,92	-7,57
		1	12,65	24	26	-16,94	-7,63
	2	0.5	10,28	23	26	-4,74	-5,15
		1	12,31	29	26	-15,27	-7,02
6	1	0.5	8,13	44	21	-3,85	-1,35
		1	12,14	23	26	-12,56	-8,97
	1.5	0.5	8,06	45	21	-5,82	-5,52
		1	12,55	22	23	-15,77	-7,66
	2	0.5	9,13	25	23	-4,25	-3,59
		1	12,69	21	25	-16,55	-6,29

Increasing the aperture width of the antenna from $0.5\lambda_0$ to λ_0 decreases the E-plane beamwidth while increasing the H-plane beamwidth slightly. The E-plane sidelobe level is decreased significantly with an increase in aperture width. H-plane sidelobe level also decreases as aperture width increases although the decrease is not as significant as the decrease in the E-plane sidelobe level. As mentioned earlier, the variations on the aperture width is expected to cause significant changes in E-plane radiation pattern. A wider aperture results in a narrower beamwidth with lower sidelobe levels for the E-plane pattern. The effects of aperture width variations on the H-plane radiation pattern are again through the changes in the flare angle and the change in the E-field distribution that deviates from uniform field distribution. For a fixed antenna length, the flare angle increases with increasing aperture width. Therefore the amount of tapering increases with the aperture width that result in a wider beamwidth with lower sidelobe levels in the H-plane. According to [10], an increase in aperture width of the air LTSA decreases the E-plane beamwidth and E-plane sidelobe level for longer antennas as also seen here. For short antennas, with increasing aperture width, E-plane beamwidth remains the same and E-plane sidelobe level decreases which is also the case here for an antenna length of $3\lambda_0$. The H-plane beamwidth and H-plane sidelobe level are almost constant in [10] which is also not contradictory with the data here since the changes in H-plane beamwidth and sidelobe level are not significant.

The effects of aperture width variations on the E-plane and H-plane radiation patterns for $L=5\lambda_0$ and $H=1.5\lambda_0$ are given in Figure 12 and Figure 13, respectively.

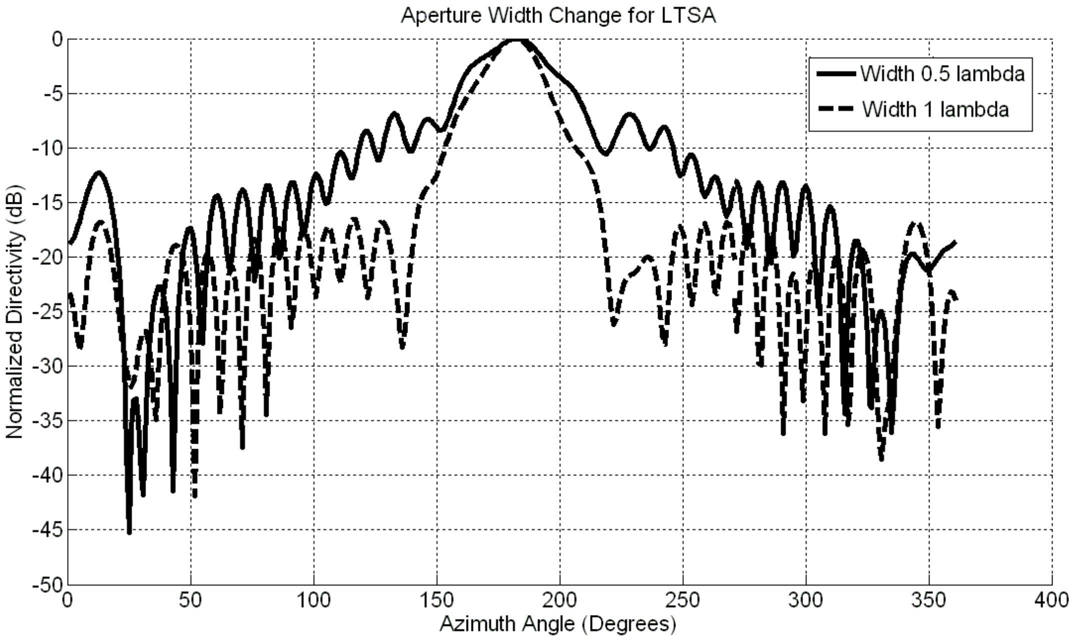

Figure 12 Effect of aperture width variations on E-Plane pattern for LTSA

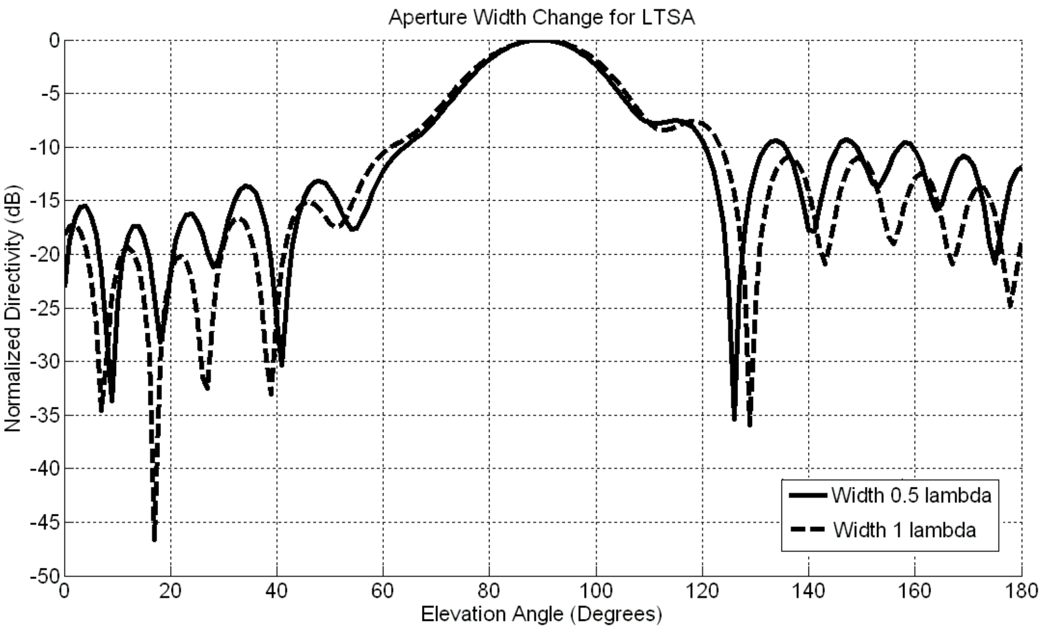

Figure 13 Effect of aperture width variations on H-Plane pattern for LTSA

Table 6 is utilized to analyze the radiation characteristics of the antenna with respect to ground extension (H) parameter. A consistent and regular impact of the ground extension parameter on the radiation pattern of the antenna could not be observed as reported in [10]. However, it should be noted that the ground extension parameter needs to be properly chosen to meet the required specifications of an antenna to be designed.

Table 6 Effects of the ground extension parameter variations for LTSA

L	W	H	Directivity (dB)	E-plane HPBW (degrees)	H-plane HPBW (degrees)	E-plane SLL (dB)	H-plane SLL (dB)
3	0,5	1	10,24	26	34	-4,19	-8,92
		1,5	9,5	40	32	-7,41	-7,62
		2	8,91	45	32	-6,85	-7,04
	1	1	11,72	26	34	-15,05	-9,16
		1,5	10,94	38	33	-12,96	-8,13
		2	10,94	40	34	-13,49	-8,95
4	0,5	1	10,03	37	27	-7,53	-8,54
		1,5	10,2	30	27	-7,02	-7,82
		2	10	33	28	-8	-6,02
	1	1	12,51	24	30	-12,15	-9,64
		1,5	12,05	28	29	-13,04	-7,84
		2	11,49	34	27	-14,49	-8,5
5	0,5	1	8,96	48	22	-5,38	-5,74
		1,5	9,72	34	24	-6,92	-7,57
		2	10,28	23	26	-4,74	-5,15
	1	1	12,83	23	26	-12,73	-9,82
		1,5	12,65	24	26	-16,94	-7,63
		2	12,31	29	26	-15,27	-7,02
6	0,5	1	8,13	44	21	-3,85	-1,35
		1,5	8,06	45	21	-5,82	-5,52
		2	9,13	25	23	-4,25	-3,59
	1	1	12,14	23	26	-12,56	-8,97
		1,5	12,55	22	23	-15,77	-7,66
		2	12,69	21	25	-16,55	-6,29

For three different values of the ground extension parameter, the E-plane and H-plane radiation patterns for an antenna with W=0.5 λ_0 and L=4 λ_0 are presented in Figure 14 and Figure 15, respectively.

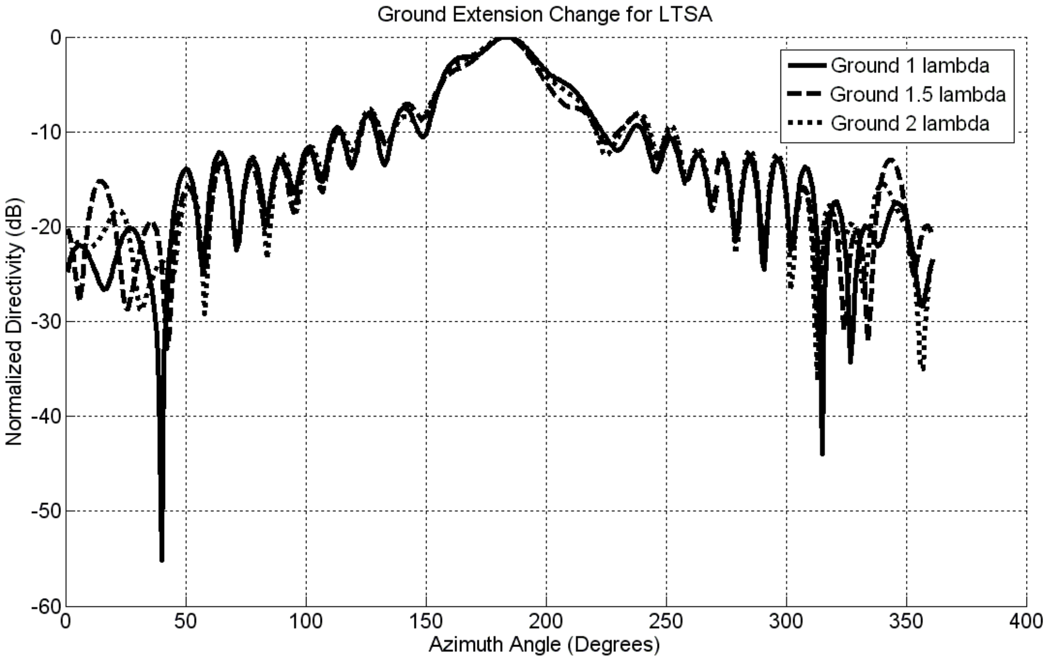

Figure 14 Effect of ground extension variations on E-Plane pattern for LTSA

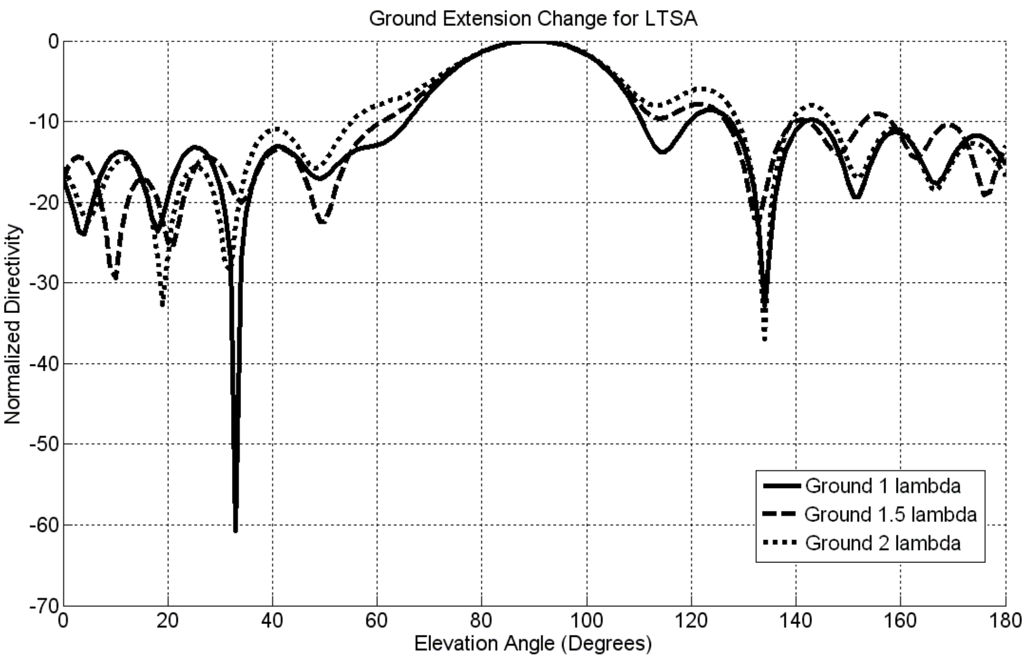

Figure 15 Effect of ground extension variations on H-Plane pattern for LTSA

2.4.Parametric Study of CWSA

The CWSA is a kind of tapered slot antenna for which the width of the radiating slot is constant over the antenna length. Since the slot line that feeds the antenna is generally narrow, there should be a tapering section between the feeding slot and the radiating slot in order to achieve better impedance matching. If such a transition is not used, there could be a high return loss due to the abrupt change in the characteristic impedance values. Two kinds of taper profiles for the CWSA are studied here, which are linear tapering and exponential tapering as shown in Figure 16. Although a wider bandwidth with the exponential taper profile is expected, the linear tapering alternative is also considered due to its simplicity in modeling and manufacturing.

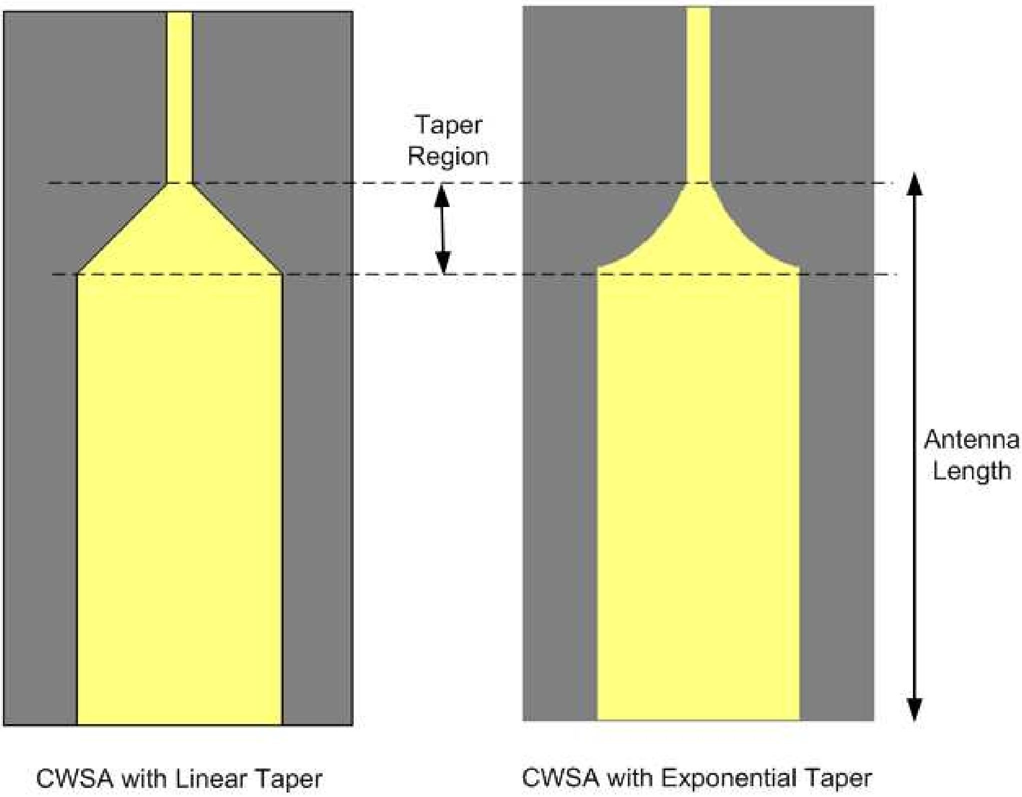

Figure 16 Tapering alternatives for CWSA

During the simulations, it was observed that the taper profile only affects the input return loss characteristics of the antenna and it does not exhibit any impact on the radiation pattern of the antenna, as expected. Consequently, the parametric study about the radiation characteristics of the antenna was performed only for CWSA with exponential tapering and the layout of the antenna is shown in Figure 17, together with the parameters considered during the parametric analysis. The taper length was chosen to be λ_0 and the taper profile was determined according to the following formula.

$$y = a.e^{bx}$$

where a and b are constants deduced from the start and end points of the parabola and x, y are coordinate axes.

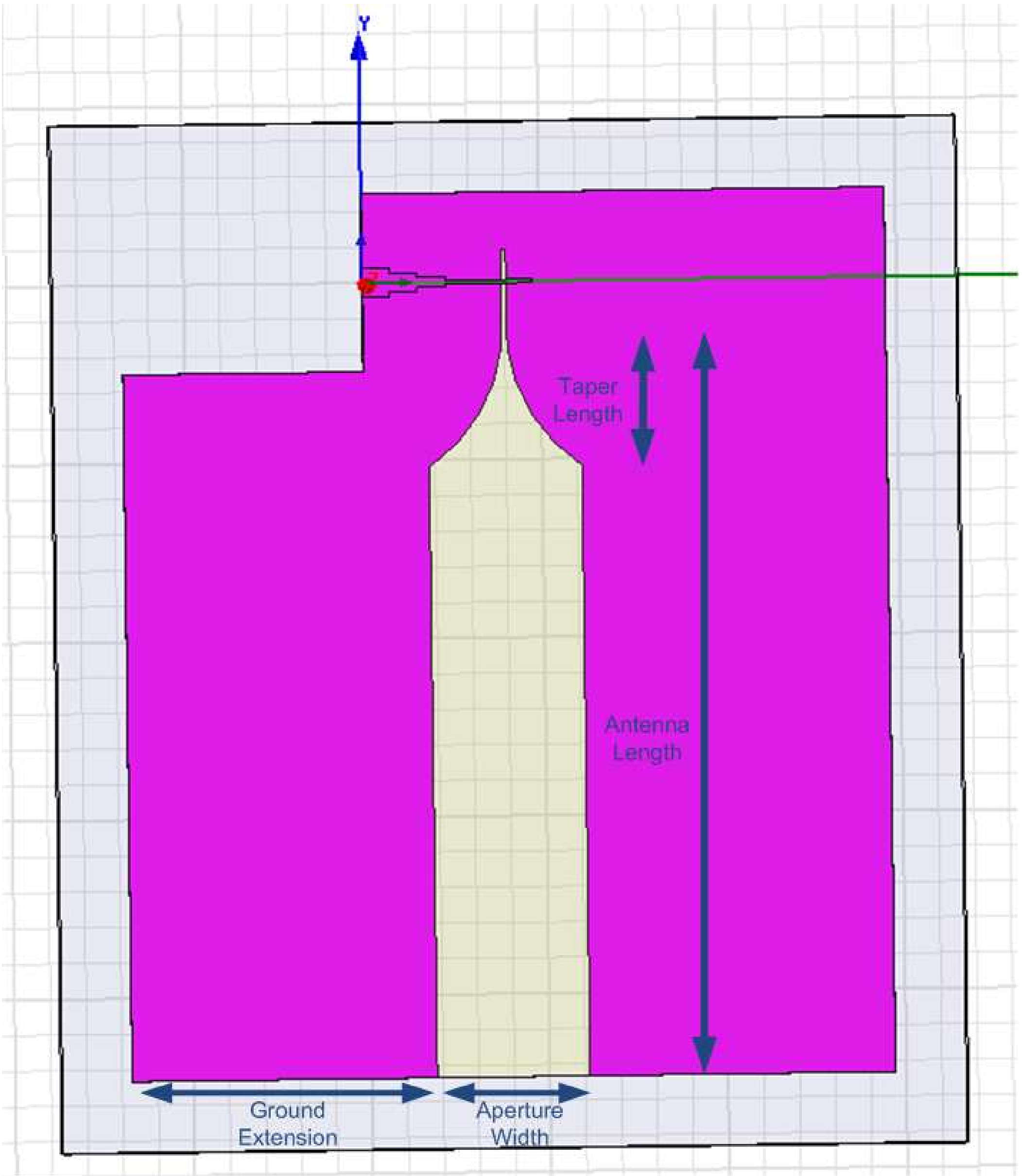

Figure 17 CWSA with Exponential Taper Geometry in HFSS

A parametric study was carried out for the CWSA by changing one of the antenna parameters while keeping the others constant. The parametric study results for CWSA with exponential taper are given in Table 7.

The row that is shaded in gray in Table 7 indicates that the antenna configuration with those parameters has a split beam characteristic so it was not taken into account in determining the effects of parameter changes.

Table 7 Parametric study results for the CWSA with exponential taper

W	H	L	Directivity (dB)	E-plane HPBW (degrees)	H-plane HPBW (degrees)	E-plane SLL (dB)	H-plane SLL (dB)
0.5	1	3	10,77	23	34	-8,12	-9,9
		4	11,06	22	28	-4,77	-11,23
		5	10,55	21	23	-3,31	-9,66
		6	9,08	48	18	-6,99	-5,21
	1.5	3	9,72	35	32	-8,63	-7,35
		4	10,49	22	26	-8,18	-7,77
		5	10,92	19	23	-8,18	-8,05
		6	10,6	19	20	-5,98	-8,76
	2	3	9,04	41	31	-7,57	-7,55
		4	9,71	32	25	-8,3	-5,73
		5	10,58	21	22	-6,29	-4,32
		6	11	15	21	-5,86	-4,38
1	1	3	9,71	20	32	-8,87	-6,85
		4	10,54	18	29	-8,09	-8
		5	11,14	16	25	-7,68	-9,88
		6	11,16	15	23	-4,78	-12,56
	1.5	3	8,55	32	29	-9,51	-5,62
		4	9,31	23	25	-7,27	-4,71
		5	10,05	17	23	-6,97	-4,72
		6	10,81	14	22	-5,34	-6,91
	2	3	8,66	30	30	-9,32	-7,08
		4	8,54	28	25	-7,82	-6
		5	9,06	26	21	-7,07	-4,05
		6	10,19	18	21	-5,88	-3,26

As the length of the antenna increases, the E-plane beamwidth becomes narrower and E-plane sidelobe level increases. The beamwidths in H-plane plane also decrease as the length of the antenna increases. However, a consistent behavior for sidelobe levels in the H-plane with changing antenna length is not observed.

For an antenna with aperture width of λ_0 and ground extension of $1.5\lambda_0$, the effect of antenna length variations on E-plane and H-plane radiation patterns can be seen in Figure 18 and Figure 19, respectively.

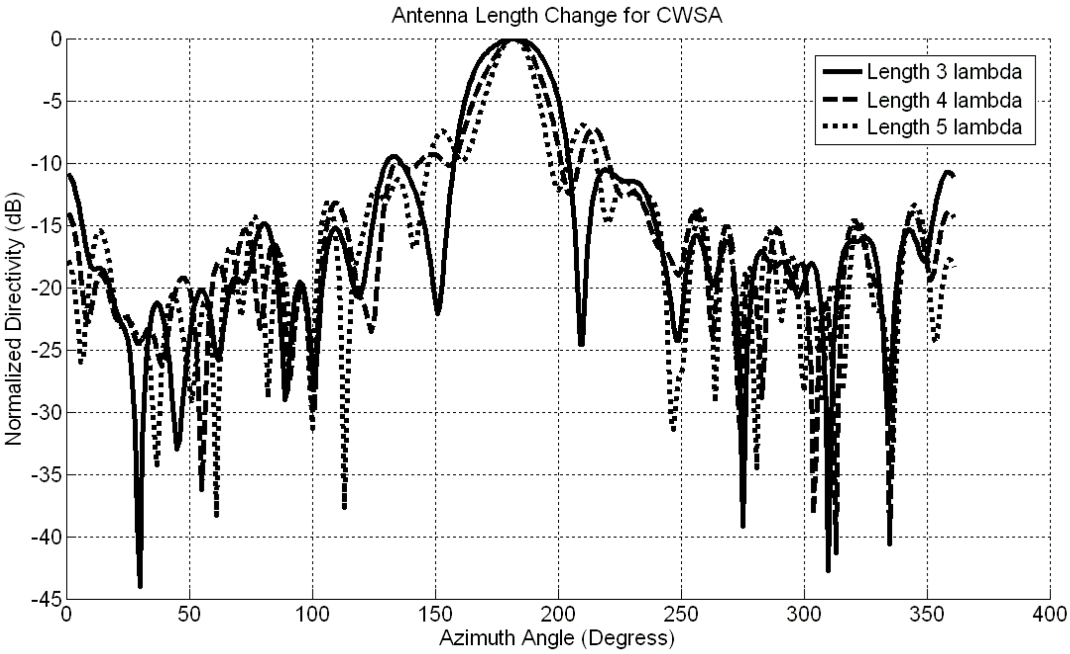

Figure 18 Effect of antenna length variations on E-Plane pattern for CWSA

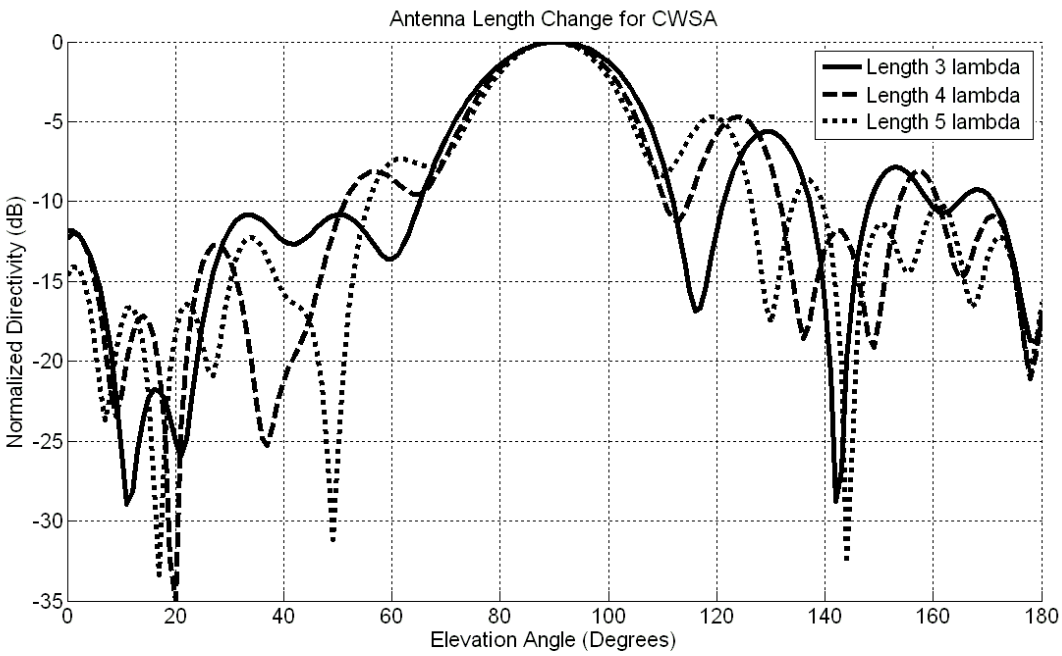

Figure 19 Effect of antenna length variations on H-Plane pattern for CWSA

In order to easily observe the effects of the aperture width parameter on E-plane and H-plane radiation patterns, Table 7 is rearranged as Table 8.

Table 8 Effects of the aperture width change for CWSA

L	H	W	Directivity (dB)	E-plane HPBW (degrees)	H-plane HPBW (degrees)	E-plane SLL (dB)	H-plane SLL (dB)
3	1	0.5	10,77	23	34	-8,12	-9,9
		1	9,71	20	32	-8,87	-6,85
	1.5	0.5	9,72	35	32	-8,63	-7,35
		1	8,55	32	29	-9,51	-5,62
	2	0.5	9,04	41	31	-7,57	-7,55
		1	8,66	30	30	-9,32	-7,08
4	1	0.5	11,06	22	28	-4,77	-11,23
		1	10,54	18	29	-8,09	-8
	1.5	0.5	10,49	22	26	-8,18	-7,77
		1	9,31	23	25	-7,27	-4,71
	2	0.5	9,71	32	25	-8,3	-5,73
		1	8,54	28	25	-7,82	-6
5	1	0.5	10,55	21	23	-3,31	-9,66
		1	11,14	16	25	-7,68	-9,88
	1.5	0.5	10,92	19	23	-8,18	-8,05
		1	10,05	17	23	-6,97	-4,72
	2	0.5	10,58	21	22	-6,29	-4,32
		1	9,06	26	21	-7,07	-4,05
6	1	0.5	9,08	48	18	-6,99	-5,21
		1	11,16	15	23	-4,78	-12,56
	1.5	0.5	10,6	19	20	-5,98	-8,76
		1	10,81	14	22	-5,34	-6,91
	2	0.5	11	15	21	-5,86	-4,38
		1	10,19	18	21	-5,88	-3,26

It is inferred from the parametric study results that an increase in the aperture width decreases the E-plane beamwidth except for long antennas with wide ground extension while it has no significant effect on H-plane beamwidth. The E-plane sidelobe level also decreases with an increase in aperture width for antennas with small length. As the antenna gets longer the E-plane sidelobe level is not much affected by a change in aperture width.

The antenna pattern changes for antenna length of $3\lambda_0$ and ground extension of $2\ \lambda_0$ in E and H-planes due to aperture width change can be seen in Figure 20 and Figure 21, respectively.

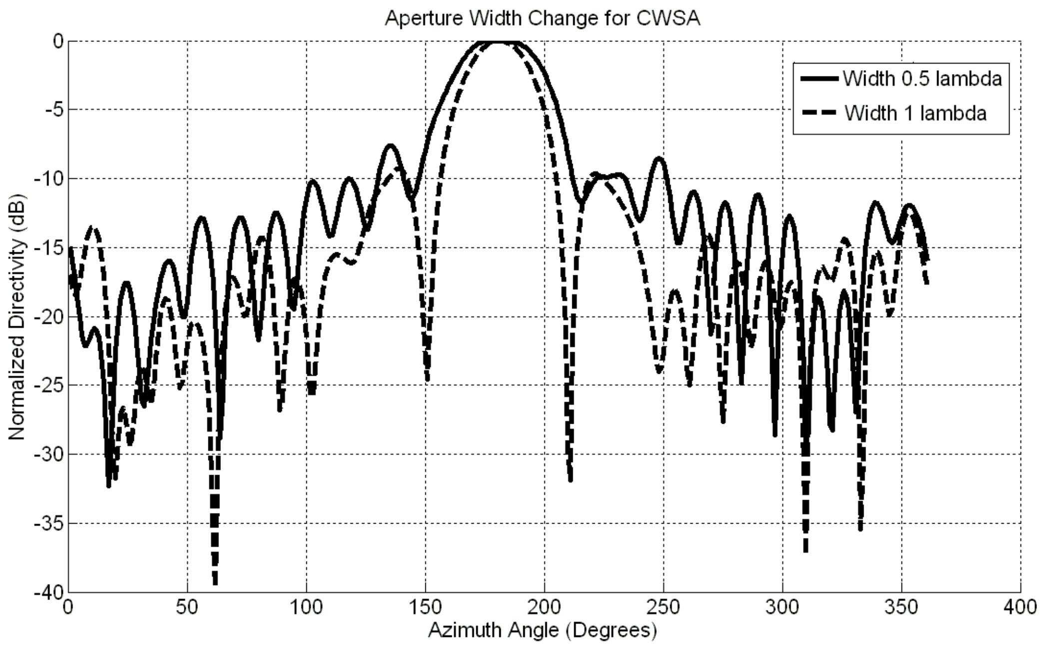

Figure 20 Effect of aperture width variations on E-Plane pattern for CWSA

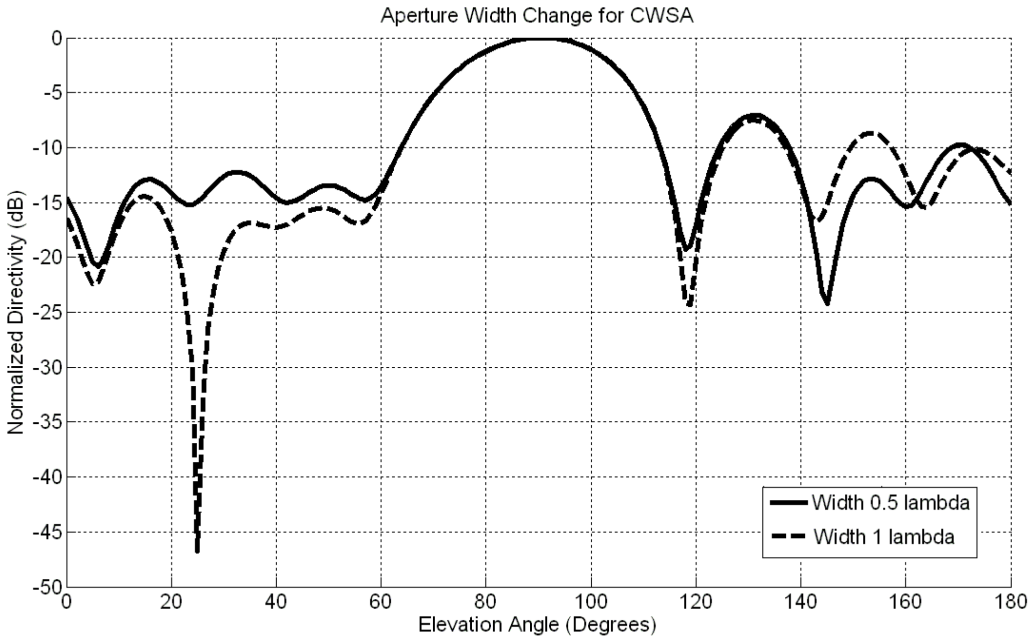

Figure 21 Effect of aperture width variations on H-Plane pattern for CWSA

Table 9 is utilized to interpret the parametric study results in terms of the ground extension parameter (H).

Table 9 Effects of the ground extension parameter for CWSA

L	W	H	Directivity (dB)	E-plane HPBW (degrees)	H-plane HPBW (degrees)	E-plane SLL (dB)	H-plane SLL (dB)
3	0,5	1	10,77	23	34	-8,12	-9,9
		1,5	9,72	35	32	-8,63	-7,35
		2	9,04	41	31	-7,57	-7,55
	1	1	9,71	20	32	-8,87	-6,85
		1,5	8,55	32	29	-9,51	-5,62
		2	8,66	30	30	-9,32	-7,08
4	0,5	1	11,06	22	28	-4,77	-11,23
		1,5	10,49	22	26	-8,18	-7,77
		2	9,71	32	25	-8,3	-5,73
	1	1	10,54	18	29	-8,09	-8
		1,5	9,31	23	25	-7,27	-4,71
		2	8,54	28	25	-7,82	-6
5	0,5	1	10,55	21	23	-3,31	-9,66
		1,5	10,92	19	23	-8,18	-8,05
		2	10,58	21	22	-6,29	-4,32
	1	1	11,14	16	25	-7,68	-9,88
		1,5	10,05	17	23	-6,97	-4,72
		2	9,06	26	21	-7,07	-4,05
6	0,5	1	9,08	48	18	-6,99	-5,21
		1,5	10,6	19	20	-5,98	-8,76
		2	11	15	21	-5,86	-4,38
	1	1	11,16	15	23	-4,78	-12,56
		1,5	10,81	14	22	-5,34	-6,91
		2	10,19	18	21	-5,88	-3,26

The change in the E-plane beamwidth due to ground extension is dependent also on the antenna length. For antenna lengths below 5 λ_0, increasing the ground extension also increases the E-plane beamwidth. However above 5 λ_0, the E-plane beamwidth is not affected considerably by a change in ground extension. H-plane beamwidth is not also affected by ground extension changes. For the sidelobe level behavior, it can be said that the E-plane sidelobe level is not affected and the H-plane sidelobe level is increased with an increase in ground extension parameter.

The effect of the ground extension change on antenna pattern for antenna length of 6 λ_0 and aperture width of λ_0 can be observed in Figure 22 and Figure 23, respectively.

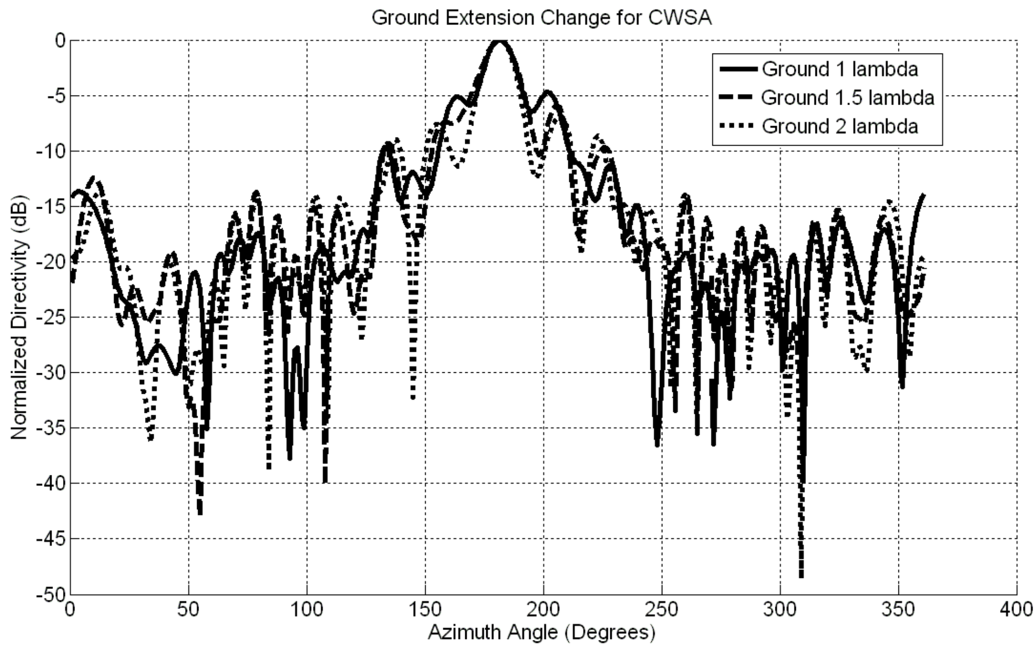

Figure 22 Effect of ground extension variations on E-Plane pattern for CWSA

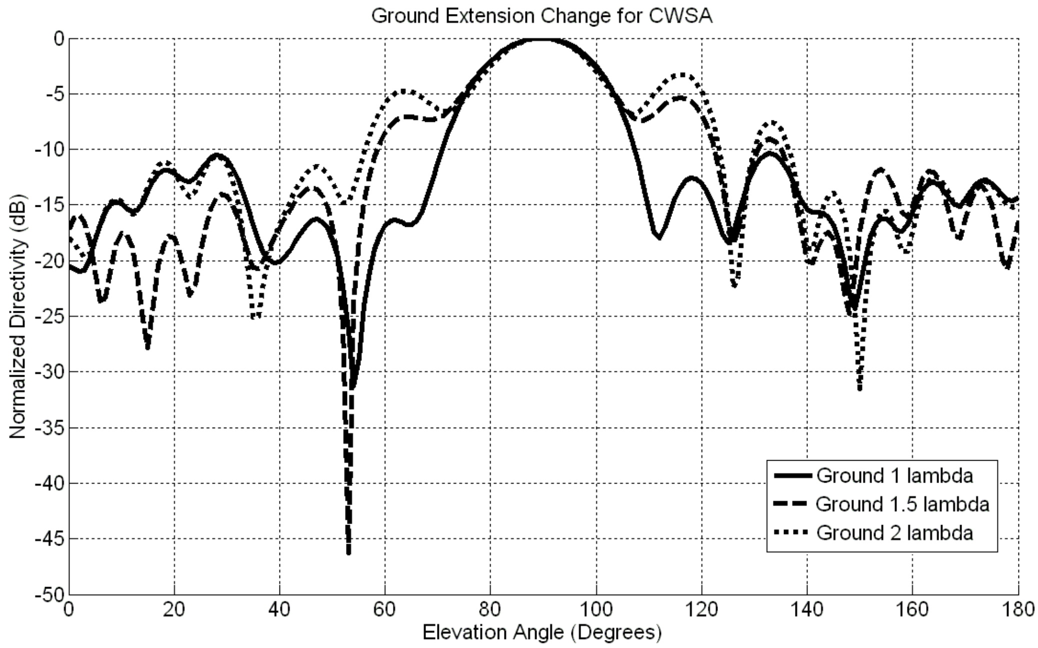

Figure 23 Effect of ground extension variations on H-Plane pattern for CWSA

2.5.Effect of Taper Profile on Bandwidth of CWSA

Since the general behavior of the antenna radiation characteristics with the parameter changes are the same for CWSA with exponential taper and with linear taper, only their bandwidth characteristics were compared. The first simulated configuration is a CWSA having an antenna length of $3\lambda_0$, aperture width of 1 λ_0 and ground extension of 1 $\lambda_{0.}$ The return loss graphs of CWSA with linear taper and CWSA with exponential taper are given in Figure 24. As seen in Figure 24, the return loss value of the CWSA with exponential taper profile is below that of CWSA with linear taper profile in the whole band of 25-45 GHz except a narrow frequency region near 30 GHz. For frequencies near 35 GHz, the usable bandwidth that the return loss value is below -10dB is the same for both types of taper profiles of CWSA. The exponential taper configuration has also a usable bandwidth between below 25GHz to nearly 29 GHz and an acceptable return loss value between 37.5 GHz and 45 GHz.

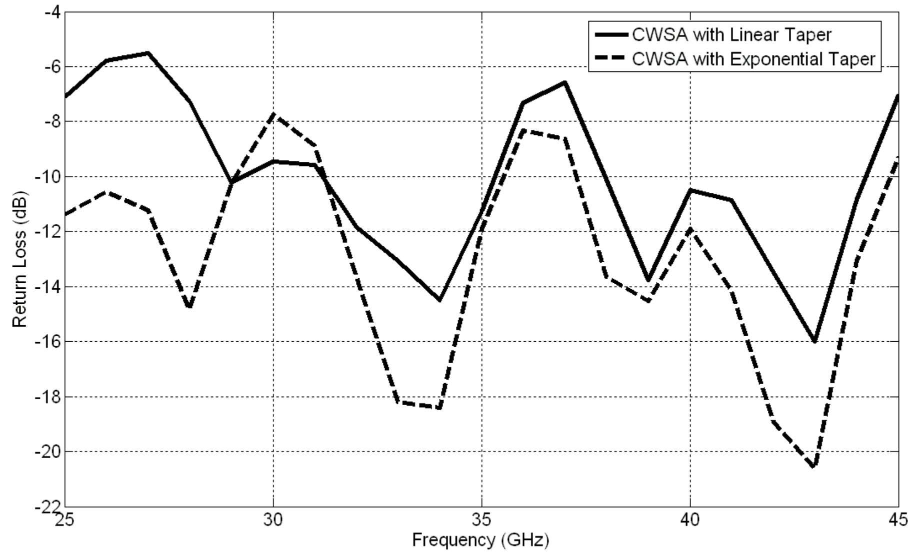

Figure 24 Bandwidth comparison of CWSAs with exponential and linear taper with L=3λ_0, W=1 λ_0, H=1 λ_0

Another antenna with antenna length of 5λ_0, aperture width of 0.5λ_0 and ground extension of λ_0 was considered to investigate an example with narrow aperture. As seen in Figure 25, the return loss behaviors of linearly and exponentially tapered antennas do not differ significantly over the 25-45 GHz band for the antenna with aperture width of 0.5λ_0. This is an expected result since linear and exponential taper profiles start to resemble each other as the width of the antenna becomes smaller.

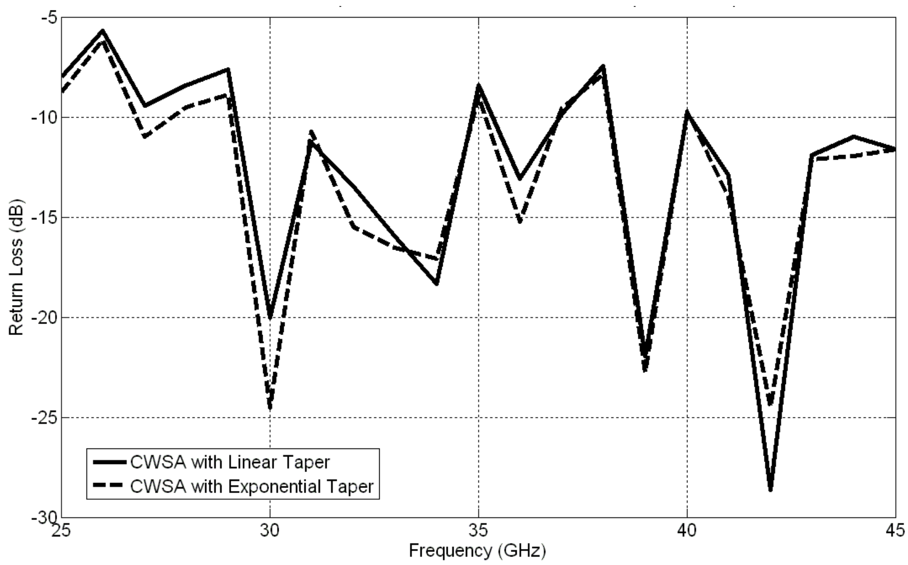

Figure 25 Bandwidth comparison of CWSAs with exponential and linear taper with L=5λ_0, W=0.5 λ_0, H=1 λ_0

To observe the effect of the taper on antenna bandwidth for longer antennas, another simulation was carried out for a CWSA with antenna length of $6\lambda_0$, aperture width of λ_0 and ground extension of $1.5\lambda_0$. As seen in Figure 26, again the exponentially tapered antenna has lower return loss values compared to the linearly tapered antenna. Only the exponentially tapered CWSA can be utilized for lower frequency bands like 25-29 GHz.

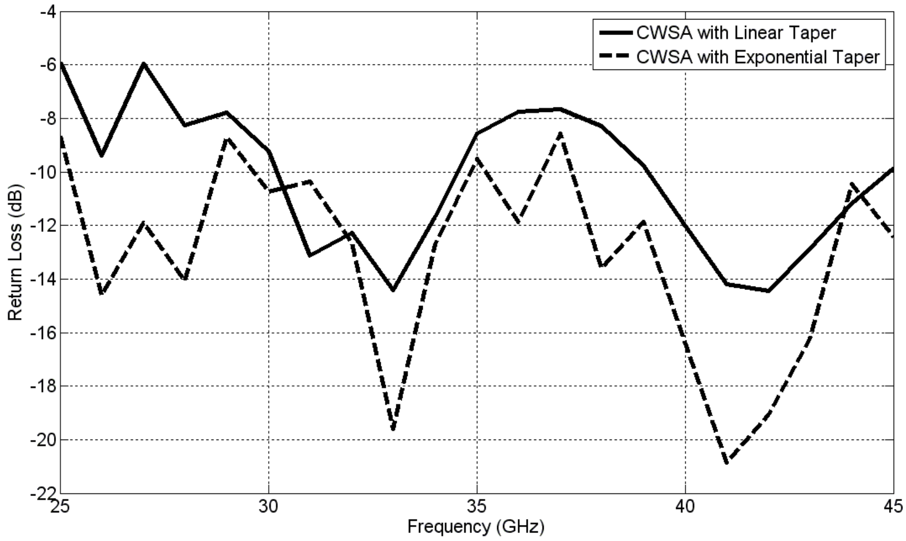

Figure 26 Bandwidth comparison of CWSAs with exponential and linear taper with $L=6\lambda_0$, $W=1\ \lambda_0$, $H=1.5\ \lambda_0$

CHAPTER 3

RECONFIGURABILITY IN THE RADIATION PATTERN OF TAPERED SLOT ANTENNAS

As mentioned in Chapter 1, one of the aims of this study is to provide pattern reconfigurability between an LTSA and a CWSA at 35 GHz. Up to now, the LTSA and CWSA designs and antenna patterns were studied with respect to variations in antenna parameters. These parametric study results were discussed and general conclusions about design of LTSA and CWSA were derived. In this chapter, the radiation patterns of LTSA and CWSAs will be compared to each other.

3.1. LTSA-CWSA Pattern Comparison and Reconfigurability

In the parametric study, LTSA simulation results were compared with other LTSA results, same is also true for CWSA. To obtain pattern reconfigurability between these two types of antennas, the antenna patterns of the two kinds, LTSA and CWSA, shall be compared.

The compared antenna configurations should have same antenna parameters like antenna length, aperture width and ground extension in order to achieve efficient switching between different antenna layouts. Both antennas will be fed by using the same microstrip line to slot line transition. Figure 27 illustrates the possible layout of the reconfigurable antenna.

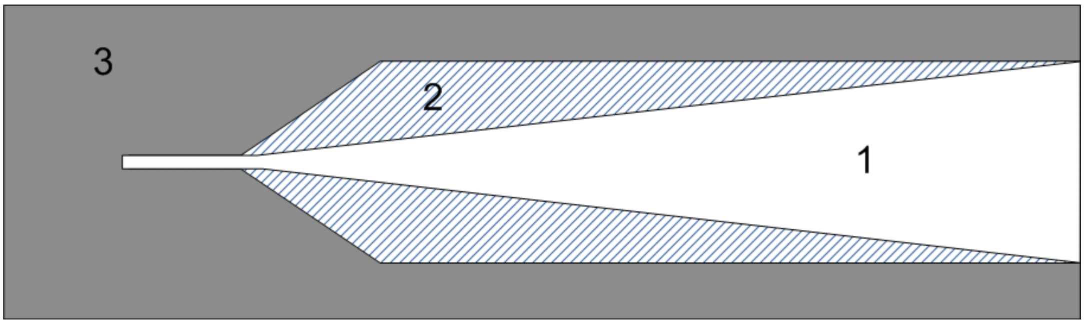

Figure 27 Reconfigurable antenna layout

The region numbered as 1 in Figure 27 contains no metalization so this region is directly the substrate. Region 2 will be formed by a special material that will behave like conductor when excited optically and like an insulator when excitation is not applied, and Region 3 is the metal layer. When Region 2 is not excited, the antenna will have the CWSA configuration. When Region 2 is excited, the antenna will have the LTSA geometry. Hence, excitation of Region 2 provides switching between LTSA and CWSA configurations. The taper region of Region 2 can be designed to be linear or exponential according to the intent of taper profile in CWSA. The CWSA configurations with exponential taper profile are used instead of linear taper since they provide wider frequency bands.

The special material proposed to be used in Region 2 could be a photosensitive dielectric material like photoconductive polymer or photo-induced plasma in silicon. Recently, these types of photosensitive materials started to be used in various reconfigurable antenna and array applications [23]-[26], since the optical excitation of these materials eliminate the use of bias lines required for the actuation of electronic control components utilized in conventional reconfigurable antenna structures.

The parametric study results for LTSA and CWSA with exponential taper can be seen in Table 10. For a transition from LTSA configuration to CWSA configuration, the reductions in the E-plane and H-plane beamwidths and the change in the E-plane and H-plane sidelobe levels are presented in the related columns of Table 10. Using the parametric study results, the LTSA configurations that show largest beamwidth change when compared to CWSA with the same antenna parameters need to be determined.

Table 10 Pattern comparison between LTSA and CWSA

			LTSA				CWSA with Exponential Taper				Reduction in Beamwidth		Increase in SLL	
L	W	H	BW_E	BW_H	SLL_E	SLL_H	BW_E	BW_H	SLL_E	SLL_H	BW_E	BW_H	SLL_E	SLL_H
		1	26	34	-4,19	-8,92	23	34	-8,12	-9,9	3	0	-3,93	-0,98
		1,5	40	32	-7,41	-7,62	35	32	-8,63	-7,35	5	0	-1,22	0,27
	0,5	2	45	32	-6,85	-7,04	41	31	-7,57	-7,55	4	1	-0,72	-0,51
		1	26	34	-15,0	-9,16	20	32	-8,87	-6,85	6	2	6,18	2,31
		1,5	38	33	-12,9	-8,13	32	29	-9,51	-5,62	6	4	3,45	2,51
3	1	2	40	34	-13,4	-8,95	30	30	-9,32	-7,08	10	4	4,17	1,87
		1	37	27	-7,53	-8,54	22	28	-4,77	-11,2	15	-1	2,76	-2,69
		1,5	30	27	-7,02	-7,82	22	26	-8,18	-7,77	8	1	-1,16	0,05
	0,5	2	33	28	-8	-6,02	32	25	-8,3	-5,73	1	3	-0,3	0,29
		1	24	30	-12,1	-9,64	18	29	-8,09	-8	6	1	4,06	1,64
		1,5	28	29	-13,0	-7,84	23	25	-7,27	-4,71	5	4	5,77	3,13
4	1	2	34	27	-14,4	-8,5	28	25	-7,82	-6	6	2	6,67	2,5
		1	48	22	-5,38	-5,74	21	23	-3,31	-9,66	27	-1	2,07	-3,92
		1,5	34	24	-6,92	-7,57	19	23	-8,18	-8,05	15	1	-1,26	-0,48
	0,5	2	23	26	-4,74	-5,15	21	22	-6,29	-4,32	2	4	-1,55	0,83
		1	23	26	-12,7	-9,82	16	25	-7,68	-9,88	7	1	5,05	-0,06
		1,5	24	26	-16,9	-7,63	17	23	-6,97	-4,72	7	3	9,97	2,91
5	1	2	29	26	-15,2	-7,02	26	21	-7,07	-4,05	3	5	8,2	2,97
		1	44	21	-3,85	-1,35	48	18	-6,99	-5,21	-4	3	-3,14	-3,86
		1,5	45	21	-5,82	-5,52	19	20	-5,98	-8,76	26	1	-0,16	-3,24
	0,5	2	25	23	-4,25	-3,59	15	21	-5,86	-4,38	10	2	-1,61	-0,79
		1	23	26	-12,5	-8,97	15	23	-4,78	-12,5	8	3	7,78	-3,59
		1,5	22	23	-15,7	-7,66	14	22	-5,34	-6,91	8	1	10,43	0,75
6	1	2	21	25	-16,5	-6,29	18	21	-5,88	-3,26	3	4	10,67	3,03

When Table 10 is observed, it is seen that most of the configurations exhibit a change in sidelobe levels when a transition from LTSA to CWSA is applied. The only configuration that has negligible sidelobe level change and a high beamwidth change with the transition is the configuration with antenna length 5λ0, aperture width of 0.5 λ0 and ground extension of 1.5 λ0. The radiation pattern of this configuration for LTSA and CWSA cases can be seen in Figure 28 and Figure 29.

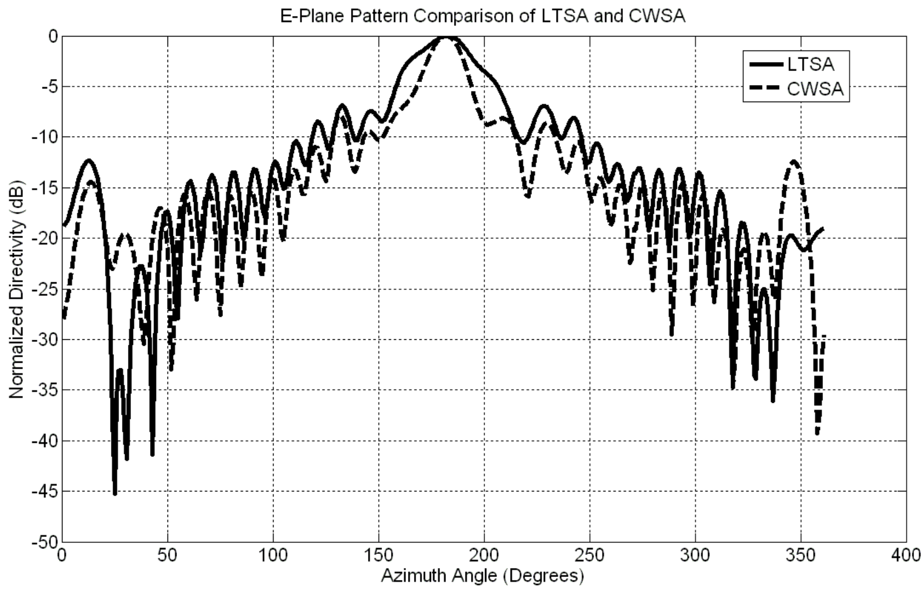

Figure 28 E-Plane pattern comparison for LTSA and CWSA with L=5λ_0, W=0.5λ_0, H=1.5 λ_0

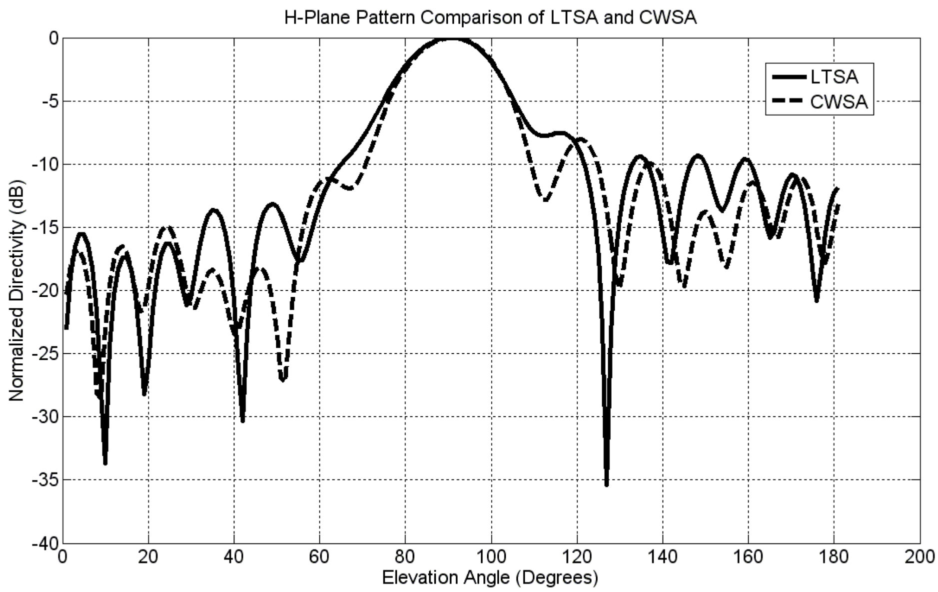

Figure 29 H-Plane pattern comparison for LTSA and CWSA with L=5λ_0, W=0.5 λ_0, H=1.5 λ_0

Since this configuration has high sidelobe levels for LTSA case, other configurations that show higher sidelobe level change were also considered.

It was seen in the parametric study that the sidelobe levels in both planes for an LTSA is highly dependent on aperture width value. Wider aperture width configurations will be utilized for pattern reconfigurability between LTSA and CWSA since LTSAs with wider aperture provide lower sidelobe levels.

One of the configurations that show a high beamwidth change also with sidelobe level change when a transition between LTSA and CWSA occurs is the antenna with antenna length of $3\lambda_0$, aperture width of λ_0 and a ground extension of $2\lambda_0$. The E-plane patterns of LTSA and CWSA having the physical parameters mentioned are plotted in Figure 30. As seen in Figure 30, the CWSA half power beamwidth is smaller than the LTSA case by approximately 10 degrees in E-plane. When the first sidelobe levels of the LTSA and CWSA configurations are compared, it is seen that the sidelobe level is higher as much as approximately 4 dB relative to LTSA configuration. So it can be concluded that when a transition from LTSA to CWSA is provided, the beam will be narrower with a tradeoff of an increased sidelobe level in E-plane.

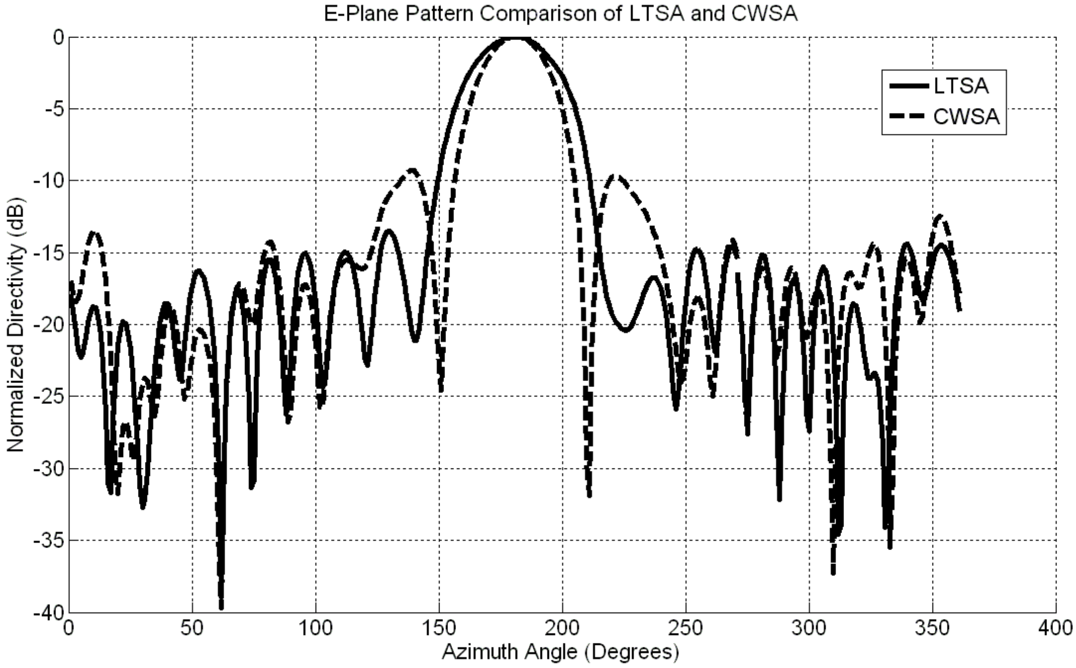

Figure 30 E-Plane pattern comparison for LTSA and CWSA with L=3λ_0, W=1λ_0, H=2 λ_0

The H-plane pattern comparison for the same configurations is given in Figure 31. The conclusions obtained for the E-plane reconfigurability also holds for the H-plane case. The H-plane beamwidth of CWSA case is smaller as compared to the LTSA case although not as much as E-plane case. The beamwidth difference between two configurations is on the order of 4 degrees. The sidelobe level is slightly larger for CWSA.

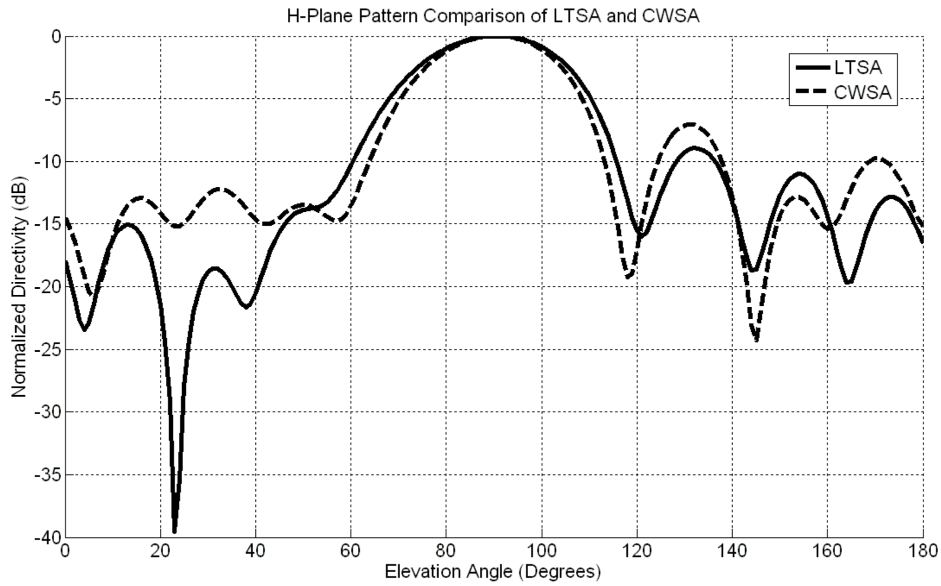

Figure 31 H-Plane Pattern Comparison for LTSA and CWSA for LTSA and CWSA with L=3λ_0, W=1λ_0, H=2 λ_0

Another antenna configuration that exhibits a good variation in pattern with a transition from LTSA to CWSA is the one having an antenna length of 4λ_0, aperture width of 1λ_0 and a ground extension of 1.5λ_0. The E-plane pattern comparison of the LTSA and CWSA with these physical parameters can be seen in Figure 32. The main beam is narrower for the CWSA as compared with LTSA. The difference between the beamwidths of the two antenna types is approximately 5 degrees. If the sidelobe levels between the antennas are observed, it can be seen that the LTSA has a lower sidelobe level of as much as 6dB.

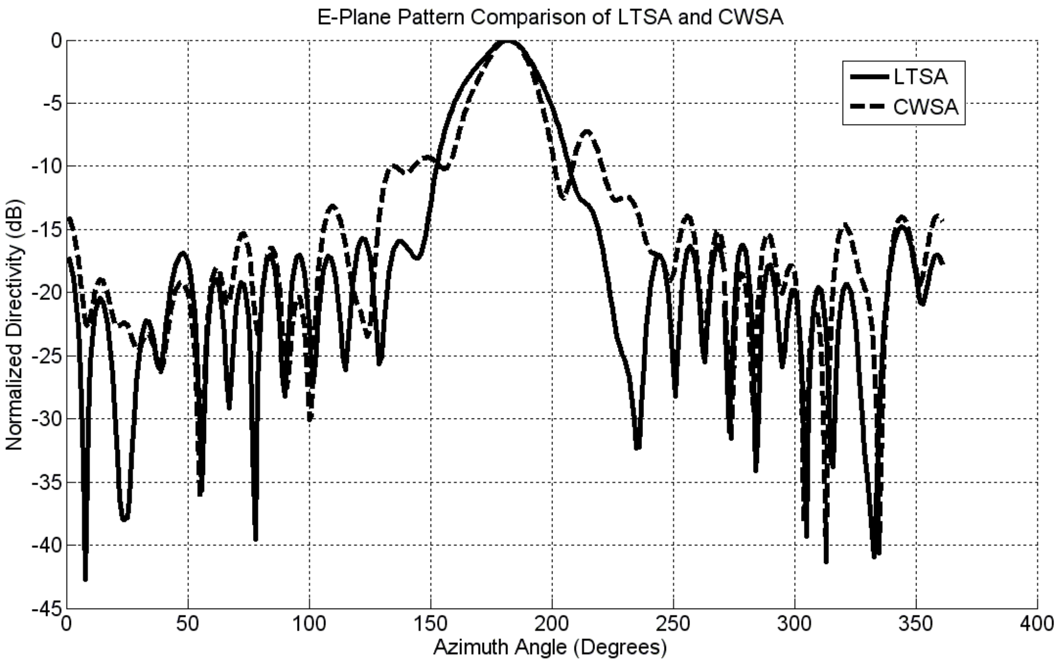

Figure 32 E-Plane Pattern Comparison for LTSA and CWSA for LTSA and CWSA with L=4λ_0, W=1λ_0, H=1.5 λ_0

The H-plane pattern comparison can be seen in Figure 33. A transition from LTSA to CWSA provides a beamwidth decrease of 4 degrees and a sidelobe level rise of 3 dB in H-plane.

Figure 33 H-Plane Pattern Comparison for LTSA and CWSA for LTSA and CWSA with L=4λ_0, W=1λ_0, H=1.5 λ_0

Another example is the configuration with an antenna length of $5\lambda_0$, an aperture width of 1 λ_0 and a ground extension of 1.5 λ_0. The E-plane and H-plane patterns are shown in Figure 34 and Figure 35, respectively.

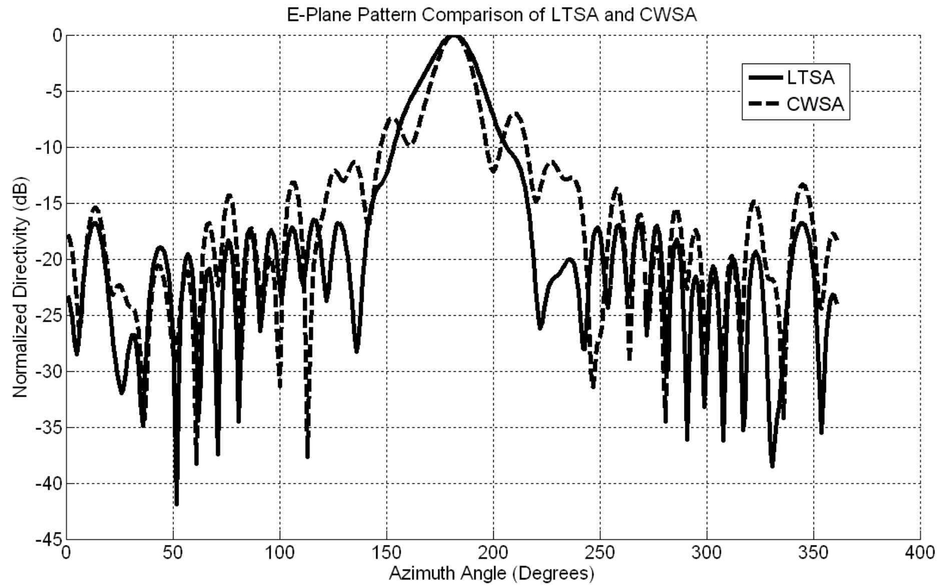

Figure 34 E-Plane Pattern Comparison for LTSA and CWSA with L=$5\lambda_0$, W=$1\lambda_0$, H=1.5 λ_0

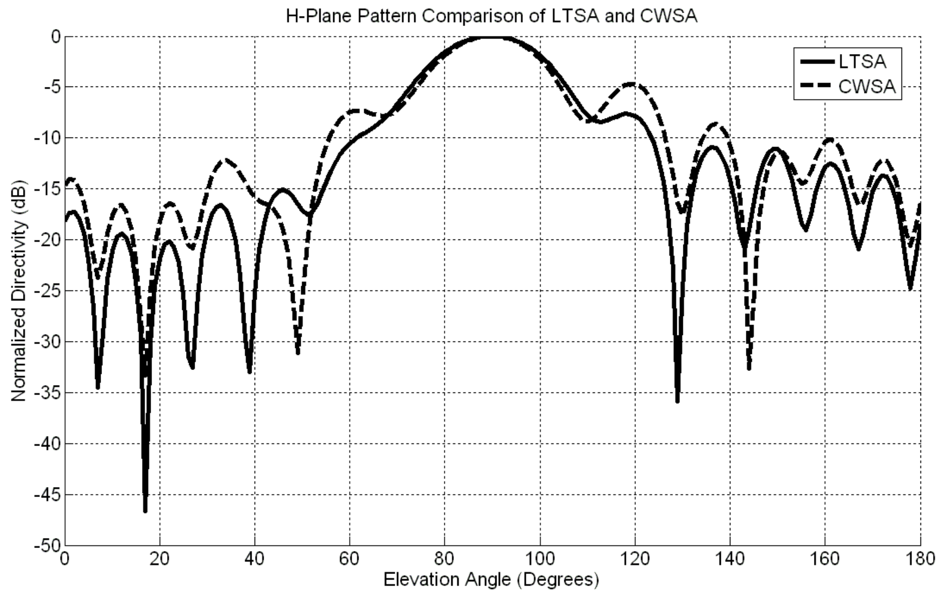

Figure 35 H-Plane Pattern Comparison for LTSA and CWSA with L=$5\lambda_0$, W=$1\lambda_0$, H=1.5 λ_0

Figure 36 shows the E-plane patterns of the antennas with an antenna length of $6\lambda_0$, an aperture width of $1\lambda_0$ and a ground extension of 1.5 λ_0. The reduction in the beamwidth is about 8 degrees in E-plane pattern. The sidelobe level is as much as 11 dB lower in LTSA case than CWSA. The H-plane patterns of the antennas having these physical properties do not show significant difference between LTSA and CWSA configurations as seen in Figure 37.

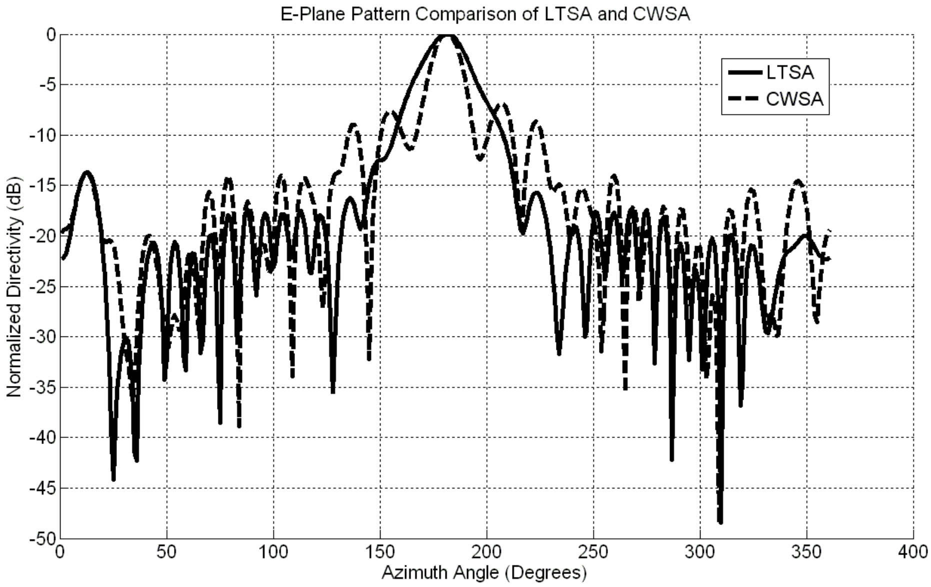

Figure 36 E-Plane Pattern Comparison for LTSA and CWSA with L=$6\lambda_0$, W=$1\lambda_0$, H=1.5 λ_0

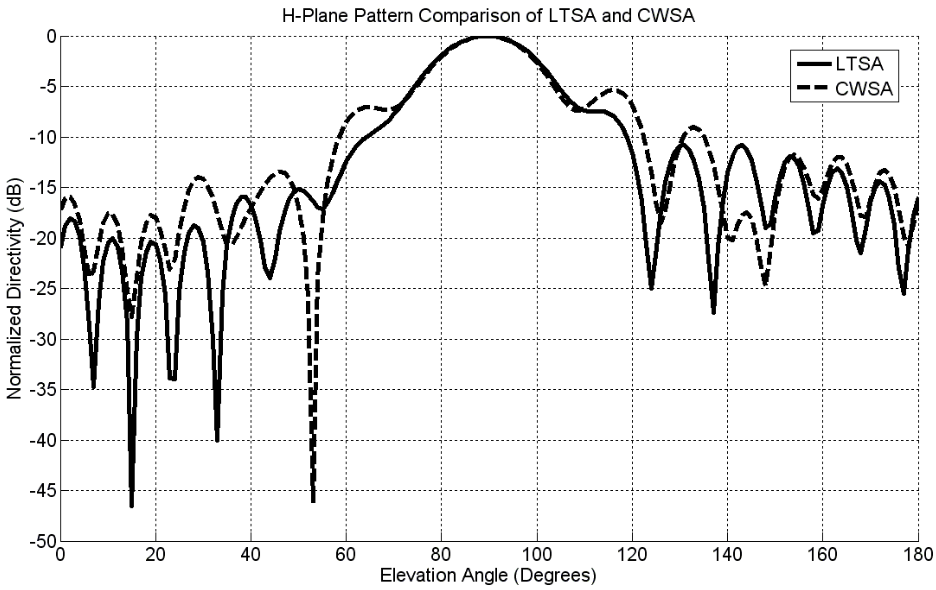

Figure 37 H-Plane Pattern Comparison for LTSA and CWSA with L=6λ_0, W=1λ_0, H=1.5 λ_0

3.2.LTSA-CWSA Bandwidth Comparison

The operating bandwidths of CWSA with exponential taper and LTSA were also compared in order to investigate if a degradation in input return loss characteristics of the antenna occurs when switching between two different antenna configurations. The return loss comparison of CWSA with exponential taper and LTSA for an antenna length of 3 λ_0, aperture width of 1 λ_0 and ground extension of 1 λ_0 can be seen in Figure 38. The return loss value on the band 25-45GHz generally follows the same trend for CWSA and LTSA. The return loss is below -10dB under 29GHz for CWSA so the CWSA is usable below 29GHz whereas LTSA is not. Likewise, the LTSA is usable for 29-32GHz however CWSA is not.

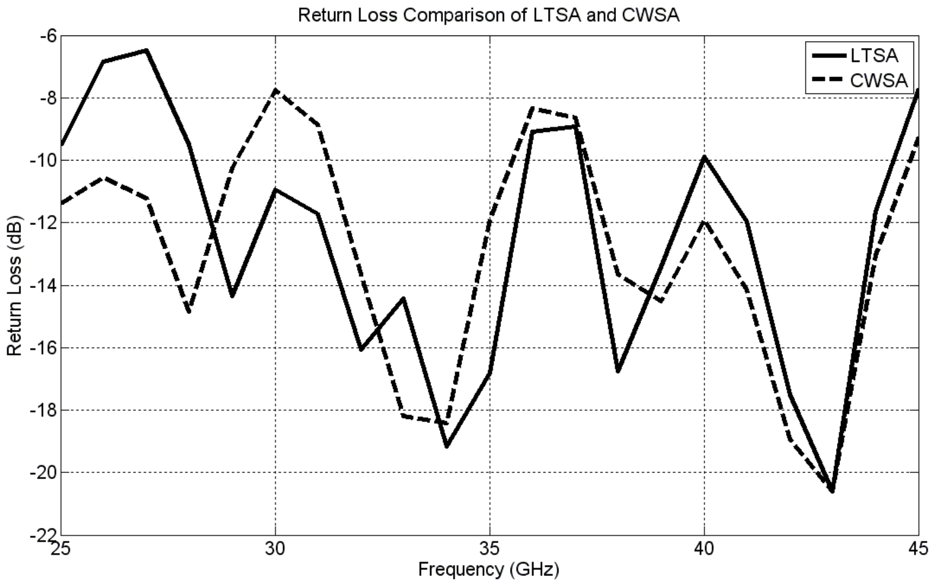

Figure 38 Bandwidth Comparison of CWSA with Exponential and LTSA with $L=3\lambda_0$, $W=1\lambda_0$, $H=1\lambda_0$

Figure 39 shows the return loss comparison for the case of 4 λ_0 antenna length, 0.5 λ_0 aperture width and 1.5 λ_0 ground extension. For narrow aperture width, there is no significant difference between the return loss characteristics of CWSA and LTSA.

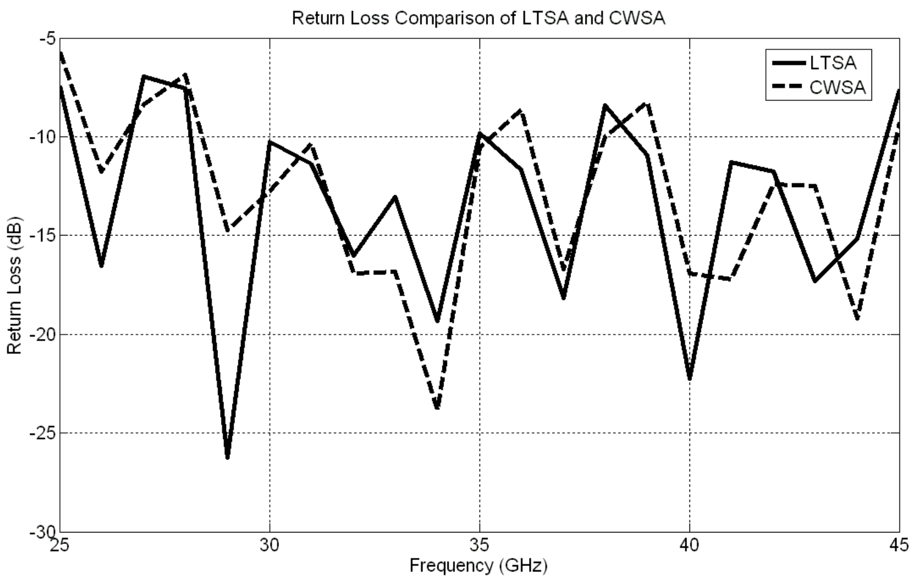

Figure 39 Bandwidth Comparison of CWSA with Exponential and LTSA with $L=4\lambda_0$, $W=0.5\lambda_0$, $H=1.5\lambda_0$

To observe the effect of aperture width on return loss another antenna with 5 λ_0 of antenna length, 0.5 λ_0 of aperture width and 1 λ_0 of ground extension is simulated. Figure 40 shows the results of bandwidth comparison of CWSA and LTSA for this antenna configuration. As seen in Figure 40, the return loss and the usable frequency bands again do not differ between CWSA and LTSA configurations with narrow aperture width.

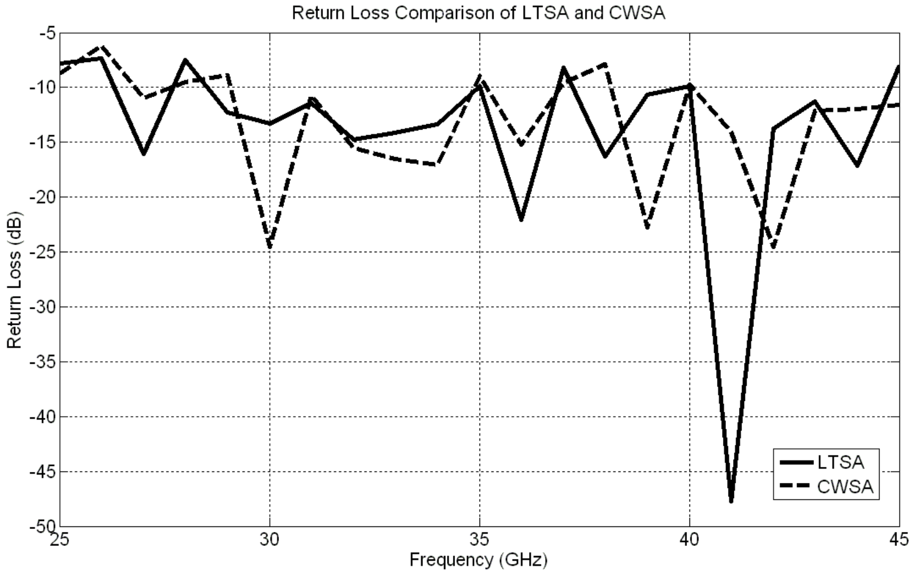

Figure 40 Bandwidth Comparison of CWSA with Exponential and LTSA with $L=5\lambda_0$, $W=0.5\lambda_0$, $H=1\lambda_0$

The return loss comparison of LTSA and CWSA with antenna length of 5 λ_0, aperture width of 1 λ_0 and ground extension of 2 λ_0 can be observed in Figure 41. The LTSA configuration shows better return loss for below 35GHz, whereas the return loss of CWSA is better for above 35GHz. However the usable bandwidth where the return loss is below -10dB do not show difference between LTSA and CWSA.

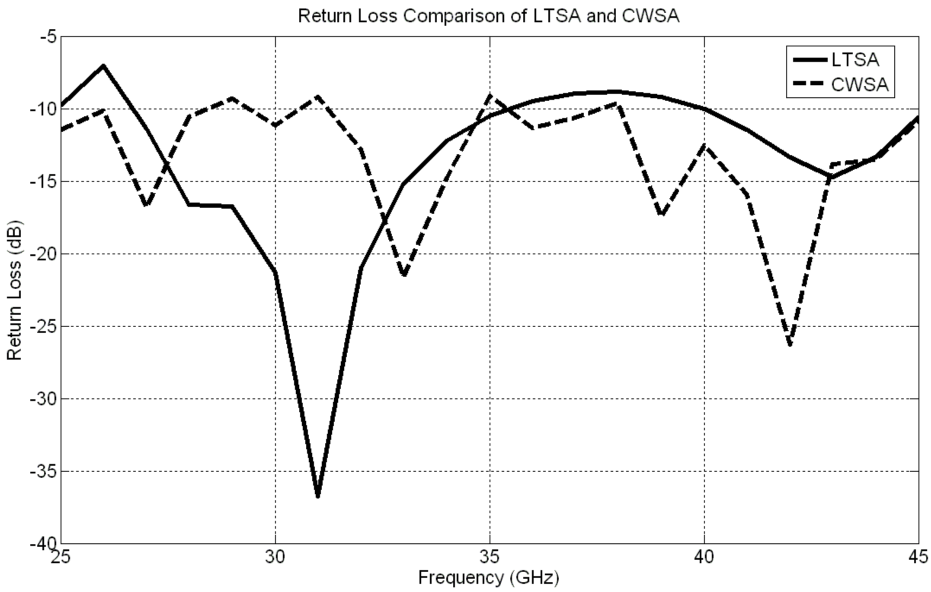

Figure 41 Bandwidth Comparison of CWSA with Exponential and LTSA with $L=5\lambda_0$, $W=1\lambda_0$, $H=2\lambda_0$

The final configuration used to compare the bandwidths of LTSA and CWSA is with an antenna length of 6 λ_0, aperture width of 1 λ_0 and ground extension of 1.5 λ_0. The LTSA again shows better return loss below 35GHz whereas CWSA's return loss is lower above 35GHz. As a result it can be concluded that, the usable bandwidth that has return loss below -10dB does not differ much for the LTSA and CWSA with exponential taper.

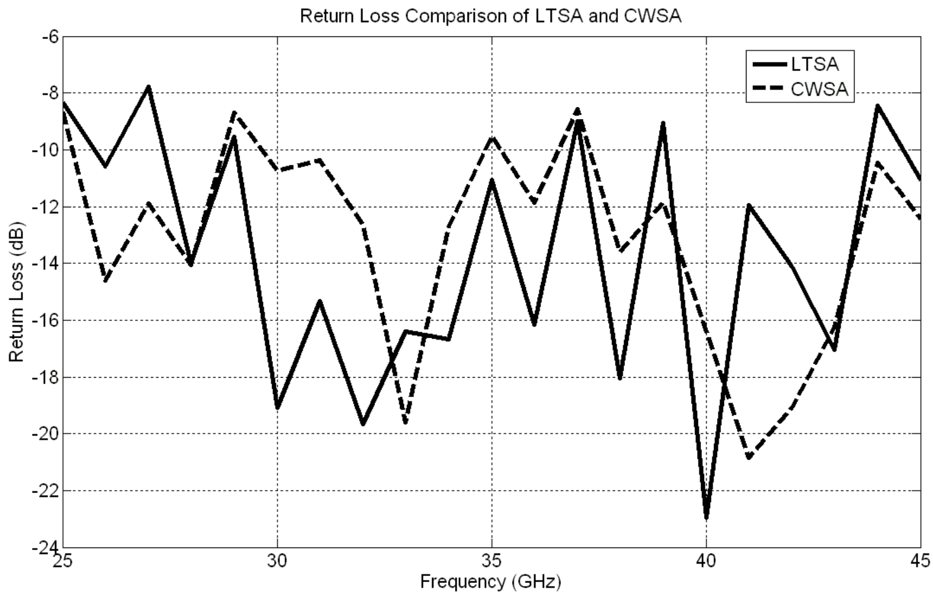

Figure 42 Bandwidth comparison of CWSA with exponential tapering and LTSA with L=6λ_0, W=1λ_0, H=1.5λ_0

It was stated in Chapter 2.2 that the designed antenna is aimed to operate at the frequency band of 30-40GHz centered at 35 GHz. The return loss characteristics previously mentioned proves that the bandwidth aim is met in terms of return loss. Next, the simulation results for the radiation patterns of LTSA and CWSA configurations were observed for 30GHz and 40GHz in order to see the radiation patterns at the frequency band boundaries.

3.3.Radiation Patterns of LTSA and CWSA With Respect to Frequency

The E-plane and H-plane radiation patterns for three different frequencies of the LTSA with an antenna length of 3λ_0, aperture width of 1 λ_0 and ground extension of 2 λ_0 can be seen in Figure 43 and Figure 44. The radiation patterns are not normalized in order to observe the variations in the directivity of the antenna with frequency. The maximum value in the radiation patterns indicates the directivity of the antenna. As seen from the radiation patterns, the antenna keeps its endfire radiating characteristics and exhibits similar directivity levels for frequencies between 30GHz and 40GHz which implies that the antenna has a pattern bandwidth of at least 30-40GHz. It is also observed that as the frequency increases, half power beamwidths in both planes decrease which is expected as a result seen from the parametric study. Due to the decrease in beamwidths, the directivity of the antenna slight increases at higher frequencies. The E-plane SLL is almost the same and the H-plane SLL slightly increases.

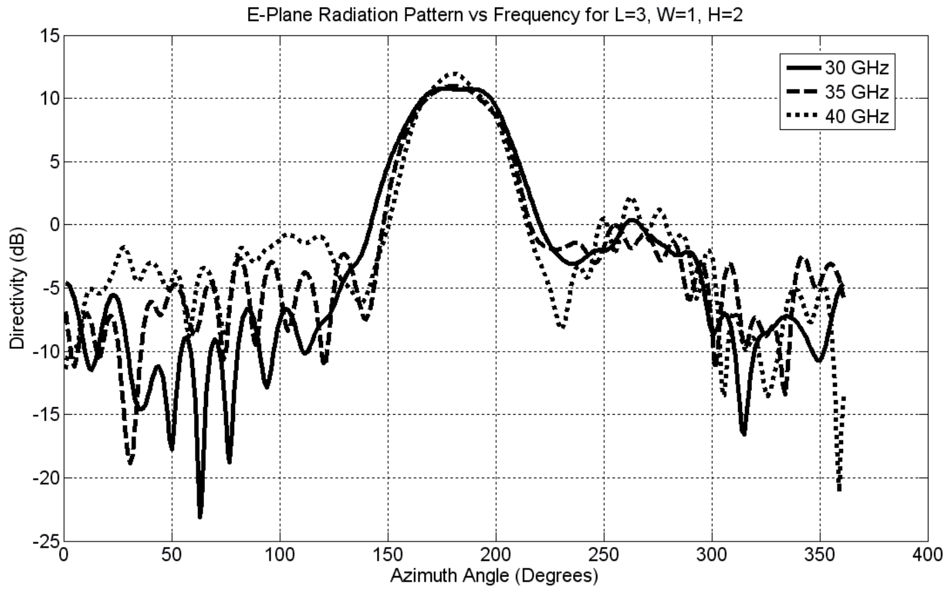

Figure 43 E-Plane Radiation Pattern of LTSA with L=3 λ_0, W=1 λ_0, H=2 λ_0 at different frequencies

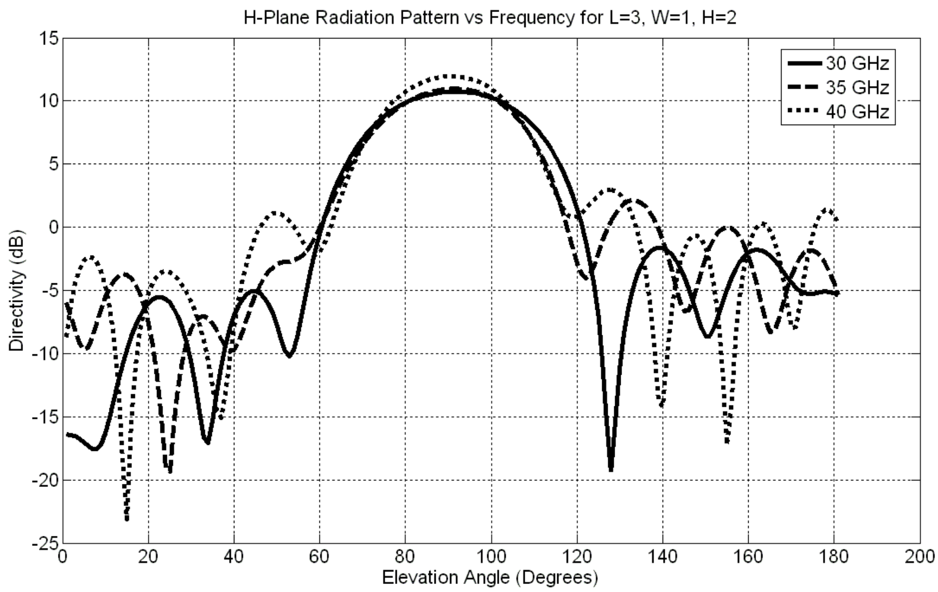

Figure 44 H-Plane Radiation Pattern of LTSA with L=3 λ_0, W=1 λ_0, H=2 λ_0 at different frequencies

The E-plane and H-plane radiation patterns for three different frequencies of the CWSA with an antenna length of $3\lambda_0$, aperture width of 1 λ_0 and ground extension of 2 λ_0 can be seen in Figure 45 and Figure 46.

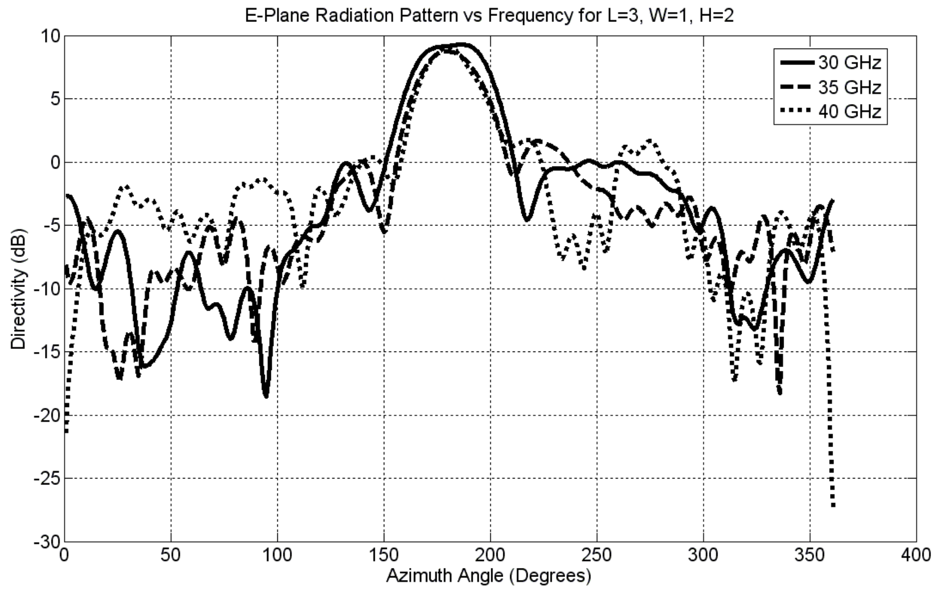

Figure 45 E-Plane Radiation Pattern of CWSA with L=3 λ_0, W=1 λ_0, H=2 λ_0 at different frequencies

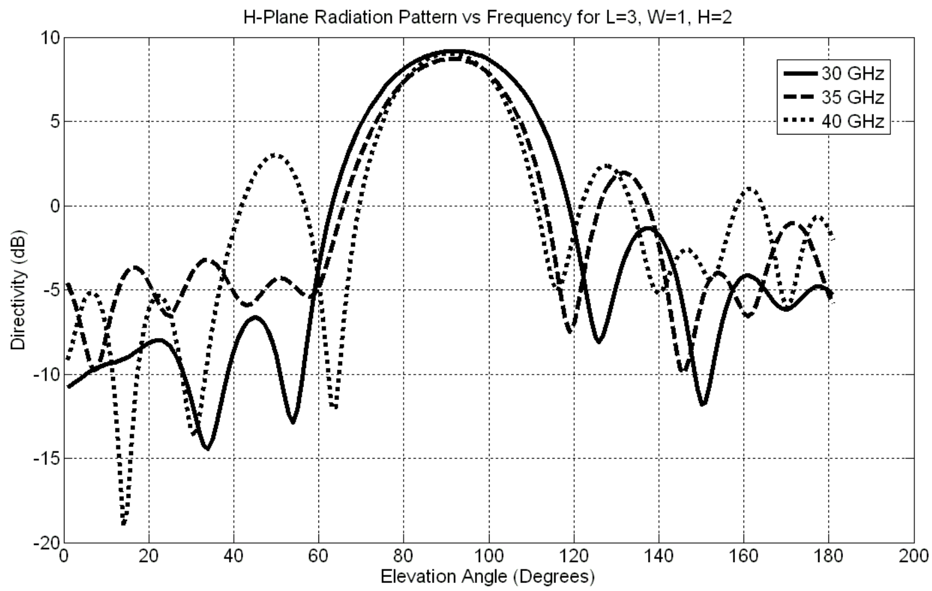

Figure 46 H-Plane Radiation Pattern of CWSA with L=3 λ_0, W=1 λ_0, H=2 λ_0 at different frequencies

The CWSA has a usable pattern bandwidth of 30-40GHz as well. An increase in frequency implies an increase in the electrical dimensions (physical dimensions normalized with respect to wavelength) of the antenna so the decrease in beamwidths and increase in H-plane SLL is compliant with the parametric study results of CWSA. It should be noted that the increase in sidelobe levels with increasing frequency is more dominant in CWSA compared to LTSA. Consequently, although the beamwidths become narrower with increasing frequency, an increase in the directivity of CWSA is not observed, since higher sidelobe levels reduce the directivity of the antenna.

The E-plane and H-plane radiation patterns are plotted for another configuration with antenna length of 6 λ_0, aperture width of 1 λ_0 and ground extension of 1.5 λ_0 for three different frequencies of the LTSA in Figure 47 and Figure 48. The radiation pattern again is suitable in the frequency band of 30-40 GHz for an endfire radiating antenna. It is observed that for shorter antenna (L=3λ_0), the directivity is almost constant with changing frequency, whereas for longer antenna (L=6 λ_0) the directivity change is higher. For L=6λ_0 case, the variation in the beamwidths (especially in E-plane) with frequency is not as significant as L=3λ_0 case. However, the increase in the H-plane side lobe levels with increasing frequency is more pronounced compared to L=3λ_0 case. Consequently, the directivity of the antenna decreases with increasing frequency.

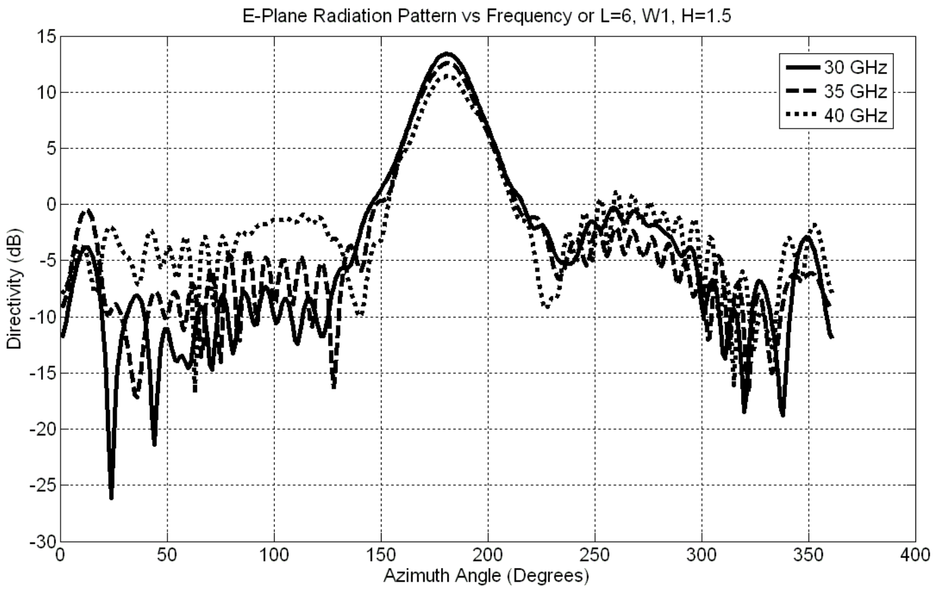

Figure 47 E-Plane Radiation Pattern of LTSA with L=6 λ_0, W=1 λ_0, H=1.5 λ_0 at different frequencies

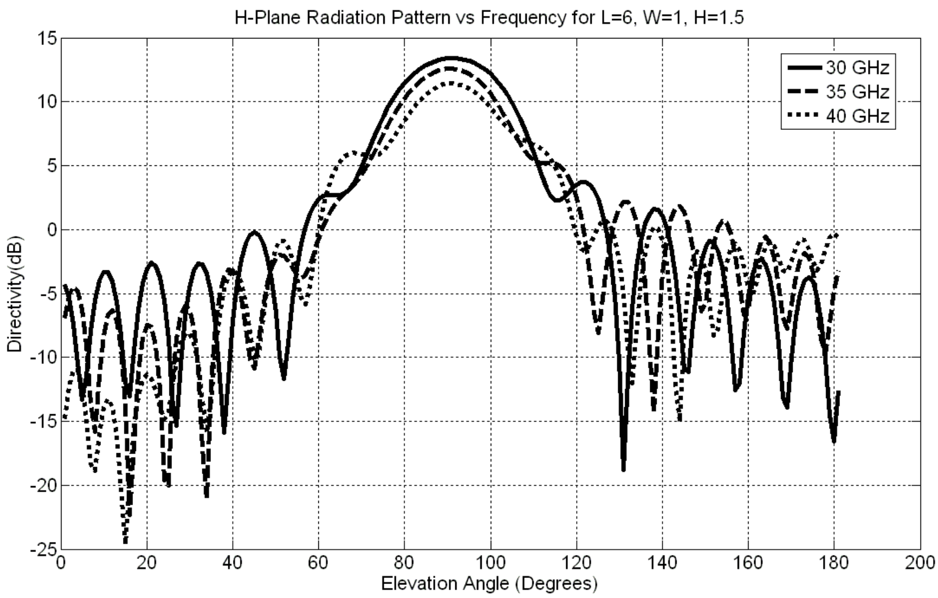

Figure 48 H-Plane Radiation Pattern of LTSA with L=6 λ_0, W=1 λ_0, H=1.5 λ_0 at different frequencies

The E-plane and H-plane radiation patterns for three different frequencies of the CWSA with an antenna length of $6\lambda_0$, aperture width of 1 λ_0 and ground extension of 1.5 λ_0 can be seen in Figure 49 and Figure 50.

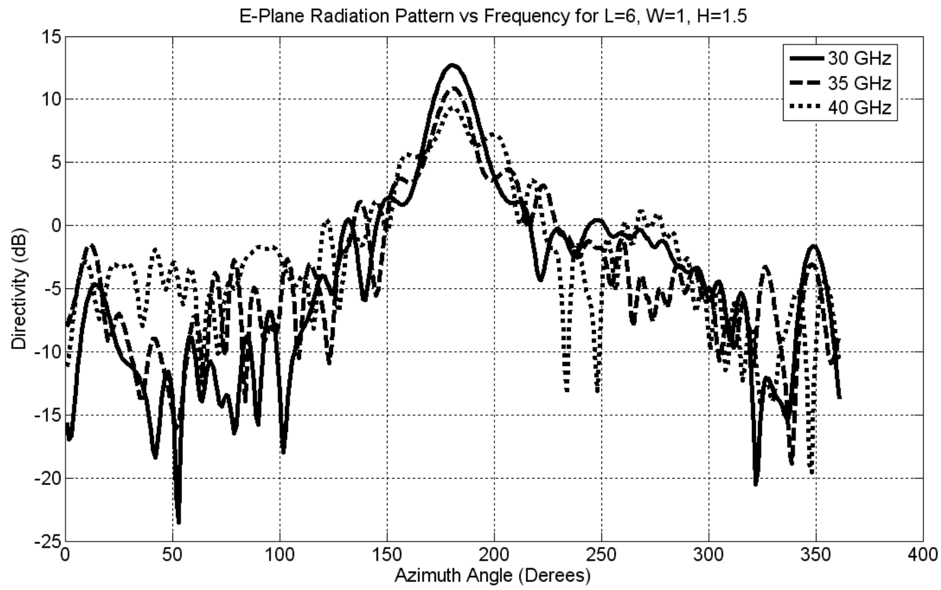

Figure 49 E-Plane Radiation Pattern of CWSA with L=6 λ_0, W=1 λ_0, H=1.5 λ_0 at different frequencies

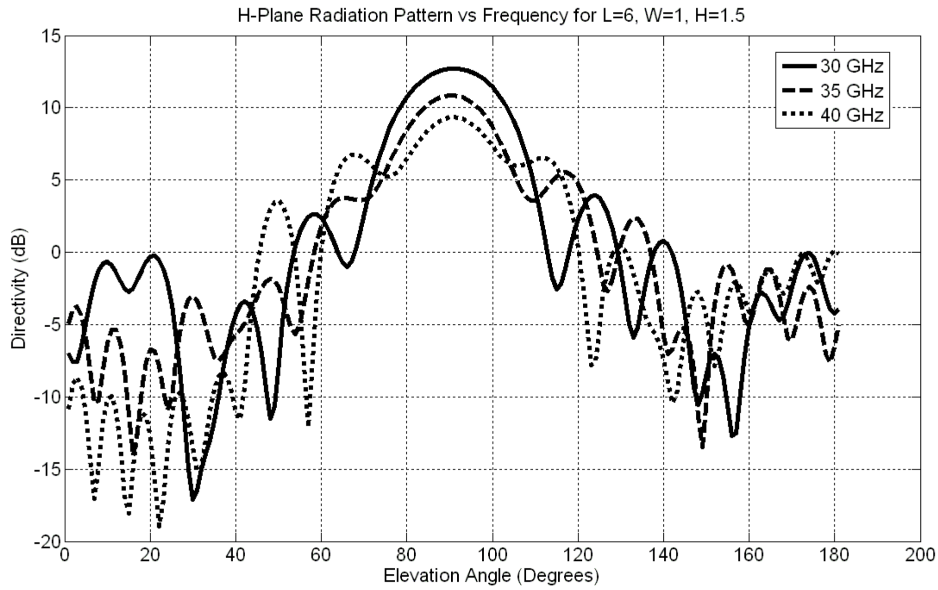

Figure 50 H-Plane Radiation Pattern of CWSA with L=6 λ_0, W=1 λ_0, H=1.5 λ_0 at different frequencies

As seen from Figure 49 and Figure 50, the decrease in the directivity of the antenna with increasing frequency is more effective compared to LTSA. Also the increase in the sidelobe levels is so significant that the sidelobes start to merge with the main beam with increasing frequency. Hence, it can be concluded that the radiation pattern bandwidth of the LTSA is wider compared to CWSA as expected.

CHAPTER 4

MEASUREMENT RESULTS

In this chapter, the antenna manufacturing phase will be explained and the antenna measurement results will be given. First, the measurement results will be compared to the simulation results to investigate the accuracy of the simulation tool. Then, measured radiation patterns for LTSA and CWSA will be compared to explore the possibility of pattern reconfigurability.

4.1. Antenna Manufacturing Phase

Among the antenna geometries proposed in Chapter 3, two configurations for each of LTSA and CWSA have been manufactured. One of these configurations have the physical parameters of antenna length $3\lambda_0$, aperture width of 1 λ_0, ground extension of 2 λ_0 and the other configuration have the antenna length of 4 λ_0, aperture width of 1 λ_0 and ground extension of 1.5 λ_0.

For these four antennas, it was seen that the last microstrip segment of the impedance transformer of microstrip line to slot line transition was too narrow to be manufactured and also the substrate was not suitable for etching the metal layer above the substrate.

In order to obtain a design that can be manufactured, the substrate was changed to RO4003 and another microstrip line to slot line transition was designed on HFSS that does not have an impedance transformer and has a wider microstrip line width. The dielectric permittivity, thickness and loss tangent of RO4003 substrate are 3.38, 0.51mm and 0.0027 respectively. So the effective dielectric thickness is 0.049 as can also be seen in Table 1. Although the effective thickness value for this substrate is larger than the maximum recommended effective thickness value which is 0.03;

RO4003 was chosen due to the availability of the substrate and the ease of etching the metal layer.

In the new transition design, the microstrip line width was calculated to be 1.1mm that corresponds to an impedance of 50Ω on RO4003 substrate and a slotline width of 0.3mm was seen to be appropriate for manufacturing purposes.

An orthogonal transition was designed between microstrip line and slot line carrying out a parametric study on HFSS. The geometry of the new transition can be seen in Figure 51.

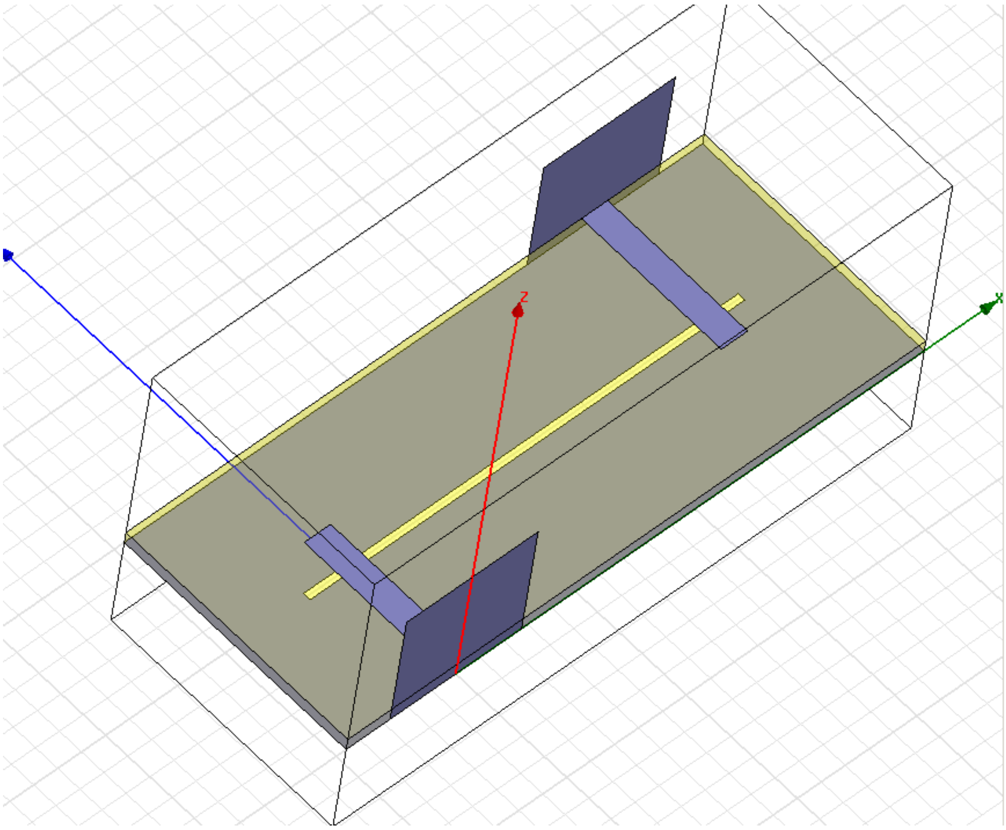

Figure 51 The Geometry of the New Microstrip Line to Slotline Transition

The transition contains no impedance transformer and is compliant with the w=v case given in detail in [18]. For the parametric study of the new transition, the microstrip line width was kept constant at 1.1mm and the slot line width was kept constant at 0.3mm. The parameters that were changed are the microstrip stub length and slot line stub length values as seen in Figure 52. These two parameters were changed with 0.1mm increments and the return loss and insertion loss values of two transitions connected back to back through the slot line were evaluated to determine the optimum values of these parameters.

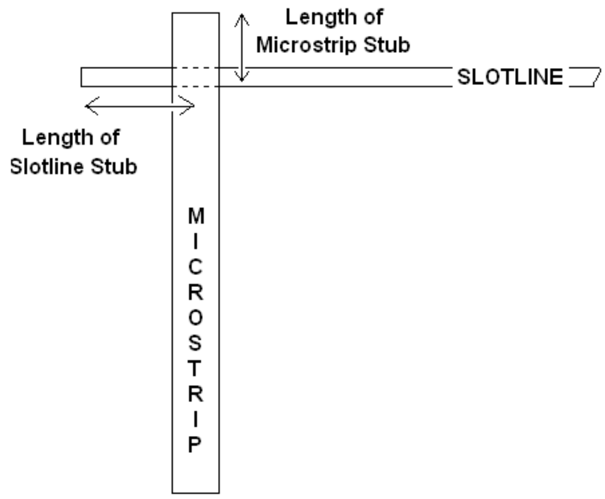

Figure 52 Parameters of the New Microstrip Line to Slot line Transition

As a result of the parametric study, the transition that has a microstrip line stub length and slot line stub length of 0.8mm each was found to exhibit the lowest return loss and the best insertion loss characteristics. The performance of the transition can be observed in Figure 53.

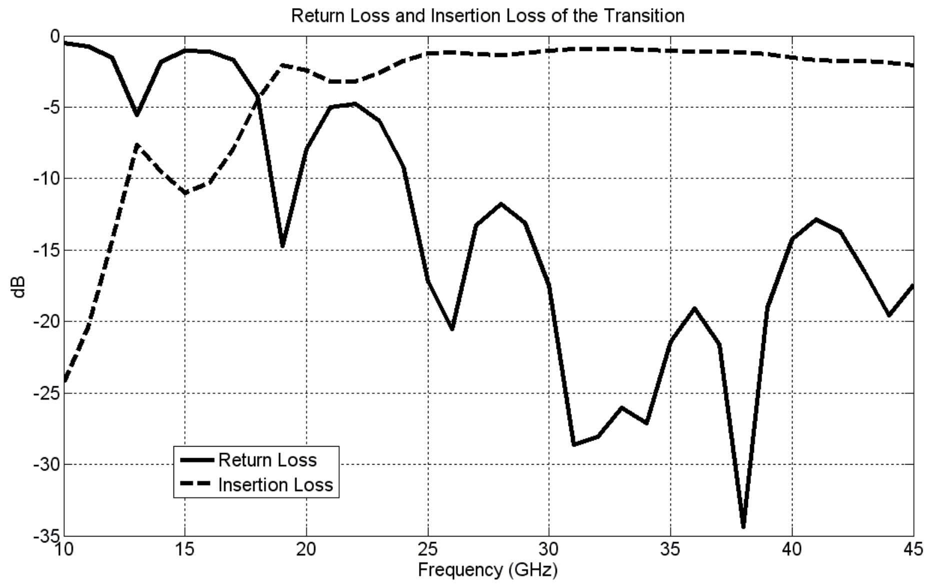

Figure 53 Return and Insertion Loss of the Transition

The return loss of the transition is seen to be below -10dB and insertion loss below 2 dB for the frequency band of 23-45GHz.

Using the designed transition, four antennas were manufactured:

[1] LTSA with L=3 $\lambda_{0,}$ W=1 $\lambda_{0,}$ H=2 λ_0

[2] CWSA with L=3 λ_0, W=1 λ_0, H=2 λ_0

[3] LTSA with L=4 λ_0, W=1 λ_0, H=1.5 λ_0

[4] CWSA with L=4 λ_0, W=1 λ_0, H=1.5 λ_0

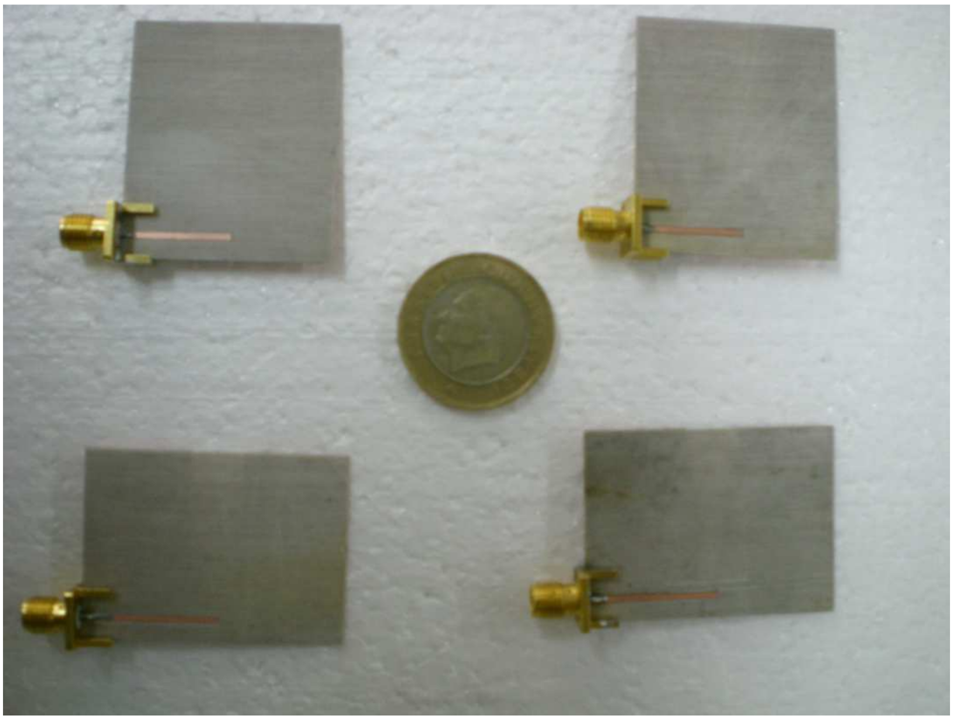

Figure 54 Manufactured Antennas-Top Side

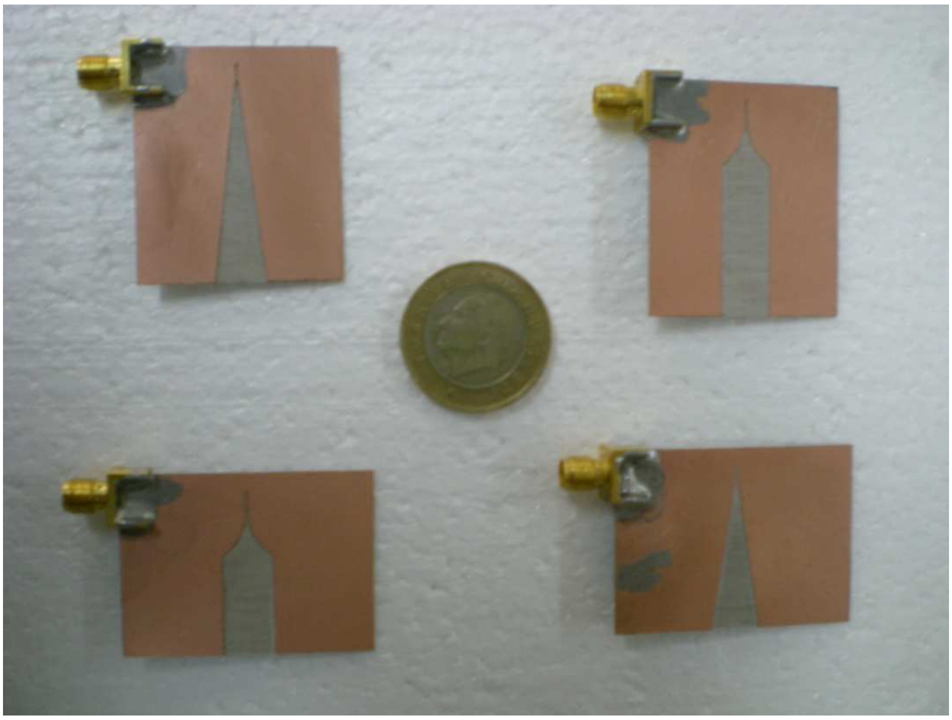

Figure 55 Manufactured Antennas-Bottom Side

4.2. Antenna Pattern Measurement Results

For each of the four antennas manufactured, two sets of pattern measurement (one for E-plane and one for H-plane) were performed which makes a total of eight sets of measurements. For each set of measurement, multiple frequency patterns were measured from 28 to 40 GHz. The set-up given in Figure 56 was used for the antenna pattern measurements in the anechoic chamber.

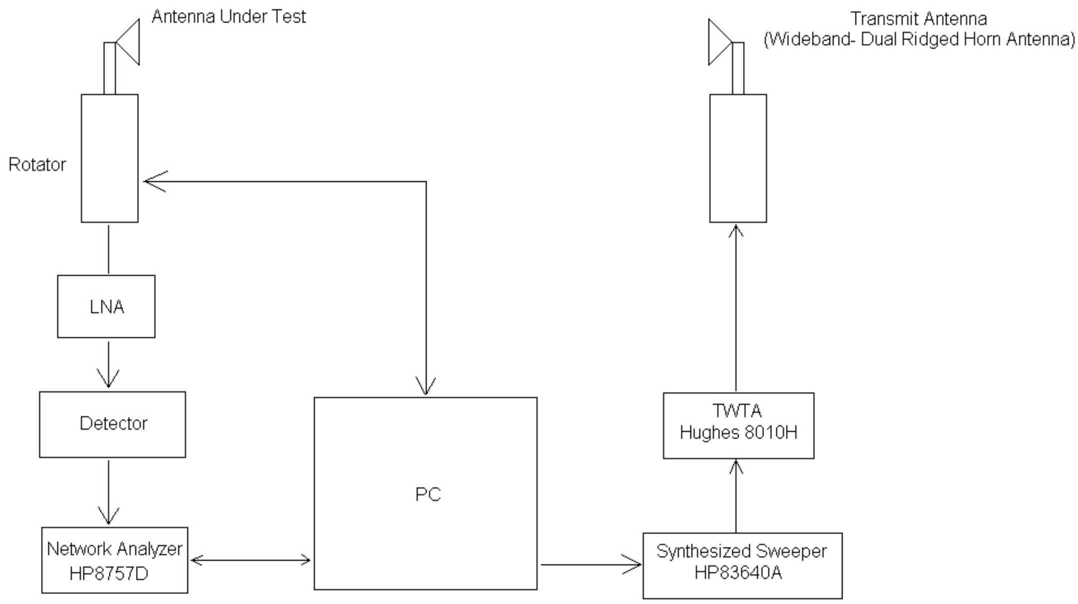

Figure 56 Antenna Measurement Set-Up

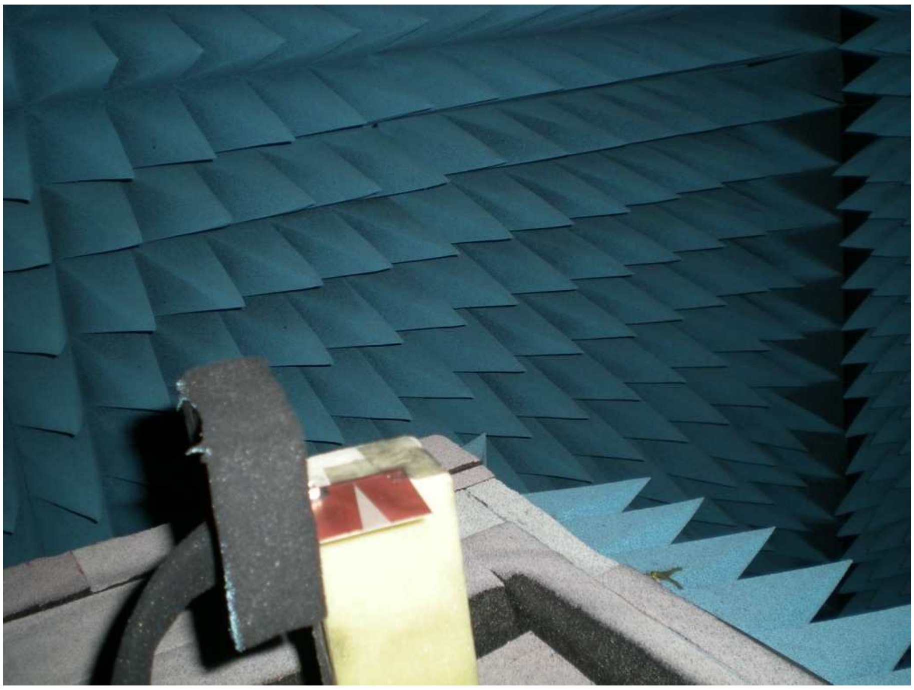

Figure 57 Antenna Under Test

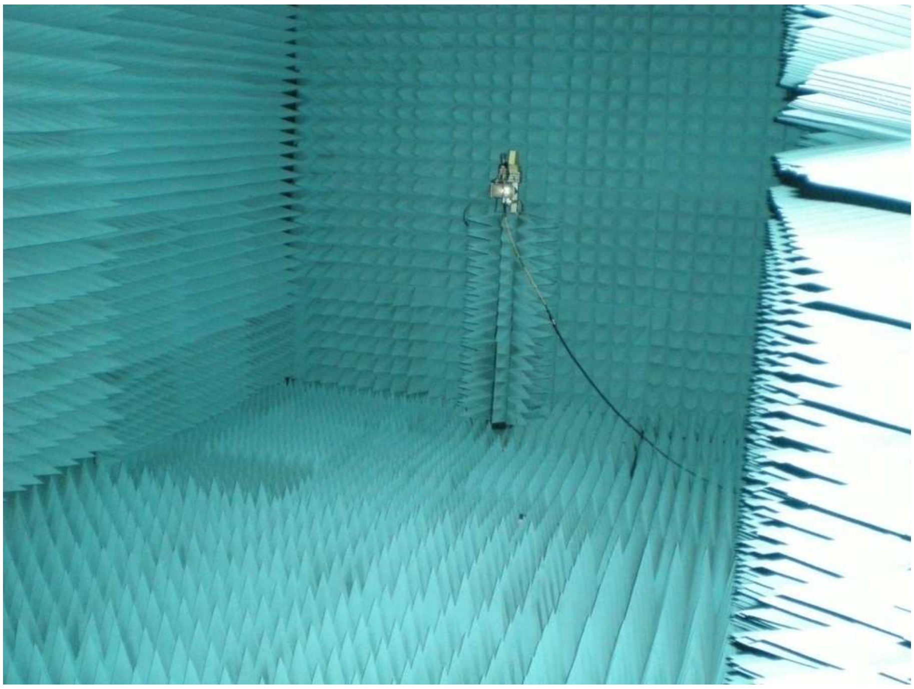

Figure 58 Anechoic Chamber and the Transmit Antenna

The four antenna configurations were also simulated in HFSS to see if there is consistency between the simulated and measured antenna patterns. The comparison between simulated and measured E-plane and H-plane radiation patterns of LTSA with L=3λ_0 , W=1 λ_0 and H=2 λ_0 can be seen in Figure 59 and Figure 60, respectively at 35GHz.

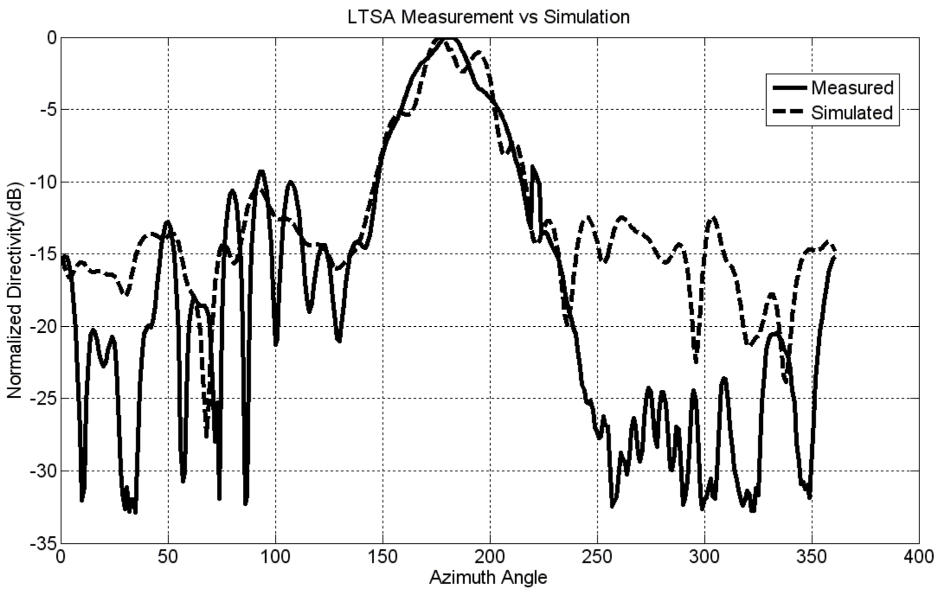

Figure 59 E-Plane Radiation Pattern of LTSA with L=3λ_0, W=1λ_0 and H=2λ_0

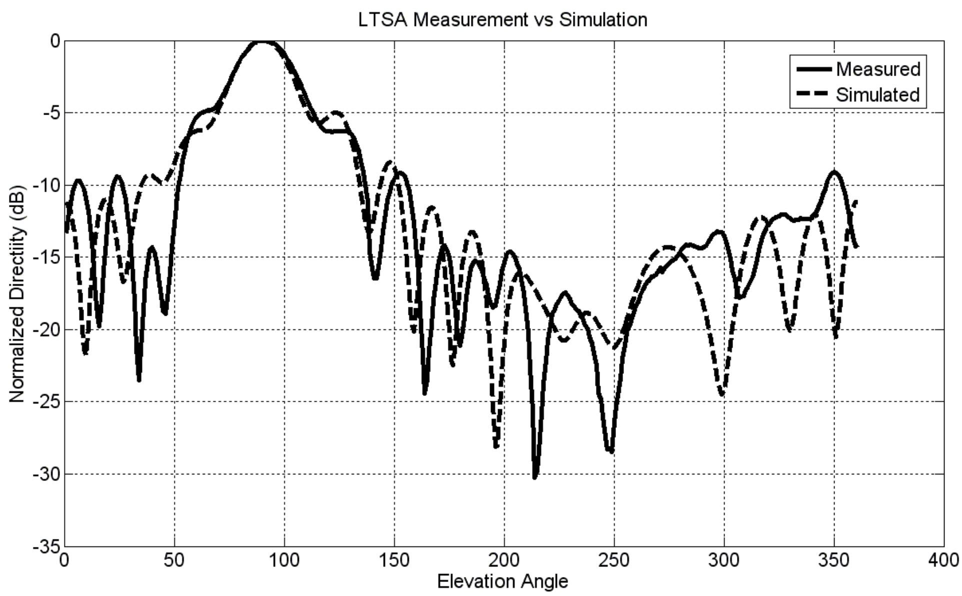

Figure 60 H-Plane Radiation Pattern of LTSA with L=3λ_0, W=1λ_0 and H=2λ_0

As seen from Figure 59 and Figure 60, there is a good agreement between the measured radiation pattern and simulated radiation pattern for both planes. The only difference in the patterns can be seen in the E-plane radiation pattern on the region through the direction of the microstrip feed line on top of the substrate. In this region, the simulation result predicts a higher radiation whereas in the measurement a lower radiation level is seen. The reason for this is believed to be due to the measurement set-up where the microstrip line lies between supporting foam and the substrate. So the feed radiation seen in simulations might have been absorbed by the supporting foam in the measurement.

The comparison between simulated and measured E-plane and H-plane radiation patterns of LTSA with $L=4\lambda_0$, $W=1\ \lambda_0$ and $H=1.5\ \lambda_0$ can be seen in Figure 61 and Figure 62, respectively at 35GHz.

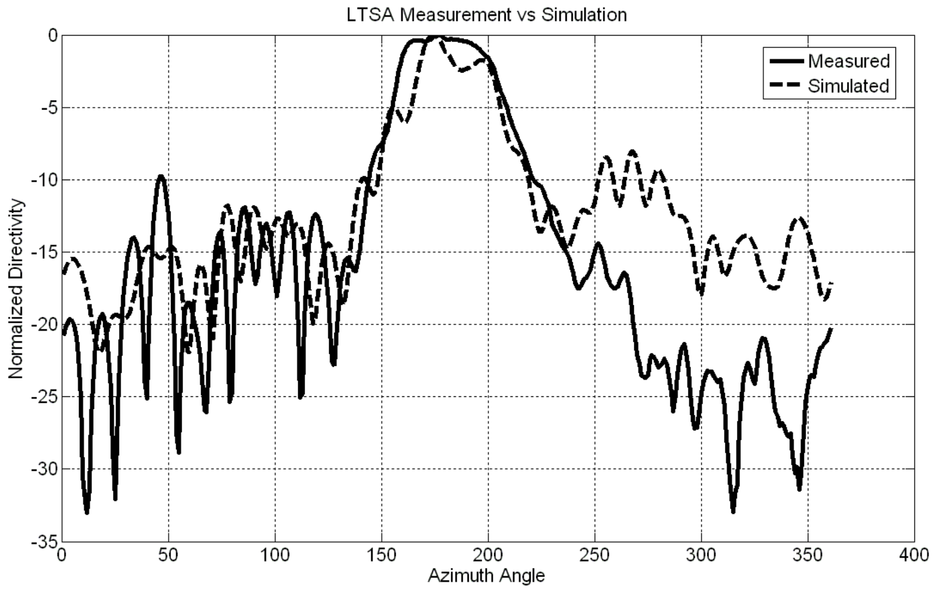

Figure 61 E-Plane Radiation Pattern of LTSA with $L=4\lambda_0$, $W=1\lambda_0$ and $H=1.5\lambda_0$

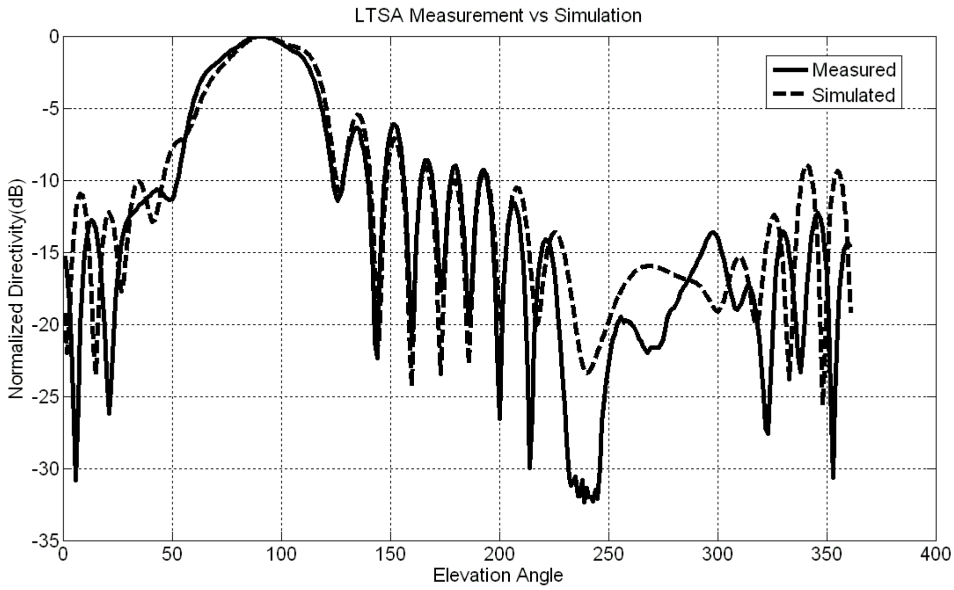

Figure 62 H-Plane Radiation Pattern of LTSA with L=4λ_0, W=1λ_0 and H=1.5λ_0

There is again a good agreement between simulation and measurement results except for the microstrip feed region in E-plane.

The comparison between simulated and measured E-plane and H-plane radiation patterns of CWSA with L=3λ_0, W=1 λ_0 and H=2 λ_0 can be seen in Figure 63 and Figure 64, respectively at 35GHz.

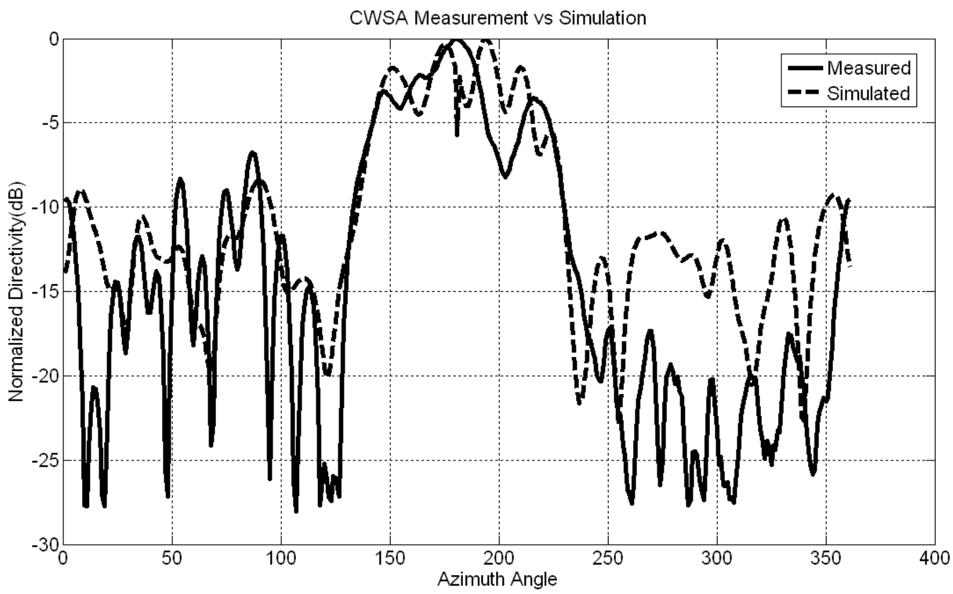

Figure 63 E-Plane Radiation Pattern of CWSA with L=3λ_0, W=1λ_0 and H=2λ_0

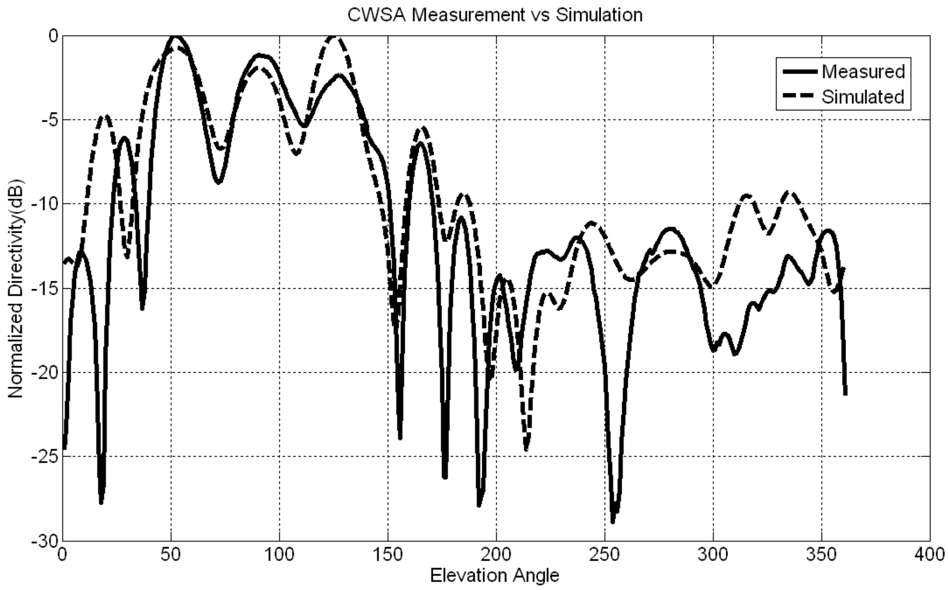

Figure 64 H-Plane Radiation Pattern of CWSA with L=3λ_0, W=1λ_0 and H=2λ_0

CWSA is seen to be deviating from the endfire radiation characteristics due to the split in the main beam and unsymmetrical pattern with respect to endfire direction. It was stated in section 4.1 that RO4003 substrate was used in manufactured antennas with a substrate thickness of 0.51mm which causes an effective thickness value larger than the value proposed in [19]. This fact is believed to be the reason for the deviation in antenna patterns from endfire radiation characteristics. It can be concluded that the manufactured antennas are not well-behaved endfire radiating antennas because of the high effective dielectric thickness.

The comparison between simulated and measured E-plane and H-plane radiation patterns of CWSA with L=4λ_0, W=1 λ_0 and H=1.5 λ_0 can be seen in Figure 65 and Figure 66, respectively at 35GHz.

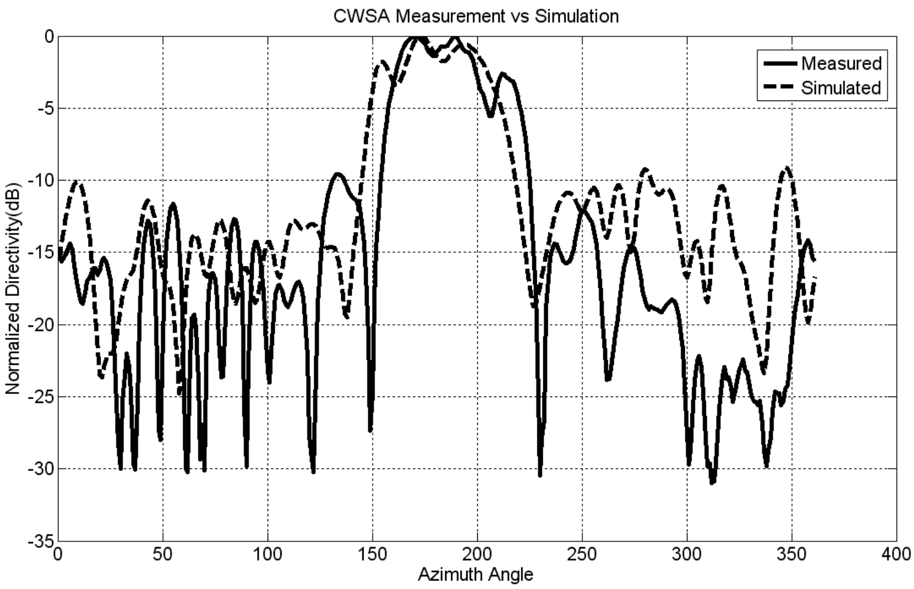

Figure 65 E-Plane Radiation Pattern of CWSA with L=4λ_0, W=1λ_0 and H=1.5λ_0

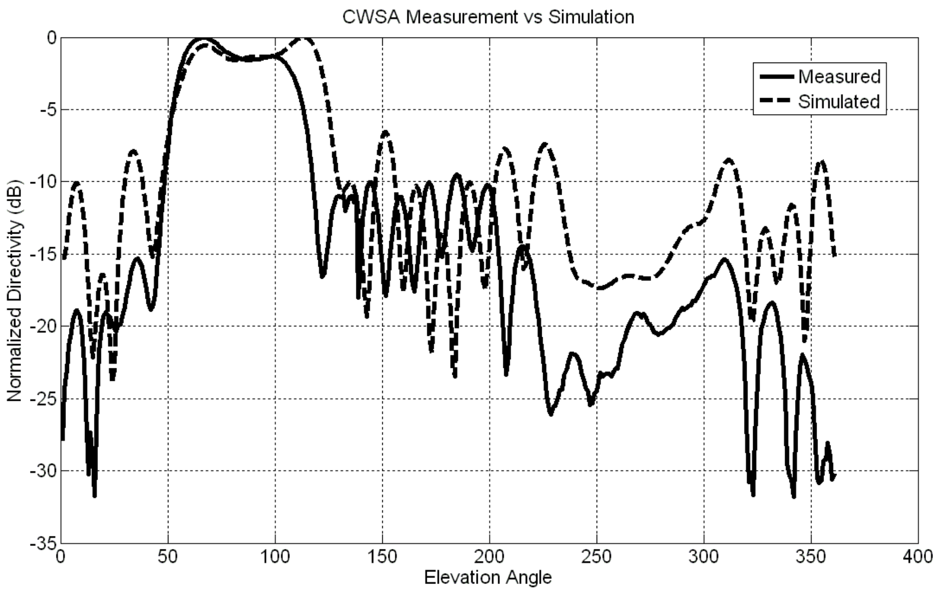

Figure 66 H-Plane Radiation Pattern of CWSA with L=4λ_0, W=1λ_0 and H=1.5λ_0

4.3. Radiation Pattern Comparison of LTSA and CWSA

The LTSA and CWSA pattern measurement results will be compared next. Figure 67 and Figure 68 show the E-plane and H-plane radiation pattern comparison between LTSA and CWSA with the same physical parameters as antenna length of 3λ_0, aperture width of 1 λ_0 and ground extension of 2 λ_0 for 35GHz.

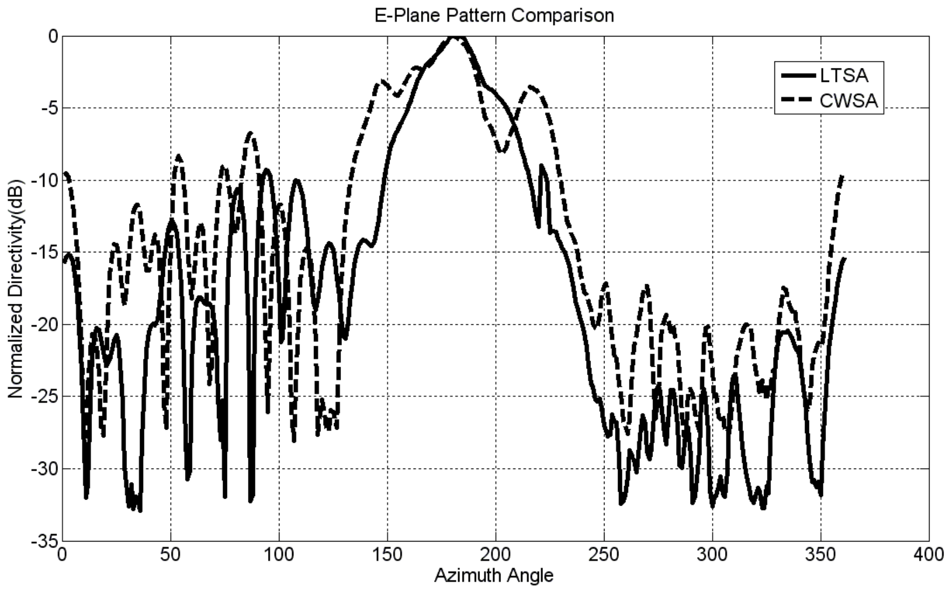

Figure 67 E-Plane Pattern Comparison of LTSA&CWSA with L=3λ_0, W=1λ_0 and H=2 λ_0

Figure 68 H-Plane Pattern Comparison of LTSA&CWSA with L=3λ_0, W=1λ_0 and H=2 λ_0

For LTSA and CWSA with antenna length of 4λ_0, aperture width of 1 λ_0 and ground extension of 1.5 λ_0, the E-plane and H-plane radiation pattern measurement result comparison can be seen in Figure 69 and Figure 70.

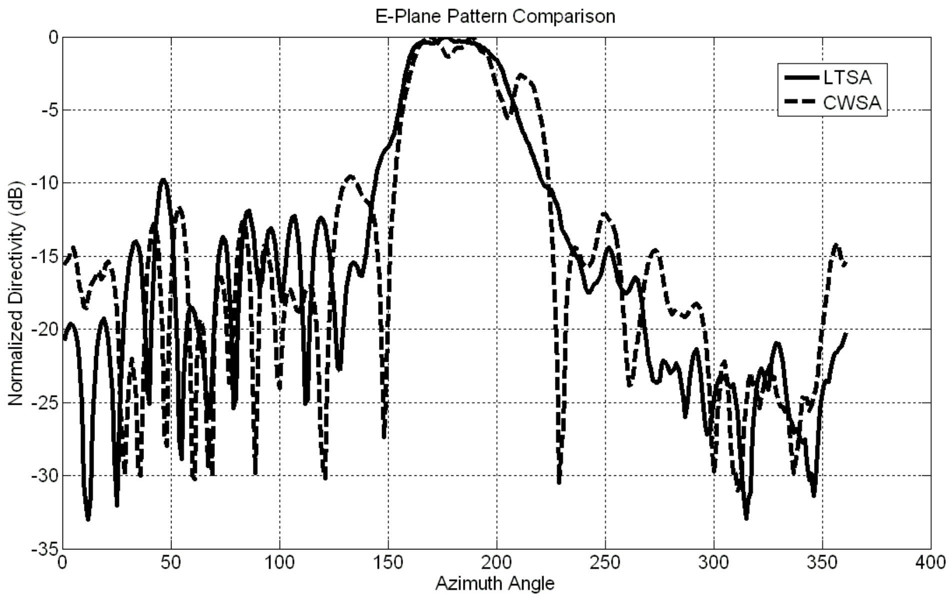

Figure 69 E-Plane Pattern Comparison of LTSA&CWSA with L=4λ_0, W=1λ_0 and H=1.5 λ_0

Figure 70 H-Plane Pattern Comparison of LTSA&CWSA with L=4λ_0, W=1λ_0 and H=1.5 λ_0

Since the radiation patterns for the CWSA are far from proper endfire radiation characteristics, it is not meaningful to make a comparison with LTSA.

4.4. Measured Radiation Patterns with Respect to Frequency

In order to be able to see the pattern bandwidth of the manufactured antennas, the radiation patterns are plotted for three different frequency values as 30GHz, 35GHz and 40GHz.

The E-plane radiation patterns of LTSA with L=3λ_0, W=1 λ_0 and H=2 λ_0 at three different frequencies are given in Figure 71.

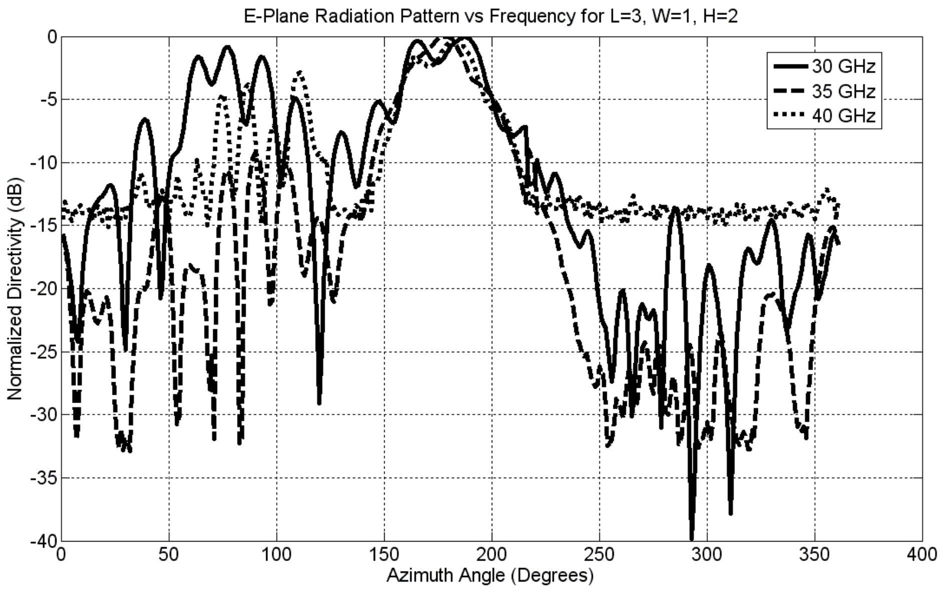

Figure 71 E-Plane Radiation Pattern vs Frequency for LTSA with L=3λ_0, W=1λ_0 and H=2 λ_0

It can be seen from Figure 71 that for 40GHz, the received power is almost constant for azimuth angles between 220^0 and 360^0. This might be due to the fact that the signal level on the antenna is too low to be measured by the detector in the set-up because of the fact that the maximum recommended usable frequency of the test set-up is 40 GHz and the SMA connectors used in the antennas have high loss values above 18 GHz.

Concerning the patterns for different frequencies, the antenna seems to keep its endfire radiation characteristics in the 30-40GHz band although the sidelobe level at 30 GHz is too high.

The H-plane radiation patterns of LTSA with L=3λ_0, W=1λ_0 and H=2λ_0 at three different frequencies are given in Figure 72. For the H-plane characteristics, the antenna has a tilted beam for 40GHz and the sidelobe level for 30GHz is higher than the main beam directivity.

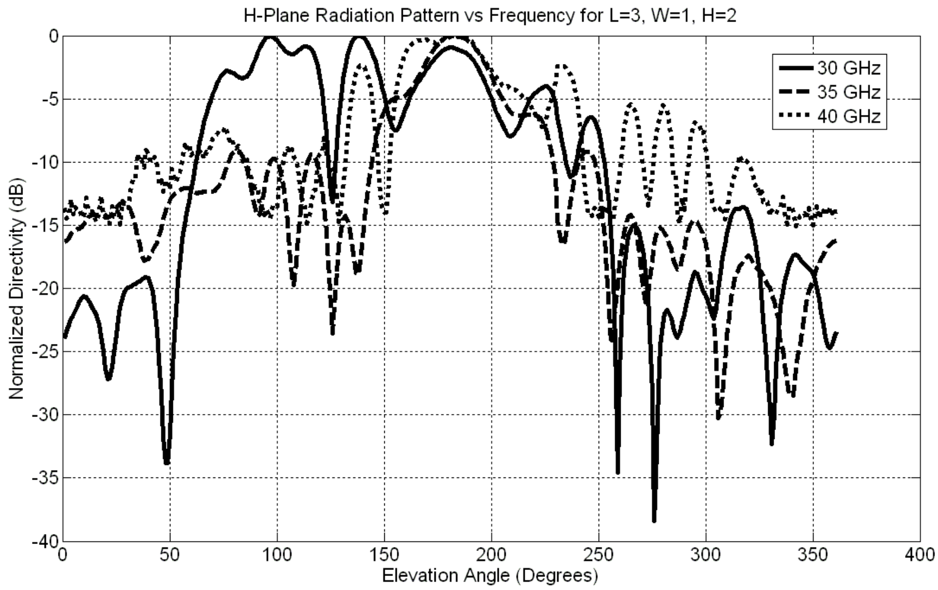

Figure 72 H-Plane Radiation Pattern vs Frequency for LTSA with L=3λ_0, W=1λ_0 and H=2 λ_0

The E-plane and H-plane radiation patterns of CWSA with L=3λ_0, W=1 λ_0 and H=2 λ_0 at three different frequencies are given in Figure 73 and Figure 74. The CWSA deviates from endfire characteristics at 40GHz with a tilted beam.

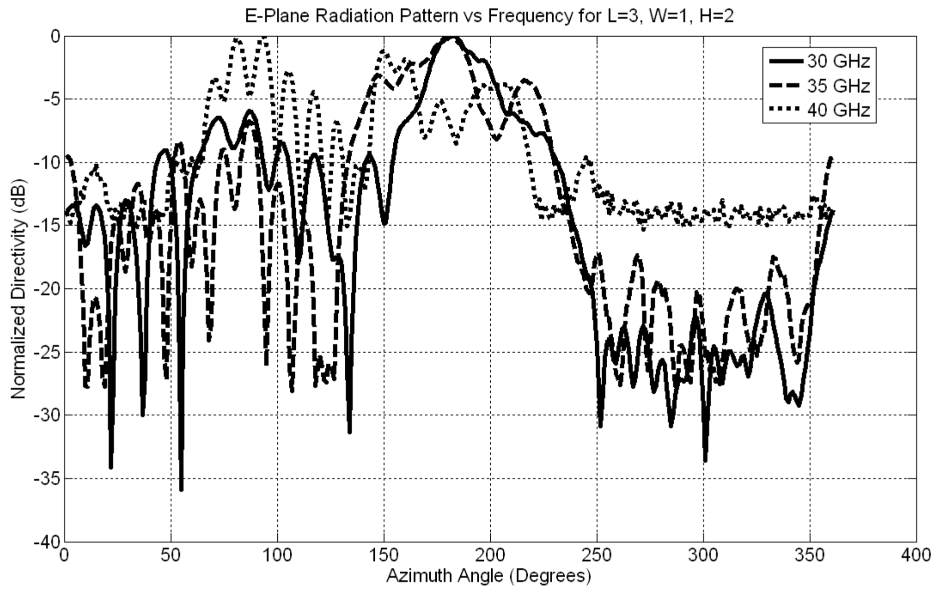

Figure 73 E-Plane Radiation Pattern vs Frequency for CWSA with L=3λ_0, W=1λ_0 and H=2 λ_0

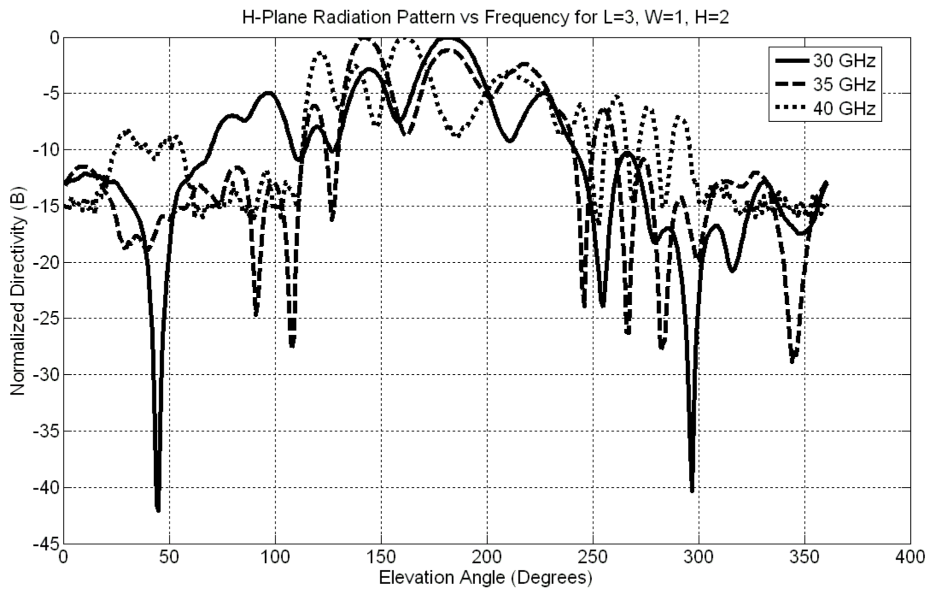

Figure 74 H-Plane Radiation Pattern vs Frequency for CWSA with L=3λ_0, W=1λ_0 and H=2 λ_0

The E-plane and H-plane radiation patterns of LTSA with L=4λ_0, W=1 λ_0 and H=1.5 λ_0 for different frequencies are given in Figure 75 and Figure 76. For this LTSA configuration, the antenna keeps its endfire characteristics for the frequency range of

30-40 GHz. The increase in the sidelobe level for 30GHz is again need to be noted. The H-plane beamwidth is narrower than 35GHz case for both 30GHz and 40GHz.

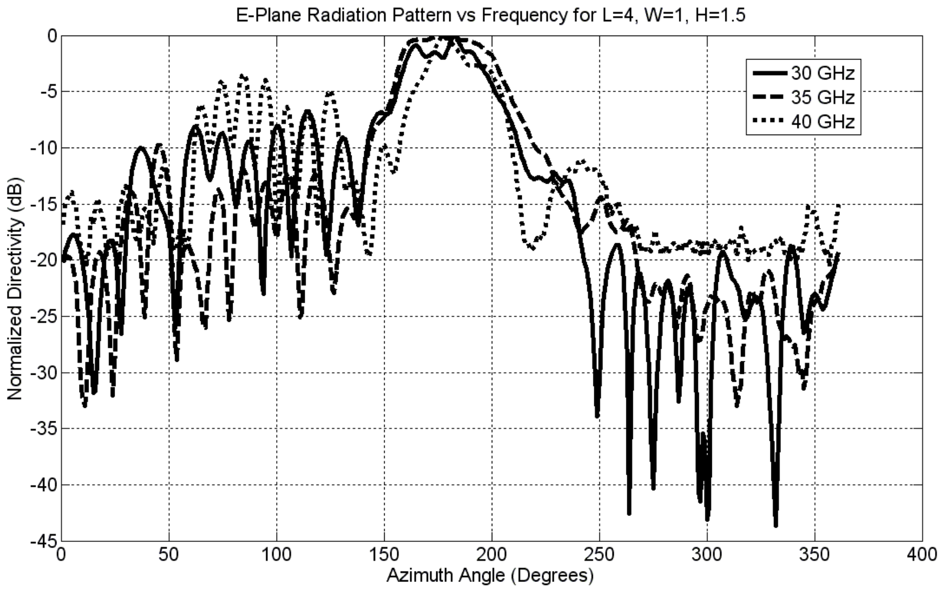

Figure 75 E-Plane Radiation Pattern vs Frequency for LTSA with L=4λ_0, W=1λ_0 and H=1.5 λ_0

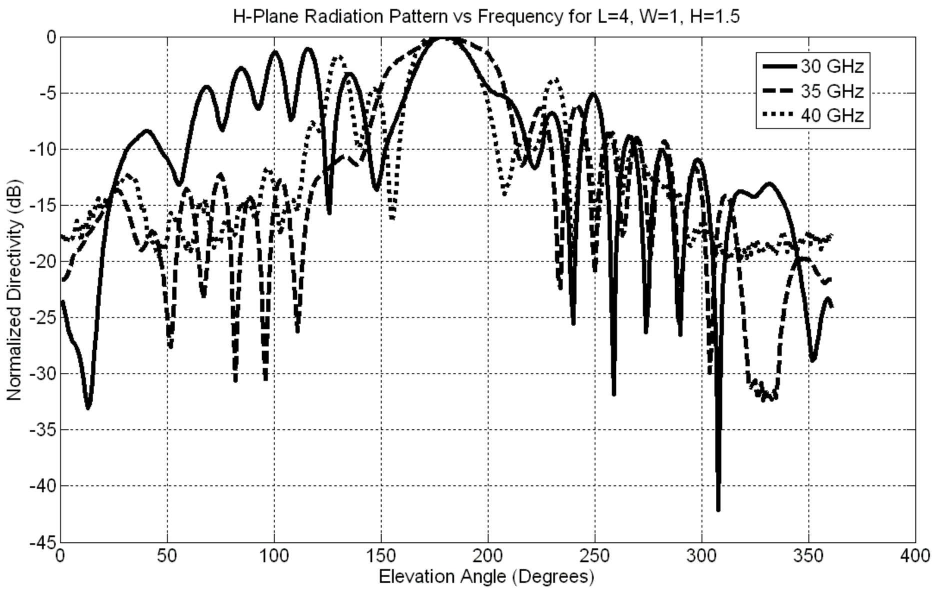

Figure 76 H-Plane Radiation Pattern vs Frequency for LTSA with L=4λ_0, W=1λ_0 and H=1.5 λ_0

The E-plane and H-plane radiation patterns of CWSA with L=4λ_0, W=1 λ_0 and H=1.5 λ_0 at three different frequencies are given in Figure 77 and Figure 78. The CWSA deviates from endfire characteristics for the frequency of 30GHz.

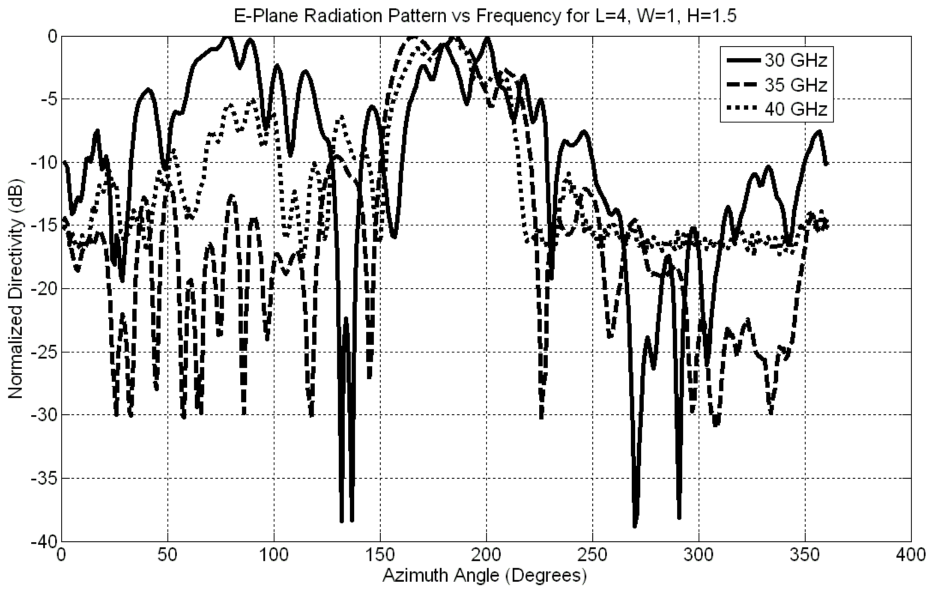

Figure 77 E-Plane Radiation Pattern vs Frequency for CWSA with L=4λ_0, W=1λ_0 and H=1.5 λ_0

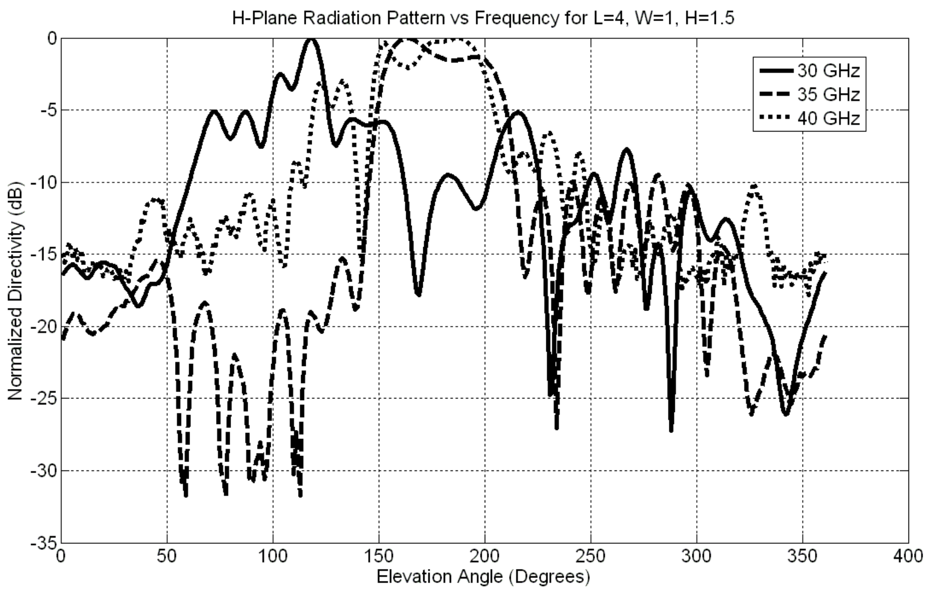

Figure 78 H-Plane Radiation Pattern vs Frequency for CWSA with L=4λ_0, W=1λ_0 and H=1.5 λ_0

Although for these configurations, some of the antennas have split or tilted beams for some different frequencies, it is mandatory to note that even at the center frequency, the effective thickness value of the substrate does not satisfy the condition required to achieve good travelling wave antenna characteristics.

CHAPTER 5

CONCLUSION

A parametric study on the radiation characteristics of LTSA and CWSA was performed. According to the results of this parametric study a reconfigurable antenna configuration operating at 35 GHz was proposed.

Since tapered slot antennas are a class of travelling wave antennas composed of a slot line that gets wider through the antenna until the wave detaches to air and microstrip line was chosen as the antenna feed, a microstrip line to slot line transition was needed to be designed. To obtain a wideband antenna, a wideband microstrip line to slot line transition was designed through the use of Chebyshev impedance transformer circuit. The designed microstrip line to slot line transition showed good return loss characteristics in the frequency band of 26-47 GHz according to the simulation results carried out in HFSS.

A parametric study about the relationship between physical antenna parameters (aperture width, antenna length and ground extension) and the radiation pattern was performed for both LTSA and CWSA. In this study, simulations in HFSS were carried out by changing one of the parameters of the antenna while keeping others constant. Then, the variations in the E-plane and H-plane beamwidths and sidelobe levels were observed and discussed. The results of this study were also compared with a similar study presented in [10], and a good agreement between these studies was observed.

The conclusions drawn from the parametric studies are summarized in Table 11.

Table 11 Summary of the Parametric Study Results

	LTSA				CWSA			
	E-BW	H-BW	E-SLL	H-SLL	E-BW	H-BW	E-SLL	H-SLL
Increasing Antenna Length	↓	↓	–	↑	↓	↓	↑	–
Increasing Aperture Width	↓	↑	↓	↓	↓	↔	↓	↑
Increasing Ground Extension	–	–	–	–	–	↔	↔	↑

The up-arrow in the table indicates that the pattern parameter is increasing with the increase in the antenna parameter, down-arrow indicates a decrease, the horizontal arrow indicates no change and a dash means that the pattern change is dependent on at least one more physical parameter so a generalization can not be done.

As seen in Table 11, the general effects of the physical parameter change on antenna pattern are similar for the LTSA and CWSA cases. Generally, increasing the length of the antenna decreases the half-power beamwidths in both planes. An increase in the aperture width acts as to decrease both the beamwidth and the sidelobe level in E-plane. The change in the ground extension has no significant effect on H-plane beamwidth or E-plane sidelobe level, but increasing the ground extension increases the H-plane sidelobe level.

The CWSA needs some kind of taper in order to get a reasonable return loss value from the antenna. Two different taper profiles as exponential and linear taper were considered and according to the results of the HFSS simulations, it was seen that there is not a significant difference in the antenna pattern for the linear taper and exponentially tapered CWSA cases. The exponential taper simulations were used in the parametric study. Although there is not a significant change in antenna pattern with taper profile, the usable antenna bandwidth depends on it. For narrow aperture width CWSAs, the return loss is not affected by the taper profile, however for an aperture width of $1\lambda_0$, the CWSA with exponential taper exhibits lower return loss in comparison with linear taper.

The main aim of the thesis study was to get an understanding of the possible chance of using a transition between LTSA and CWSAs to obtain reconfigurability in the antenna radiation pattern. It was expected to get a narrower beam with a tradeoff of higher sidelobe level for a transition from LTSA to CWSA. As a result of the parametric study, it was seen that for most of the configurations, the desired pattern change could be obtained. The configurations that show more significant pattern change and the radiation pattern graphs for these configurations are given in Chapter 3. The amount of fall in the beamwidth is on the orders of 5-15 degrees and the rise in the sidelobe levels are on the order of 5-10 dB for a transition between LTSA and CWSA with same antenna parameters.

To prove the results of the parametric study obtained from simulations, antenna pattern measurements for four antennas were made. Due to the problems in manufacturing phase, the substrate (Duroid 5880) that was used in the parametric study simulations was not used in the manufactured antennas. So a new transition from microstrip line to slot line was designed. Four antennas were manufactured with the new transition design on the new substrate (RO4003). The pattern measurements of these antennas were performed in both planes and a good agreement between measurement and simulation results were observed. When the measured patterns of LTSAs and CWSAs having the same physical sizes were compared, it was seen that the desired reconfigurability was not achieved due to the split beam characteristics of CWSAs, also seen in simulations. This was due to the fact that the dielectric constant of the new substrate used in the manufactured antennas was too high and not suitable to be used in the design of TSAs. Therefore the conclusion drawn through the measurement results is the importance of the choice of the dielectric substrate for the design of TSAs. The dielectric constant of the substrate should be low for the proper radiation of the antenna. If a substrate with high dielectric constant is chosen as in this work, then the effective dielectric constant need to be lowered by introducing a cavity under the antenna or by drilling holes in the substrate as proposed in [12] and [13], respectively.

REFERENCES

[1] Balanis, Constantine A., *Antenna theory : analysis and design,* John Wiley & Sons, Inc., New York : 1982.

[2] Milligan, T. A., Traveling-Wave Antennas, Chapter 10 in *Modern Antenna Design,* Second Edition, John Wiley & Sons, Inc., NJ, USA. : 2005.

[3] Amena Kauser Syeda, "Design of a Wideband Vivaldi Antenna Array and Performance Enhancement of Small Vivaldi Arrays Using Baffles," B.E., Electronics and Communication Engineering, Osmania University, India, 2003.

[4] K.S. Yngvesson, T.L. Korzienowski, Y.S. Kim, "The Tapered Slot Antenna-A New Integrated Element for Millimeter-Wave Applications," *IEEE Trans. on Microwave Theory and Techniques*, vol. MTT-37, pp. 365-374, Feb. 1989.

[5] P. J. Gibson, "The Vivaldi Aerial," *Proc. 9th European Microwave Conf. Brighton, U.K,* pp. 101-105, *1979.*

[6] S.N. Prasad, S. Mahapatra, "A Novel MIC Slot-Line Antenna," *Proc. 9th European Microwave Conf. Brighton, U.K,* pp.120-124, 1979.

[7] K. Sigfrid Yngvesson, Daniel H. Schaubert, Thomas L. Korzienowski et al, "Endfire Tapered Slot Antennas on Dielectric Substrates," *IEEE Transactions on Antennas and Propagation*, Vol. AP-33, No. 12, December 1985.

[8] R. Janaswamy, "Radiation Pattern Analysis of the Tapered Slot Antenna," Ph.D. dissertation, Univ. Massachusetts, USA, 1986.

[9] J.F. Johansson, "A Moment Method Analysis of Linearly Tapered Slot Antennas," *IEEE Antennas and Propagation Society International Symposium,* pp. 383-386, 1989.

[10] Adnan Köksal, "Characterization and Optimization of Linearly Tapered Slot Antenna Pattern," *International Journal of Infrared and Millimeter-Waves,* Vol.18, No.8, pp. 1525-1537, 1997.

[11] Dong-Sik Woo; Young-Gon Kim; Kang Wook Kim; Young-Ki Cho; , "Ultra-wideband millimeter-wave tapered slot antennas," *IEEE Antennas and Propagation Society International Symposium,* pp.1969-1972, June 2007.

[12] I.K. Kim, N. Kidera, S. Pinel, J. Papapolymerou, J. Laskar, J.G. Yook, M.M. Tentzeris, "Linear Tapered Cavity-Backed Slot Antenna for Millimeter-Wave LTCC Modules," *IEEE Antennas and Wireless Propagation Letters,* Vol.5, No.1, pp.175-178, Dec. 2006.

[13] Jeremy B. Muldavin, Gabriel M. Rebeiz, “MM-Wave Tapered Slot Antennas on Synthesized Low Permittivity Substrates,” *IEEE Transactions on Antennas and Propagation,* Vol.47, No.8, pp.1276-1280, August 1999.

[14] Y.S. Kim, K.S. Yngvesson, “Characterization of Tapered Slot Antenna Feeds and Feed Arrays,” *IEEE Transactions on Antennas and Propagation,* Vol.38, No.10, pp.1559-1564, October 1990.

[15] J.H.G. Ender, A.R. Brenner, “PAMIR - a wideband phased array SAR/MTI system,” *IEE Proceedings Radar, Sonar and Navigation*, Vol.150, No.3, pp.165 – 172, June 2003.

[16] Ian Wood, “Linear Tapered Slot Antenna for Imaging Arrays,” Ph.D. dissertation, University of Victoria, USA, 2005.

[17] Simons, R. N. Coplanar Waveguide Transitions, Chapter 10 in *Coplanar Waveguide Circuits, Components, and Systems*, John Wiley & Sons, Inc., New York, USA. : 2002.

[18] Bernd Schüppert, “Microstrip/Slotline Transitions: Modelling and Experimental Investigation,” *IEEE Trans. Microwave Theory Tech.* Vol.36, No.8, August 1988.

[19] Johnson, Richard C., *Antenna Engineering Handbook,* 3rd Edition, pp: 8.5-8.6, McGraw-Hill. : 1993.

[20] R. Janaswamy, D.H. Schaubert, “Characteristic Impedance of a Wide Slotline on Low-Permittivity Substrates,” *IEEE Trans. Microwave Theory Tech.* Vol MTT-34, No 8, August 1986.

[21] J. Thaysen, K.B. Jakobsen, J. Appel-Hansen, “A Wideband Balun-How Does It Work?,” *Applied Microwave&Wireless*, Vol.12, No.10, pp.40-50, October 2000.

[22] Nai-Biao Wang, Yang-Chang Jiao et al, “A Simple Low-Loss Broadband 1-14 GHz Microstrip-to-Slotline Transition,” *Microwave and Optical Technology Letters,* Vol.51, No.9, September 2009.

[23] B. Boyer, J. Haidar, A. Vilcot, and M. Bouthinon, “Tunable microwave load based on photoinduced plasma in silicon,” *IEEE Transaction on Microwave Theory and Techniques*, vol.45, issue 8, pp. 1362-1367, Aug. 1997.

[24] R.K. Shevgaonkar and S. Shevgaonkar, “Study of optically controlled microwave devices” *Proceedings of International Union of Radio Science (URSI): XXIX General Assembly*, August 7 - 16, 2008, Chicago, USA.

[25] M.R. Chaharmir, J. Shaker, M. Cuhaci and A. Sebak, “Novel photonically-controlled reflectarray antenna,” *IEEE Transactions on Antennas and Propagation*, vol. 54, no. 4, pp. 1134-1142, April 2006.

[26] T. Morolari, “Characterization of Optically Sensitive Polymer and Application to Microwave Antenna,” M.A.Sc. Thesis Dissertation, Carleton University, Ottawa, Canada, Dec. 2009.

APPENDIX A - Calculation of characteristic impedance of slot lines and microstrip lines

The characteristic impedance of a slot line can be calculated as:

$$Z_0 = 60 + 3.69\sin\left[\frac{(\varepsilon_r - 2.22)\pi}{2.36}\right] + 133.5\ln(10\varepsilon_r)\sqrt{\frac{W}{\lambda_0}} +$$

$$2.81\left[1 - 0.011\varepsilon_r(4.48 + \ln\varepsilon_r)\right]\left(\frac{W}{h}\right)\ln\left(\frac{100h}{\lambda_0}\right) \qquad \text{(A1)}$$

$$+131.1(1.028 - \ln\varepsilon_r)\sqrt{\frac{h}{\lambda_0}} + 12.48(1 + 0.18\ln\varepsilon_r)\left(\frac{\left(\frac{W}{h}\right)}{\sqrt{\varepsilon_r - 2.06 + 0.85\left(\frac{W}{h}\right)^2}}\right)$$

where h is the height of the dielectric substrate and W is the width of the slot line.
The guided wavelength of the slot line can be found as:

$$\frac{\lambda_g}{\lambda_0} = 1.045 - 0.365\ln\varepsilon_r + \frac{6.3\left(\frac{W}{h}\right)\varepsilon_r^{0.945}}{238.64 + 100\left(\frac{W}{h}\right)} - \left(0.148 - \frac{8.81(\varepsilon_r + 0.95)}{100\varepsilon_r}\right)\ln\left(\frac{h}{\lambda_0}\right) \qquad \text{(A2)}$$

The effective dielectric constant and characteristic impedance of a microstrip line can be calculated as:

For W/h<1:

$$\varepsilon_{eff} = \frac{\varepsilon_r + 1}{2} + \frac{\varepsilon_r - 1}{2}\left[\frac{1}{\sqrt{1 + \frac{12h}{W}}} + 0.04\left(1 - \frac{W}{h}\right)^2\right] \qquad \text{(A3)}$$

$$Z_c = \frac{60}{\sqrt{\varepsilon_{eff}}}.\ln\left(\frac{8h}{W} + \frac{W}{4h}\right) \qquad \text{(A4)}$$

For W/h>1:

$$\varepsilon_{eff} = \frac{\varepsilon_r + 1}{2} + \frac{\varepsilon_r - 1}{2}\left(\frac{1}{\sqrt{1 + \frac{12h}{W}}}\right) \tag{A5}$$

$$Z_c = \frac{120\pi}{\sqrt{\varepsilon_{eff}}} . \frac{1}{\left[\frac{W}{h} + 1.393 + \left(0.677.\ln\left(\frac{W}{h} + 1.444\right)\right)\right]} \tag{A6}$$

where W is the width of the microstrip line.

APPENDIX B - Design of Chebyshev Impedance Transformer

The impedance calculation formulas for Chebyshev impedance transformer with three sections is presented here.

$$\sec\theta_m = \cosh\left[\frac{1}{N}\cosh^{-1}\left(\frac{\ln(Z_L/Z_0)}{2\Gamma_m}\right)\right] = \cosh\left[\frac{1}{3}\cosh^{-1}\left(\frac{\ln(152.76/50)}{2\times 0.05}\right)\right] = 1.5849 \qquad \text{(B1)}$$

$$2\Gamma_0 = A\sec^3\theta_m = 0.05\times(1.5849)^3 \Rightarrow \Gamma_0 = 0.0995 \qquad \text{(B2)}$$

$$2\Gamma_1 = 3A\left(\sec^3\theta_m - \sec\theta_m\right) = 3\times 0.05\left(1.5849^3 - 1.5849\right) \Rightarrow \Gamma_1 = 0.1797 \qquad \text{(B3)}$$

$$\ln Z_1 = \ln Z_0 + 2\Gamma_0 = \ln 50 + (2\times 0.1797) \Rightarrow Z_1 = 61.01\Omega \qquad \text{(B4)}$$

$$\ln Z_2 = \ln Z_1 + 2\Gamma_1 = \ln 61.01 + (2\times 0.1797) \Rightarrow Z_2 = 87.39\Omega \qquad \text{(B5)}$$

$$\ln Z_3 = \ln Z_2 + 2\Gamma_2 = \ln 87.39 + (2\times 0.1797) \Rightarrow Z_3 = 125.19\Omega \qquad \text{(B6)}$$

where, $A=\Gamma_m=0.05$, $\Gamma_2=\Gamma_1$ due to symmetry and $N=3$.